The Cost and Benefit of Bulk Energy Storage in the Arizona Power Transmission System

by

John Ruggiero

A Thesis Presented in Partial Fulfillment
of the Requirements for the Degree
Master of Science

Approved November 2013 by the
Graduate Supervisory Committee:

Gerald Heydt, Chair
Rajib Datta
George Karady

ARIZONA STATE UNIVERSITY

December 2013

ABSTRACT

This thesis addresses the issue of making an economic case for energy storage in power systems. Bulk energy storage has often been suggested for large scale electric power systems in order to levelize load; store energy when it is inexpensive and discharge energy when it is expensive; potentially defer transmission and generation expansion; and provide for generation reserve margins. As renewable energy resource penetration increases, the uncertainty and variability of wind and solar may be alleviated by bulk energy storage technologies. The quadratic programming function in MATLAB is used to simulate an economic dispatch that includes energy storage. A program is created that utilizes quadratic programming to analyze various cases using a 2010 summer peak load from the Arizona transmission system, part of the Western Electricity Coordinating Council (WECC).

The MATLAB program is used first to test the Arizona test bed with a low level of energy storage to study how the storage power limit effects several optimization out-puts such as the system wide operating costs. Very high levels of energy storage are then added to see how high level energy storage affects peak shaving, load factor, and other system applications. Finally, various constraint relaxations are made to analyze why the applications tested eventually approach a constant value. This research illustrates the use of energy storage which helps minimize the system wide generator operating cost by "shaving" energy off of the peak demand.

ACKNOWLEDGMENTS

Foremost, I would like to extend my deepest appreciation to my advisor, Dr. Gerald T. Heydt, for his continuous support of my M.S. study and research, his patience, immense knowledge, and guidance. Without his assistance and motivation, the completion of this thesis would not have been possible. I could not have imagined a better advisor and mentor for my M.S study and I am immensely thankful. I also would like to thank Dr. George Karady and Dr. Rajib Datta for offering their time and effort to be part of my graduate supervisory committee.

I would also like to acknowledge the Power Systems Engineering Research Center (PSERC), a National Science Foundation 'Industry – University Cooperative Research Center' for their financial assistance. The NSF center is a Generation III Engineering Research Center supported by industry and the U.S. National Science Foundation under grant EEC-0968993.

Last but not least, I would like to thank my parents, Don and Linda Ruggiero, for their continuous support and encouragement throughout my thesis. Their love provided inspiration and was the driving force that kept me going during times of stress and frustration. I cannot thank them enough for all of the help they offered throughout my educational career.

TABLE OF CONTENTS

Page

CHAPTER Page

LIST OF TABLES

Table Page

LIST OF FIGURES

Figure Page

Figure Page

NOMENCLATURE

a	The quadratic coefficient of the approximation for the cost of generation
A	Coefficient matrix (m *x* n) of inequality constraints
A_{eq}	Coefficient matrix (k *x* n) of equality constraints
ACE	Area control error
AGC	Automatic generation control
b	The linear coefficient of the approximation for the cost of generation
b	Vector (m *x 1*) of inequality right-hand side constraints
B	Frequency bias (MW/mHz); part of supplementary control
b_{eq}	Vector (k *x 1*) of equality right-hand side constraints
B_k	Susceptance of transmission element k
c	The coefficients of the cost function of generator g
c	The no load coefficient of the approximation for the cost of generation
CA	Combined cycle steam part
CAES	Compressed air energy storage
C_g	The linear coefficient, b, of the cost function of generator g
CSP	Concentrated solar power
CT	Combined cycle combustion turbine part
D	Frequency independent component of the load in AGC
DP	Dynamic programming
ED	Economic dispatch
E/P	The ratio of maximum energy stored in a pumped hydro facility to the maximum power (i.e., rated power). E is usually in MWh and P in MW.

EPAct	Energy policy act
E_s	The energy stored in storage unit *s* in MWh
$E_{s,max}$	Maximum energy capacity of storage unit *s* in MWh
E_T	Total energy supplied in MWh
F_C	Generator fuel cost in $/MBTU
FES	Flywheel energy storage
Governor	Measures speeds and adjusts steam valves to change generation
GT	Gas turbine
i	Interval number
K/s	Gain of the AGC integral controller; part of supplementary control
k(. ,n)	Set of transmission assets with *n* as the 'FROM' node
k(n, .)	Set of transmission assets with *n* as the 'TO' node
l	Vector of lower bound variables
LMP	Locational marginal price
Load	Represents the transfer function of a specified load. Parameter *M* is the frequency dependent component and *D* is the frequency independent component
LP	Linear programming
M	Frequency dependent component of the load in AGC
m,n	Bus number (nodes)
MIPs	Mixed integer programming
P_g	The real power output of generator *g* in MW
$P_{g,max}$	Maximum power capacity of generator *g* in MW
$P_{g,min}$	Minimum power capacity of generator *g* in MW

PHES	Pumped hydro energy storage
P_k	The power flow of transmission line *k* in MW
$P_{k,max}$	Maximum line flow rating of transmission element *k* in MW (generally $P_{k,max} = -P_{k,max}$)
P_l	The active power of load *l* in MW
PM	Prime mover; provides torque necessary to turn the shaft of a generator
P_{peak}	Peak power demand in MW
P_s	The real power output of storage unit *s* in MW
$P_{s,max}$	Maximum power capacity of storage unit *s* in MW
$P_{s,min}$	Minimum power capacity of storage unit *s* in MW
PSO	Particle swarm optimization
PV	Photovoltaic
Q_g	The quadratic coefficient, *a*, of the cost function of generator *g*
QP	Quadratic programming
1/R	Speed droop characteristic of the generator (included in the governor system)
R_g	Ramp rate limit of generator *g* in $\frac{MW}{hr}$
RPS	Renewable portfolio standard
s	Laplace transform variable
SCES	Supercapacitor energy storage
SLP	Successive linear programming
SMES	Superconductor magnetic energy storage
SRP	Salt River Project
ST	Steam turbine

T	Time period in hours
T/s	Tie line constant
TES	Thermal energy storage
u	Vector of upper bound variables
V_{OM}	Generator variable operation and maintenance costs in $/MWh
$WECC$	Western Electricity Coordinating Council
x	The vector generated system variable outputs
x_j	Variables that must be integers
δ_k	Bus voltage angle at node k
ΔP_{Tie}	Tie line power flow between areas one and two
Δt	Length of the time interval i in hours
$\Delta\omega$	Change in area frequency, r/s

CHAPTER 1

OBJECTIVES RELATING TO BULK ENERGY STORAGE IN POWER TRANSMISSION SYSTEMS

1.1 Introduction and research objectives

This research addresses the economic case for bulk energy storage optimized for multiple objectives including cost, congestion, and peak shaving for increasing levels of renewable resource penetration. The test bed used is the Arizona electric transmission system.

Arizona, like most states, has put forth a road map plan for the incorporation of renewable energy resources [1]. This type of plan is generally known as a Renewable Portfolio Standard (RPS). High penetration of solar and wind resources is inevitable as the RPS is implemented. There are a variety of proposal methods to address the variability issues associated with wind and solar renewable sources. It is possible to rely on conventional generators to provide ancillary services and backup generation; however this may reduce the value of renewable resource investment. Energy storage provides a potentially attractive resource for matching supply to load. The central question relating bulk storage use is an economic question: when does bulk energy storage and its concomitant transmission deferral possibilities, reserve margin alleviation, and other enhancements offset the potentially high cost of storage. This is the main subject of this thesis.

This research focuses on how energy storage can be used to potentially reduce conventional generator operating costs. The possible cost reduction will be shown through an economic dispatch model comparing the cost of generation before and after the inclusion

of energy storage in the system. The focus is on Arizona, and therefore the test bed used is the 2010 summer peak Arizona system. The analysis investigates peak shaving in order to lower the generating costs during periods of high demand. Also, the alleviation of congestion in the transmission system shall be studied for its benefits. Finally, this research will examine how bulk energy storage might be used to maximize the use of renewables.

Bulk energy storage at the transmission level will be evaluated based on benefits of:

- alleviation of uncertainty in the energy supply
- reduction of peak loading
- potential deferral of transmission expansion
- improvement in system efficiency
- incorporation of required RPS renewable generation
- maintaining system frequency by maintaining load-generation balance
- reduction of transmission congestion
- maintaining required reserve margins
- improvement of system reliability.

The objectives listed above will be applied to the state of Arizona using data provided by a statewide utility, Salt River Project (SRP), of the electric power grid. The results gathered from this test bed will be used to evaluate the practicality of bulk energy storage in Arizona.

1.2 Bulk energy storage applications

In this section, the main bulk energy storage applications in large electric power systems are discussed.

Peak shaving/ load leveling

Load leveling or peak shaving refers to the use of electric energy stored during times of low demand to supply the peak electric demand. Peak shaving reduces the need to draw on generation resources from peaking power plants or increasing the grid structure [2]. For most load profiles, the system demand is low during the early morning hours and high in the midday through the evening hours [3]. With peak shaving, during the early morning hours, the generation can be raised while storing energy. The stored energy can then be discharged during peak load hours so that the load peak is reduced. With load shaving however, the same process occurs except the goal is to flatten the load profile. Figure 1.1 shows pictorially the process of peak shaving.

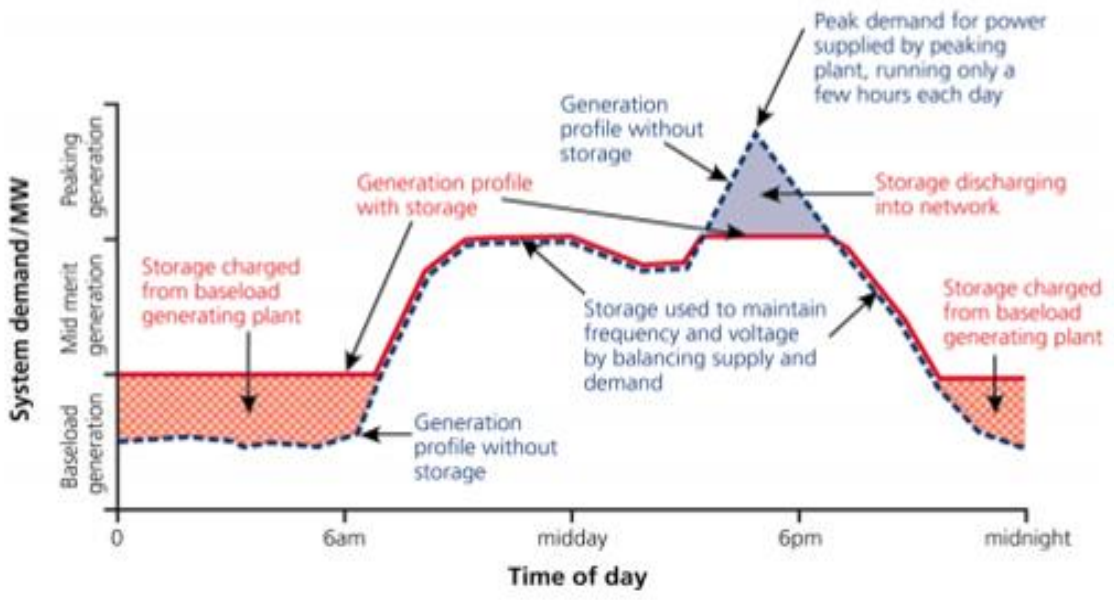

Figure 1.1 A diagram of showing peak shaving with energy storage
(taken directly from [4])

Frequency and area control error regulation

In a large interconnected power system, nominally the demand plus system losses are balanced by the generation. If there is a short term unbalance in this basic operating condition, the difference (power) comes from the rotating mass of the generating units,

$$\Delta P = \frac{dW}{dt}$$

where the difference in the power balance is ΔP and W is the system inertial energy. If energy is recovered from the rotating mass, the system frequency will change. For example, forced outage of generators can result in power unbalance. To restore the power balance, and to restore the operating frequency, power generation may be increased (or decreased). There is a limitation of how fast the power balance can be restored, and this suggests the potential use of high speed sources of power as might be available from electronically switched batteries.

The basic mechanism of frequency and system load control is accomplished using Automatic Generation Control (AGC), and Figure 1.2 shows a simplified two-area system under AGC [5]. Table 1.1 defines the nomenclature used in Figure 1.2. Analysis of a system under AGC indicates that as generation increases or load decreases, the frequency will increase (and energy storage can be used to store energy thus making the effective load higher). Similarly, energy storage may be used if generation decreases or load increases.

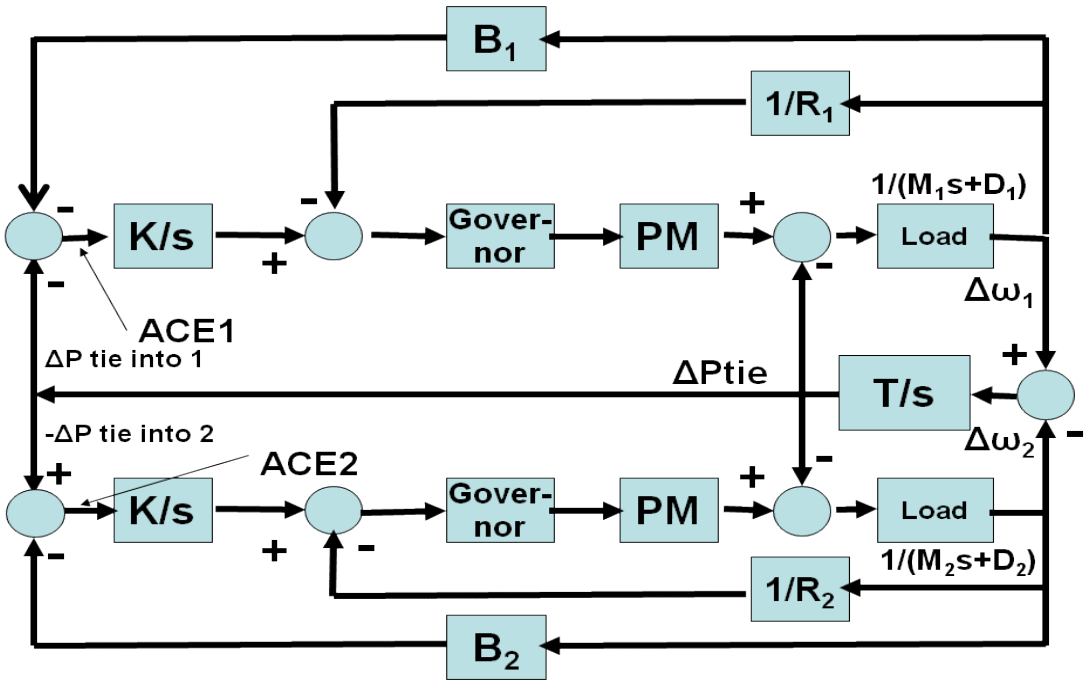

Figure 1.2 Automatic generation control of two control areas

Table 1.1 Nomenclature for an AGC system

Symbol	Meaning	Symbol	Meaning
Area control error (ACE)	Instantaneous difference between a Balancing Authority's net actual and scheduled interchange	$1/R$	Speed droop characteristic of the generator (included in the governor system).
K/s	Gain of the AGC integral controller. Part of supplementary control.	Load ($\frac{1}{Ms+D}$)	Represents the load at the specified area. Parameter *M* is the frequency dependent component and *D* is the frequency independent component.
B	Frequency bias (MW/MHz). Part of supplementary control.	*T/s*	Tie line constant
Governor	Measures speeds and adjusts steam valves to change generation.	$\Delta\omega$	Change in area frequency
Prime mover (PM)	Provides turning force necessary to turn the shaft of the generator.	ΔP_{tie}	Tie line power flow between areas one and two

Energy storage devices such as batteries have the capabilities of absorbing energy when the AGC Area Control Error (ACE) is high, and discharge the energy back into the grid when the ACE is low. Battery energy storage has a very fast response time and offers an alternative to the traditional strategy of maintaining adequate spinning reserve margins [6, 7]. Battery storage is electronically switched and can supply needed power rapidly. Energy storage can also help reduce or eliminate supplementary power from combustion turbines. With a large increase in wind generators in certain areas, there could be serious frequency problems in the electrical system because of the intermittent behavior of wind generation [8]. Again, energy storage can be used to reduce the generation uncertainty.

Transmission line expansion deferral

Transmission upgrades and new construction investments are necessary when line congestion limits the power that can be sent through an existing circuit [9]. Congestion can be avoided by using bulk energy storage on the 'receiving' end of a circuit to reduce transmission line loading. There is the potential, therefore, to reduce the need for transmission expansion and upgrades through the use of energy storage [10-13].

Other reasons for transmission line upgrades or expansion include:

- demand increase in existing networks
- demand increase due to new developments
- interconnection of renewable energy (i.e., wind or solar)
- existing lines reaching critical values of ampacity or sag
- enhancing system stability.

Integration of renewables

There is a lot of interest in the area of renewable generation in North America [10]. Renewable energy has even become popular enough that various books have been written on the subject [15-18].A large amount of wind and solar generation are likely to be added over the next 30 years in order to follow the CO2 emission reduction policies [19]. EPRI's Prism Analysis estimates about 1350 MW of new renewable generation will be added to the US grid by 2030, thus representing 15% of the generation mix. One of the major drawbacks of renewable energy is that it is time of day and weather dependent. These resources are generally undispatchable and uncontrollable. Weather data from many resources are available to predict of solar and wind levels. These predictions can be used to forecast the energy outputs, but these are only predictions and there will exist a level of uncertainty. With energy storage integrated with renewable generation, two problems may be solved [20]. First, storage can stabilize the intermittent power output of the generators and improve the capacity factor of the system. Wind generation capacity factor is currently less than 40%. Secondly, energy storage can take the energy from wind that is usually higher at night and integrate the energy into periods of higher demand [9]. With larger MW scale solar photovoltaic (PV) installations, energy storage is useful to levelize output even under conditions of cloudiness [21].

Transmission line congestion

Transmission congestion occurs when the physical limitations of a transmission infrastructure prevent electricity transactions from occurring [22]. When this occurs, Locational Marginal Prices (LMPs) increase because the system would need to be redispatched to accommodate the transmission constraints. Transmission congestion

charges are fees that are charged during periods of peak electricity usage because of the increased cost of providing power under high congestion [23]. Part of this charge is eventually passed onto the customer because of their use during peak demand times. Energy storage can alleviate response to system contingencies if the storage elements are located properly [22]. Energy storage can be sited near congestion such that it could shift the delivery of generation from off peak to on peak. When reducing congestion in transmission lines relatively smaller energy storage systems, such as batteries, can be used during peak hours [24]. Other types of storage such as PHES and CAES are possible solutions but are very location dependent [25, 26]. Battery storage also has the advantage of having a fast response time, meaning it could respond quickly to transmission lines becoming congested.

Reserve margins

In power systems, scheduling reserve margins are kept in order to maintain security of the system if an unpredicted event occurs [27]. This security is maintained by the redispatch of the generators in the system. The expected load must be predicted (short term load forecasting) and sufficient generation must be planned. Reserve generation must also be scheduled in order to account for load forecast uncertainties and possible outages of a generation plant. According to Antonio [28], a reserve margin is defined as the amount of capacity, usually on standby, to be activated only under exceptional situations, typically during peak conditions. This approach disaggregates the generation into two categories, the main generation devoted to meet the demand in "normal conditions" and the reserve devoted to face "exceptional" system conditions. For the Southwest region, reserve margin estimates for the summer of 2012 were around 14-22% [29]. This means that an electric

system must have excess capacity of 14-22% of the expected peak demand. Instead of having a high amount of generation only being used for "exceptional" conditions, energy storage can be used. The output from reserve generators may possibly vary from several hours to a few minutes but can respond instantaneously with some storage technologies. The amount of excessive generation to meet peak loads can also be reduced with storage since generated energy can be stored during off peak hours.

1.3 Principal energy storage technologies

The four main forms of energy storage that have the capability of performing some or all of the applications listed in Section 1.2 include:

Pumped Hydro Energy Storage (PHES)

PHES consists of two large reservoirs located at different elevations and a number of pump/turbine units [30]. During off peak electrical demand, water is pumped from the lower reservoir to the higher reservoir where it is stored. Once required during peak demands, the water in the upper reservoir is released through the turbines and electricity is produced from the connected generators. PHES is thus very similar to a conventional hydroelectric system. The storage capacity is very dependent on the head and the volume of the reservoirs. In order to create the highest storage capacity, pumped hydro is usually designed with the greatest hydraulic head possible. PHES has the capability of generating between 100-4000 MW of electrical power at efficiency 70-80%. PHES can be used for peak shaving and as spinning reserve. Also, with variable speed machines it can now be used for frequency regulation in pumping and generation.

Compressed Air Energy Storage (CAES)

In conventional gas turbines, 66% of the gas is used to compress the air at the time of generation. CAES pre-compresses the air using off peak electrical power, which is taken from the grid or renewable generators, to drive a motor and compress air into a large storage reservoir [30]. When the gas turbine is producing electricity during peak hours, the compressed air is released and used in the conventional gas turbine cycle. Instead of using expensive gas to compress air, cheaper off peak power is used to pre-compress it in advance. CAES has the capability of producing 50-300 MW with proposed facilities capable of up to 2700 MW and an efficiency of 68-75%. It also provides a longer lifetime than a standard gas turbine. CAES has a fast reaction time with the capability of full power from 0% in less than 10 minutes. It is ideal for acting as a large sink for bulk energy supply and demand and can undertake frequent startups and shutdowns. CAES can be used for frequency regulation, load following, and voltage control.

Battery energy storage (lead acid)

Lead-acid batteries are made up of two electrodes that are constructed using lead plates immersed in a mixture of water and sulfuric acid [30]. The battery has alternating lead and lead oxide plates. Current flows from the lead oxide cathode to the lead anode. Electrons are passed to the lead acid plate and both plates are converted to lead sulfate. When voltage is applied to the battery, which is greater than the batteries volt-age, current will flow through the battery in the reverse direction of when it is supplying current and will charge the battery. The rate of charge depends on the voltage difference. When the battery is switched to a load, the current will flow towards that load and the battery voltage will begin to drop due a decrease in the internal resistance. Lead acid batteries use these

operating characteristics to store energy and release the power when it is required. They have a long lifespan, fast response, and low self-discharge rate. Batteries also have very fast ramp rates and can respond within milliseconds at full power. It has been shown that they can have capacities up to 50 MW and can store up to 200 MWh of energy at an efficiency of 75-85%. Batteries can be used for peak shaving, backup energy, load leveling, power quality, and frequency fluctuations [31-33].

Solar Thermal Energy Storage (TES)

Concentrated Solar Power (CSP) technology uses heat collected from solar thermal troughs. The heat is focused on oil (e.g., *thermoil*) in tubing [30]. The oil flows from a low temperature storage tank and uses the high concentration of the sun from solar troughs to heat the oil and raise it to high temperatures, e.g., 150–350 °C. The oil is then heat exchanged with molten salt (e.g., calcium sulfate) and stored in a high temperature storage tank. When it desired to recover the stored energy, the molten salt is released into another heat exchanger with water. The steam produced is then used in the conventional Rankine cycle power plant [34, 35]. CSP has the capability to store energy captured from the sun during off peak hours and use it during peak demand when less energy from the sun is available. Depending on the material and the size of the tank, CSP has the capability to store heat up to 24 hours. To give an idea of the capabilities of CSP, note that a large CSP plant has the ability of storing up to 400 MWh of energy at an efficiency of 85-95% with an overall plant efficiency of about 30-60%. CSP can be used for peak shaving and as spinning reserve.

Other smaller scale energy storage methods that were not considered for this project include:

Supercapacitor Energy Storage (SCES)

Supercapacitors store energy in the chemical valence states or in the so called "Helmholtz" double layer that exists around the carbon fibers in the alkaline solution [36]. The main attraction of SCES is its fast charge and discharge, combined with its extremely long life of approximately 1 x10^6cycles [30]. SCES is primarily used where pulsed power is needed in the millisecond to second time range, with discharge times up to one minute. However, SCES has a very low energy storage density leading to high capital costs for larger scale applications.

Flywheel Energy Storage (FES)

Flywheels store energy by accelerating the rotor/flywheel to a very high speed and maintaining the energy in the system as kinetic energy [30]. They release energy by reversing the charging process so that the motor is then used as a generator. Flywheels have an extremely fast dynamic response, a long life, and require little maintenance. They are used for power quality enhancements like capturing waste energy and dampening frequency variations. However, they are optimal for power or storage capacities, but the need of one application can often make the design poorly suited for the other. Also, they are kept in vacuum so it is difficult to transfer heat out of the system, thus a cooling system is usually needed.

Fuel cells

A fuel cell is an apparatus that produces power through an electrochemical reaction rather than combustion [37]. It allows the continuous supply of fuel and electricity. Fuel cells run off hydrogen 'fuel' and produce energy and waste products, mostly water vapor. They can achieve high efficiencies in energy conversion terms and have a high power

density which allows them to be a relatively compact source of electric power [38, 39]. However, they have very high costs compared to other energy system technologies.

A few applications of fuel cells at the distribution level include [40-42]:

- grid reinforcement
- deferring or eliminating the need for system upgrades
- improving system integrity, reliability, and efficiency
- generating heat for residential, commercial, or industrial applications.

Superconducting Magnetic Energy Storage (SMES)

A SMES is a device made up of a superconducting coil, a power conditioning system, a refrigerator, and a vacuum to keep the coil at a low temperature [30]. Energy is stored in the magnetic field created by the flow of direct current in the SMES. Due to the high power capacity, and its instantaneous discharge rates, it is used for protection of industrial equipment from rapid momentary voltage sags and to stabilize fluctuations within the entire network. However, due to high energy consumption of the refrigerator system, SMES is unsuitable for daily cycling applications such as peak reduction, renewable applications, and generation and transmission deferral [35].

1.4 Organization of this thesis

This thesis is organized into five chapters and three appendices:

- Chapter 2 defines the economic dispatch problem and gives different methods to solve it. Also, a method is selected to formulate the problem used throughout the thesis.
- Chapter 3 uses the algorithm from Chapter 2 to introduce energy storage in the state of Arizona, which is the chosen test bed.

- Chapter 4 uses the same test bed as Chapter 3 but analyzes an “extreme” amount of energy storage to the system.
- Chapter 5 analyzes how relaxing selected constraints in the system affects the results.
- Chapter 6 presents conclusions and suggests future work related to bulk energy storage in energy systems.
- There are also three appendices: Appendix A which provides the MATLAB code used for this research and Appendix B, which describes the quadratic programming algorithm and observation made related to the algorithm. Appendix C contains brief comments on the environmental impacts of pumped hydro energy storage. This subject is beyond the scope of this thesis, but site specific references are cited to partially document the subject of environmental impact.

CHAPTER 2

THE OPTIMIZATION TOOLS NEEDED TO ADDRESS THE ENGINEERING OF BULK ENERGY STORAGE

2.1 Economic dispatch

The goal of power Economic Dispatch (ED) is the constrained minimization of the generator operating cost [43]. This is accomplished by determining the power output of all generating units under the constraint conditions of the system topology and the system load demand. That is, this is a constrained minimization problem in which the operating cost is minimized subject to the constraint that the load is satisfied and the electric circuit laws are satisfied. Additional constraints include operation within the ratings of the circuit assets, contractual limits, and environmental limits. Figure 2.1 shows the basic concept pictorially. The figure shows the input data, the principal constraints, and the dispatch schedule that minimize the operating cost. According to EPAct, economic dispatch is defined as "the operating of generation facilities to produce energy at the lowest cost to reliably serve consumers, recognizing any operating limits of generation and transmission facilities" [44].

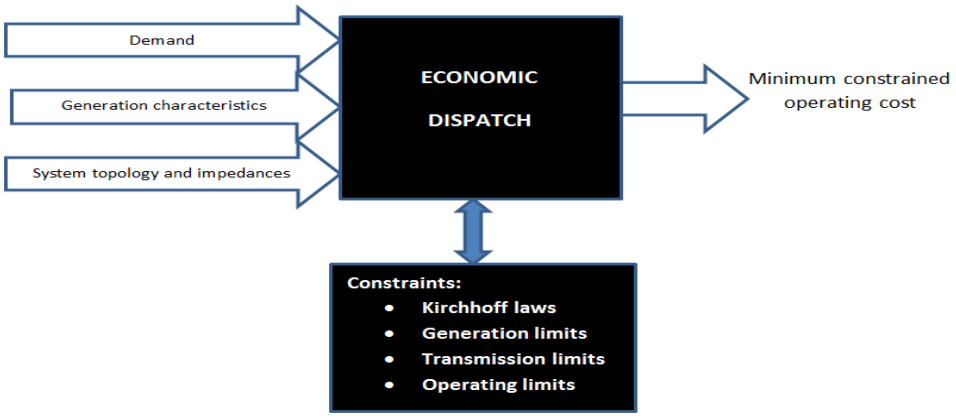

Figure 2.1 A pictorial of the economic dispatch problem

For thermal units, the input-output characteristic mentioned earlier is the generating unit fuel consumption function, or the operating cost function [43]. Generator fuel consumption is measured in *BTU*/h or its multiple 10^6 BTU/h = 1 MBTU/h. The fuel cost multiplied by the generating fuel consumption function is the operating cost expressed in*$*/h, and is denoted as *F*. The function *F* for a given generator is often expressed as an approximately quadratic function of the power output (*MW*) of the unit. The output of the generating unit is designed by P_G, the megawatt net power output. In addition to the fuel consumption cost, the operating cost includes labor cost, maintenance cost, and fuel transportation cost. It is difficult to express these costs as a function, so they are included as a fixed portion, or a no load cost. Figure 2.2 shows an example of the cost curve of a representative thermal generating unit.

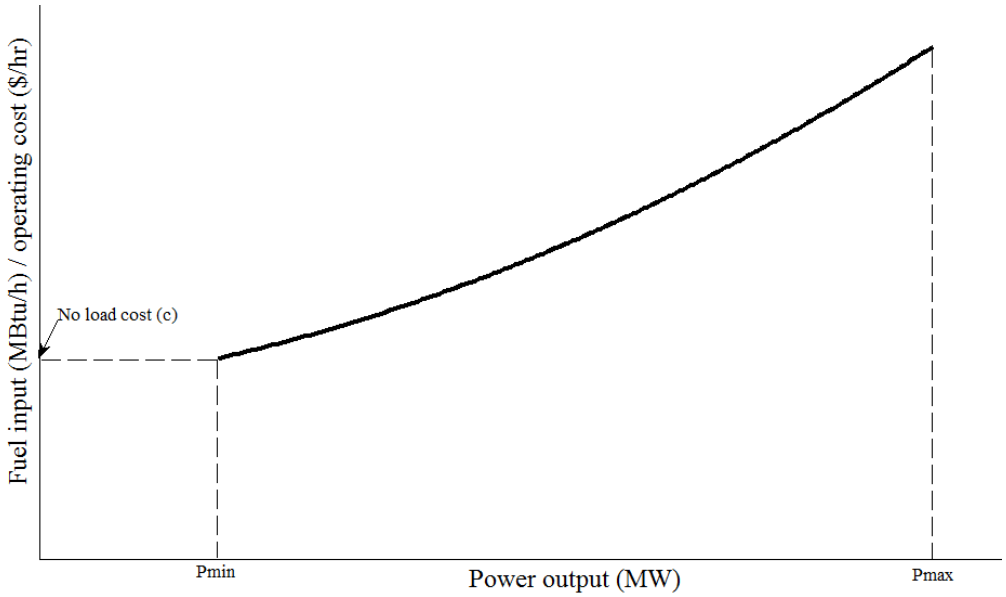

Figure 2.2 Operating cost curve of a thermal generating unit

For a given steam generating unit, the minimal power output, P_{Gmin}, is determined by technical conditions or other factors of the boiler or turbine. The incremental cost, $/MWh, or the slope of the operating cost curve, is the derivative of an assumed quadratic

function and this is linear with respect to the generator power output. The economic dispatch problem is formulated as a Lagrange multiplier problem with the Lagrangian $L(P_i, P_D)$ as [45, 46],

$$L(P_i, P_D) = F(P_i) - \lambda(\sum_{i=1}^{n} P_i - P_D) \tag{2.1}$$

where λ is a Lagrange multiplier, P_i is the power at bus i, and P_D is the total power demand. There are n generators in this formulation. The economical generation levels occur when the derivative of L in (2.1) with respect to the control variables (i.e., the individual generation levels) is zero,

$$\frac{\partial L}{\partial P_i} = 0 \quad \Rightarrow \quad \frac{\partial F(P_i)}{\partial P_i} = \lambda, \;\; i = 1, \dots, n \tag{2.2}$$

$$\frac{\partial L}{\partial \lambda} = 0 \Rightarrow \sum_{i=1}^{n} P_i - P_D = 0. \tag{2.3}$$

The result is that the incremental costs of all available generators are equal,

$$\frac{dF_1}{dP_{G1}} = \frac{dF_2}{dP_{G2}} = \cdots \frac{dF_i}{dP_{Gi}} = \lambda \tag{2.4}$$

where $\frac{dF_i}{dP_{Gi}}$ is the incremental cost of generator i. Eq. (2.4) holds for only the generators that have not yet reached their maximum (rated) output power. Eq. (2.4) is known as the *equal incremental cost rule*. The equal incremental cost rule simply says that at the minimum cost operating point of the system, the incremental cost for all operating (cycling) generators will be equal. When the load increases or decreases, the generator with the lowest incremental cost will deliver, or withdraw, the next MW. When the MW output level of a generator reaches its upper limit, the generator is fixed at that upper limit even

when a load increase occurs. Subsequently that generator is dropped out of the equal incremental cost rule. Other units which have not reached their limit will share the load increase based on the equal incremental cost rule.

Some conventional methods for solving the economic dispatch problem such as Lagrange multiplier method, lambda iteration need to compute the economic dispatch every time the load changes.

2.2 Economic dispatch methodologies

There are numerous methods that exist that can be used to solve the economic dispatch of a system. These techniques include conventional optimization methods such as lambda- iteration and the equal incremental cost rule, Linear Programming (LP), Dynamic Programming (DP), Quadratic Programming (QP), and Mixed Integer Programming (MIP) [5]. The lambda iteration method discussed below is used in several commercial economic dispatch programs because of its simplicity; however, other techniques such as MIPs are becoming more popular. Also, intelligent methods for solving the economic dispatch problem have been proposed but are largely unused: these ideas use Artificial Intelligence (AI) concepts which may or may not be suited for the economic dispatch problem [47]. An example of an AI approach is Particle Swarm Optimization (PSO), and this is discussed below.

The key to finding the most economical solution to the economic dispatch problem is solving for the system lambda, or the incremental operating cost. The system lambda method is suitable for the conventional techniques listed above when the cost function is linear or quadratic. These methods are discussed below.

Lambda-iteration method

In the lambda iteration method, the variable lambda in (2.4) is used to solve the optimization problem and λ is the Lagrange multiplier. The equations are solved using the iterative method described in steps 1-4 [5]:

Step 1- Assume a reasonable value of λ

Step 2- Calculate the individual generations, P_i for $i=1,\ldots,n$

Step 3- Calculate the equality, ε, using the equation $\varepsilon = \mathrm{P}_{\mathrm{load}} - \sum_{i=1}^{N} P_i$. If this is the first iteration, the first estimate will be incorrect. The λ value must be set to a better estimated value and the above steps must be repeated

Step 4- Check the epsilon value calculated in step 3. If ε is less than the user defined tolerance, the solution converges and the schedule is printed. If not, the projected λ is sent back to Step 2 and the above steps are rerun until the system converges.

The lambda iteration method is illustrated in Figure 2.3.

Linear programming method

Linear programming is a widely used optimization technique [5]. Linear programming seeks to find x^* to optimize a linear objective function $f(x)$ while meeting a set of linear equality and inequality constraints,

$$\min_x f(x) = \min_x \sum_g c^T x \tag{2.5}$$

subject to

$$Ax \leq b \tag{2.6}$$

$$A_{eq}x = b_{eq}. \tag{2.7}$$

where

c	The coefficients of the cost function of generator g
x	The vector generated power levels
A	Coefficient matrix (m *x* n) of inequality constraints
A_{eq}	Coefficient matrix (k *x* n) of equality constraints
b	Vector (m *x 1*) of inequality right-hand side constraints
b_{eq}	Vector (k *x 1*) of equality right-hand side constraints.

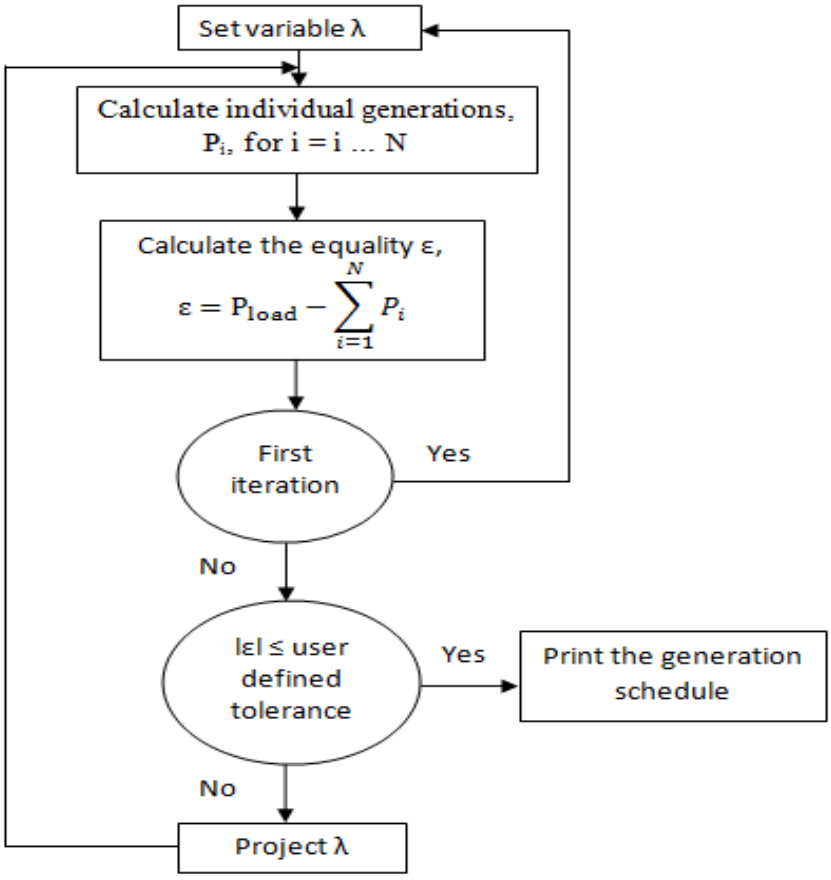

Figure 2.3 Pictorial of the lambda-iteration method

There can also be specified upper and lower limits, that is,

$$x_i^{min} \leq x_i \leq x_i^{max} \tag{2.8}$$

Eqs. (2.5)- (2.8) are then used in an iterative technique to obtain the optimal solution, thus it is called the Successive Linear Programming (SLP) method [43]. The solution procedures of SLP for economic dispatch are summarized in steps 1-7:

Step 1- Select the set of initial control variables.

Step 2- Solve the power flow problem to obtain a feasible solution that satisfies the power balance equality constraint.

Step 3- Linearize the objective function and inequality constraints around the power flow solution and formulate the LP problem.

Step 4- Solve the LP problem and obtain the optimal incremental control variables $\Delta P_{Gi.}$

Step 5- Update the control variables $P_{Gi}^{(k+1)} = P_{Gi}^{k} + P_{Gi}$.

Step 6- Obtain the power flow solutions with updated control variables.

Step 7- Check the convergence. If ΔP_{Gi}, in step 4, are below the user defined tolerance, the solution converges. Otherwise go back to step 3.

Dynamic programming method

From Bellman [48], the basic idea of the theory of dynamic programming is that of viewing an optimal policy as a policy determining the decision required at each time in terms of the present states of the system. Bellman defines the *principle of optimality* as the optimal policy having the property that whatever the initial state and initial decisions are, the remaining decisions must constitute an optimal policy with regard to the state resulting from the first decisions. The theory was designed to help solve mathematical problems

arising from the study of various multi-stage decision processes. Dynamic programming is used to determine the decision in a system at a certain state that will result in the best outcome in later states. The previous outcomes are used to guide the choice of future decisions, with the objective of extremizing a given function.

One could set up a dynamic programming algorithm to run backward in time starting from the final hour to be studied back to the initial hour [5]. Conversely, the algorithm could also be set to run forward in time from the initial hour to the final hour. One of the reasons for using the forward method is initial conditions are easily specified and the computations can go forward in time.

Mixed integer programming

A mixed integer program is a special case of a linear program in which some of the decision variables are constrained to take only integer values [49]. Given matrices A_{eq}, A, and vectors c^T, b_{eq}, and b, the general form of a MIP problem is:

$$\min_x f(x) = c^T x \tag{2.9}$$

subject to

$$Ax \leq b \tag{2.10}$$

$$A_{eq}x = b_{eq} \tag{2.11}$$

$$l \leq x \leq u \tag{2.12}$$

$$x_j \text{ integer} \tag{2.13}$$

where

c The coefficients of the cost function of generator g

x The vector generated power levels

A	Coefficient matrix (m x n) of inequality constraints
A_{eq}	Coefficient matrix (k x n) of equality constraints
b	Vector (m x 1) of inequality right-hand side constraints
b_{eq}	Vector (k x 1) of equality right-hand side constraints
l	Vector of lower bound variables
u	Vector of upper bound variables
x_j	Variables that must be integers.

The problem is inherently non-convex. It also is in the class of a *NP-complete* problem [50, 51]. This means that there is no algorithm that can guarantee solving any MIP problem in a time that is a polynomial function of the problem size, i.e., the number of decision variables and constraints (n, k, m shown above). However, with good software and modeling, many useful MIP problems can be solved quickly enough to be of practical use, even though the worst case guaranteed solution time is far longer.

The branch-and-bond algorithm is the most popular choice for solving MIP problems [52]. The great advantage of the branch-and-bound method is that, when it terminates, the solution is known to be globally optimal. This is the great benefit of the MIP approach: it can achieve globally optimal solutions for non-convex problems. The branch-and-bound algorithm begins by solving a relaxed form of the problem, replacing integrality constraints with simple bounds, and then "branching" on a chosen variable. The variable is fixed at various integer settings, each generating a new relaxed sub-problem and a better bound on the optimal solution. This procedure continues searching a "tree" with different integer settings for each branch. If the result of a relaxed sub-problem satisfies the integrality constraints, that branch does not need to be searched any further, and its

solution is a feasible solution to the original MIP. If the solution to a relaxed sub-problem is not integral, but has a cost worse than the best MIP solution found already, that branch can be terminated as further branching will only increase the cost. The search ends when all branches have been terminated. A small example of the branch and bound method is shown in Figure 2.4.

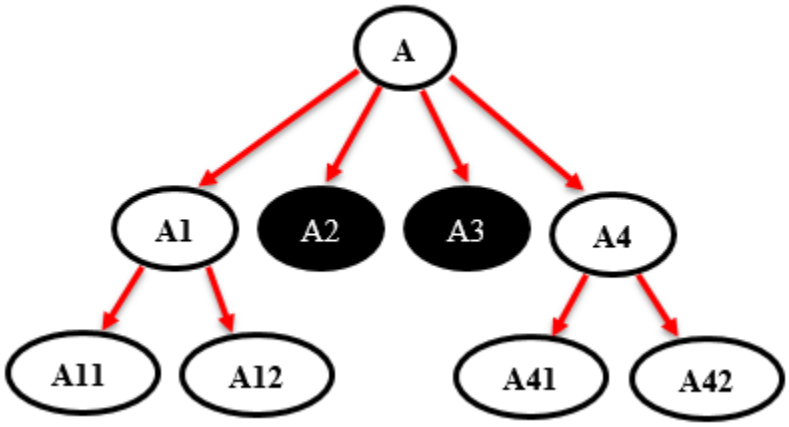

Figure 2.4 Example of the branch and bound method

The branch and bound method example shown above shows a case where the original set A is branched off into four subsets: A1, A2, A3, and A4. These subsets are all different integer relaxations of A. The subsets blacked out, A2 and A3, do not contain a feasible solution, and thus the branch is terminated. SubsetsA1 and A4 contain a feasible solution and are branched off into additional subsets. The method continues until all branches are terminated.

Quadratic programming method

A quadratic programming method contains a quadratic objective rather than the linear objective function as seen in the linear programming formulation [43]. However, both QP and LP have linear constraints. This method is usually ideal for power system

optimization because the generator cost function is often modeled in a quadratic form. A description of how quadratic programming is implemented appears in Appendix B. Quadratic programming is shown in Section 2.3 where it is used in the formulation of the optimization of the bulk energy storage problem.

This thesis uses the quadratic programming method in order to solve the economic dispatch problem. The objective function is assumed quadratic, and thus, the quadratic method is the determined as the best option. The formulation of the problem that will be used throughout this thesis is explained in the Section 2.4.

2.3 AI based optimization methods

A number of AI approaches to the economic dispatch problem have been proposed. These methods often use little mathematical information from the problem, but patterns and intelligent observations are used to obtain a solution. These methods have an advantage that the objective function $f(x)$ might be very nonlinear. Only one example is shown from the plethora of papers on these AI based methods (e.g., [53]-[59]).

Particle swarm optimization

Particle swarm optimization is a technique used to explore the search space of a given problem to find the settings or parameters required to maximize a particular objective function [60]. This technique, described by Kennedy and Eberhart in 1995 [61, 62], originates from two separate concepts: the idea of swarm intelligence based on the observation of swarming habits of certain kinds of animals, and the field of evolutionary computation.

The PSO algorithm works by retaining many possible solutions in a specified search space. During every iteration of the algorithm, each solution is assessed by the

objective function, determining the "fitness" of the solution [60]. Each possible solution can be thought of as a particle searching through the fitness landscape finding the maximum or minimum of the objective function. The PSO algorithm uses the objective function to the possible solutions, and operates upon the subsequent fitness values.

The PSO algorithm consists of three steps, which are repeated until some stopping condition is met [63]:

1. Evaluate the fitness of each particle
2. Update individual and global best fitness and positions
3. Update velocity and position of each particle.

This method uses very little mathematical information to solve a given problem and relies more on patterns and observations. It is useful in the fact that the PSO algorithm can solve very non-linear functions. However, the economic dispatch problem usually assumes a quadratic objective function and other methods with a better mathematical approach may serve as a better option.

2.4 Formulation of the bulk energy storage problem

In order to perform an accurate economic dispatch of the system being modeled, a simple linear program cannot be used. Generally, the input-output characteristic (cost curve) of a generating unit is non-linear. The cost curve of a generator is often expressed as a quadratic function,

$$F(P_i) = (A + BP_i + C * {P_i}^2)F_C + V_{OM}{P_i}^2 \tag{2.14}$$

where *A*, *B*, and *C* are the coefficients of the input-output characteristic of generator operating at a power level of P_i [64]. The variable F_C is the fuel cost in *$/MBTU* and V_{OM} represents the variable operation and maintenance costs in *$/MWh*. The coefficients depend

on the type of generator and the constant A is equivalent to the fuel consumption of the generating unit operation at $P_i = 0$, or the no-load cost. Table 2.1 displays the cost coefficients for the different types of generators [64].

Table 2.1 Cost coefficients for different types of generators

Generator Type	A	B	C	Fuel Cost ($/MBTU)	VO&M ($/MWh)
Coal Fired	0	20.000	0.01	0.761	0.22
Nuclear	0	20.000	0.01	0.72	1.28
NG (GT)	0	12.170	0.01	1.078	0.419
NG (ST)	0	11.270	0.01	1.15	0.225
NG (CT/CA)	0	12.193	0.01	1.091	0.149
Hydro	0	10.000	0	1.77	2.28

In Table 2.1, the following notation for the different generators is used:

GT Gas Turbine

ST Steam Turbine

CT Combined Cycle Combustion Turbine Part

CA Combined Cycle Steam Part

The values from Table 2.1 can be simplified to a more commonly used quadratic formula, that is,

$$F(P_i) = aP_i^2 + bP_i + c \tag{2.15}$$

where the constants *a*, *b*, and *c* include the constants F_C and V_{OM} shown in Table 2.1. Table 2.2 presents the cost coefficients for the different types of generators using the simplified cost curve shown in (2.15).

Table 2.2 Simplified cost curve coefficients by generator type

Gen. Type	Linear Cost \$/MWh	Quadratic Cost \$/(MW)^{2}h
Coal	15.44	0.00761
Nuclear	15.68	0.0072
NG(GT)	13.54	0.01078
NG(ST)	13.19	0.0115
NG(CT/CA)	13.45	0.01091
Hydro	19.98	0

For purposes of this work, MATLAB is used to run an economic dispatch of the system being modeled. To implement the non-linear cost curve of the generators, the function *quadprog* is used. *Quadprog* is an in-line MATLAB function that works similar to linear programming but allows for the minimization of a quadratic objective function rather than a linear function. The method used in *quadprog* is basically the Kuhn-Tucker-Karush method [5]. The method is gradient based, and involves the numerical solution of an expression that is the derivative of a lagrangian equal to zero. The primal of the function *quadprog* is in the form,

$$\min_X f(X) = \min_X \sum_g C_g^T X + \frac{1}{2} X^T Q_g X \tag{2.16}$$

subject to

$$AX \leq b \tag{2.17}$$

$$A_{eq} X = b_{eq}. \tag{2.18}$$

The matrix A_{eq} and vector b_{eq} model the *equalities,*

$$\sum_{\forall k(n,.)} P_k - \sum_{\forall k(.,n)} P_k + \sum_{\forall g} P_{g,n} + \sum_{\forall s} P_{s,n} = \sum_{\forall l} P_{l,n} \; \forall n, \tag{2.19}$$

$$P_k - B_k(\delta_n - \delta_m) = 0 \quad \forall k, \tag{2.20}$$

$$\sum_{\forall i} P_{s,i} = 0 \quad \forall s. \tag{2.21}$$

The matrix *A* and vector *b* model the *inequalities*,

$$-P_{k,max} \leq P_k \leq P_{k,max} \quad \forall k, \tag{2.22}$$

$$P_{g,min} \leq P_g \leq P_{g,max}; \quad \forall g, \tag{2.23}$$

$$P_{s,min} \leq P_s \leq P_{s,max} \quad \forall s, \tag{2.24}$$

$$0 \leq E_s \leq E_{s,max} \quad \forall s, \tag{2.25}$$

$$-R_g \leq \frac{P_{g,i} - P_{g,i-1}}{\Delta T} \leq R_g \qquad \forall g; \; \forall i \tag{2.26}$$

where the following notation is used:

B_k	Susceptance of transmission element *k*
C_g	The linear coefficient, *b*, of the cost function of generator *g*
E_s	The energy stored in storage unit *s* in MWh
$E_{s,max}$	Maximum energy capacity of storage unit *s* in MWh
f	The objective function, operating cost
i	Interval number
k(. ,n)	Set of transmission assets with *n* as the 'FROM' node
k(n, .)	Set of transmission assets with *n* as the 'TO' node
m,n	Bus number (nodes)
P_g	The real power output of generator *g* in MW

$P_{g,max}$ Maximum power capacity of generator g in MW

$P_{g,min}$ Minimum power capacity of generator g in MW

P_k The power flow of transmission line k in MW

$P_{k,max}$ Maximum line flow rating of transmission element k in MW (usually $P_{k,max} = -P_{k,max)}$

P_l The active power of load l in MW

P_s The real power output of storage unit s in MW

$P_{s,max}$ Maximum power capacity of storage unit s in MW

$P_{s,min}$ Minimum power capacity of storage unit s in MW

Q_g The quadratic coefficient, a, of the cost function of generator g

R_g Ramp rate limit of generator g in $\frac{MW}{hr}$

δ_k Bus voltage phase angle at node n or m

Δt Length of interval i in hrs.

The vector X includes the bus voltage phase angles (δ), line flows (P_k), generator outputs (P_g), and storage outputs (P_s) for each interval i. Note that most studies entail multiple time intervals (e.g., i = 1, 2, …, 24 for a one day study with each interval having a time span of Δt). Most of the quantities listed above need to be specified for each individual time interval, and therefore the notation indicated might also be written with an additional subscript, namely i. The equality constraints in matrix A_{eq} and vector b_{eq} include the conservation of power at each bus (2.19), the power flow across each line (2.20), and the charge/discharge of the storage elements (2.21). The inequality constraints in matrix A and vector b include the line flow limits (2.22), generator output limits (2.23), charging power

storage limits (2.24), charging energy storage limits (2.25), and the generator ramp rate limits (2.26).

Solving (2.19)-(2.26) gives the optimal $X = X^*$, and also the optimal system wide operating cost $f(X) = f^*$.The operating cost then can be compared using two different models: one including storage and another without storage to evaluate the effectiveness of storage in operating cost reduction. The program is used with a model of the Arizona power grid to demonstrate the benefits of storage.

CHAPTER 3

EXAMPLE USING THE STATE OF ARIZONA AS A TEST BED

3.1 Description of the test bed: State of Arizona

This chapter focuses on the presence of bulk energy storage and minimization of operating cost, subject to constraints, of a large test bed system. The test bed selected is essentially the state of Arizona. In this chapter, the effect of energy storage on the minimization of the objective function described in Section 2.3 is studied using the state of Arizona as a test bed. The Arizona electrical power system is part of the Western Electricity Coordinating Council (WECC). Using the present topology, generation and transmission limits, and the 2010 heavy summer load case, energy storage is added to appropriate buses in the system and operating results are evaluated. The test bed used for this purpose is an *equivalent* system, including 115 kV transmission and higher transmission voltages.

Using the system briefly described above, the objective function, or system wide operating cost*($/day*), is minimized while the constraints and formulation of the problem is the same as described in Chapter 2. Figure 3.1 is a pictorial of the basic concept.

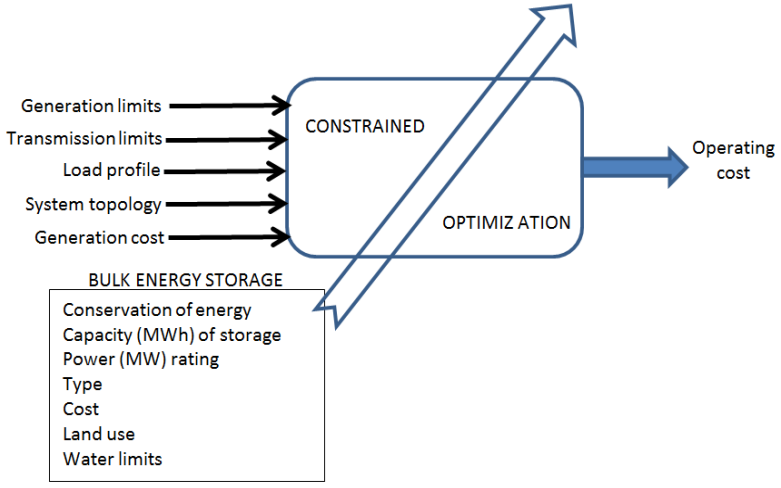

Figure 3.1 Pictorial of the concept of bulk energy storage

The quadratic programming algorithm explained in Section 2.3 is used to optimize generation while meeting the load demand at each interval and to schedule energy storage appropriately. The generation, line flow, and energy storage (charge/discharge) schedule are control variables along with the bus voltage angles. These values are calculated and the generation outputs are used to determine the system wide operating costs.

The system load is the 2010 summer peak, heavy load case. To approximate the time variation of the load in a day, the system wide load of 13,627 MW is multiplied by the function $0.45cos\left(\frac{\pi t}{12}+0.5\pi\right)+0.55$ using eight intervals of three hours each to replicate the common load profile in a 24 hour day, where *t* is the time at the beginning of each interval (e.g.,*t=0,3,6,…,21*). This can be seen in Figure 3.2. The objective of the modeled system is to economically dispatch the available generation while optimally charging/ discharging the energy storage.

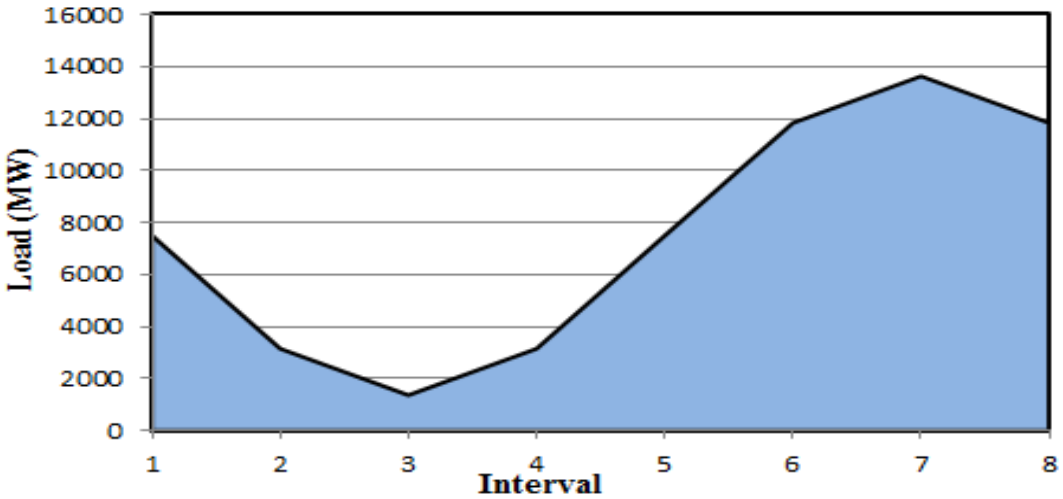

Figure 3.2 Arizona 2010 summer peak load modeled over a day
(typical, assumed values shown)

The following assumptions are made for the described test bed:

- Transmission line losses are not included in the system

- Reactive power flows are neglected
- Bus voltages are all assumed 1 per unit (*p.u.*)
- The DC load flow study approximation is used, namely the linearization of the sine function near the assumed operating point, e.g., $sin\ (\theta) \approx \theta$ [5].

The Arizona system under study has the profile shown in Table 3.1.

Table 3.1 State of Arizona system profile*

Number of buses	Number of transmission lines	Number of generators	Number of time intervals, *i*	Duration of time interval, hours
206	277	26	8	3

*This is an equivalent of the Arizona transmission system

The quadratic programming algorithm determines the total constrained optimum operating cost of the system. The cost is then multiplied by 365 to show the yearly system wide operating cost assuming the load modeled is the average over the year.

3.2 Description of test cases

The Arizona transmission system described in Section 3.1 is tested using three different cases. The first case tested is without any energy storage added to the system. This case is analyzed to determine a system wide operating cost that can be used for comparisons with the second two cases when bulk energy storage is added to the test bed.

The two cases that include bulk energy storage look at locations in Arizona where pumped hydro energy storage can be added. PHES is chosen as the technology to be simulated because it is currently the most mature form of bulk energy storage and the most feasible for very high levels of energy capacity. The locations chosen to place PHES are near existing hydroelectric dams in Arizona including: Hoover (Boulder) Dam, Glen

Canyon Dam, and Horse Mesa Dam. These locations do not currently exist and are used purely for simulation purposes. PHES is placed near existing dams because of the high amount of water in the area and the large elevation differences. Figure 3.3 shows the locations of the simulated pumped hydro energy storage added to the system.

Figure 3.3 Locations of simulated pumped hydro energy storage

Various information about the three PHES locations is shown in Tables 3.2 and 3.3. Some of the numbers, including the lower and upper reservoir volume and area, is approximated using actual Arizona PHES locations issued to FERC for approval. These locations are discussed in Chapter 4.

Table 3.2 Simulated PHES location information and operating entity

	Location	County	Nearby bus	Year of development	Water source	Operating Entity	*Power limit (MW)
★	Lake Mead	Mohave	Mead N/S	N/A	Lake Mead	WAPA[$]	2080
■	Glen Canyon	Coconino	Glen Canyon N/S	N/A	Colorado River	WAPA[$]	1296
●	Horse Mesa	Maricopa	Horse Mesa	N/A	Salt River	SRP[+]	130

[$]Western Area Power Administration, [+]Salt River Project

Table 3.3 Simulated PHES reservoir numbers

	*Lower reservoir volume (acre-ft.)	*Lower reservoir surface area (acres)	*Lower reservoir average depth (ft.)	*Upper reservoir volume (acre-ft.)	*Upper reservoir surface area (acres)	*Upper reservoir average depth (ft.)
★	25,323	265	95.6	24,624	289	85.2
■	15,778	165	95.6	15,343	180	85.2
●	1,583	17	93.1	1,539	18	85.5

*Approximations based on actual Arizona PHES locations issued to FERC

3.3 Base case for the state of Arizona

The original topology described in Section 3.1 is studied first without energy storage and is considered the base case. The economic dispatch of the generators is determined by solving the quadratic programming algorithm in MATLAB. Again, in order for the constraints listed earlier to comply, active power losses and reactive power are neglected. These constraints include:

- Generation output and ramp rate limits
- Transmission line power flow limits
- Storage power and energy charging limits.

The cost of economic dispatch of generation per day is calculated to be $3.544 million and $1.294 billion per year. As expected, the total generation output matches the total system load at each interval shown in Figure 3.2. The yearly system wide operating cost from the base case will be used for comparison with tests that include bulk energy storage.

3.4 Pumped hydro energy storage added to various buses

The system described in Section 3.1 is used again however four different cases are studied implementing possible locations in Arizona for pumped hydro energy storage. For each case included in this study, pumped storage is added to Horse Mesa Dam (bus 83) at a maximum storage of 130 MW, similar to the capacity of the existing dam. This bus is chosen to be used in combination with one of each of the four largest scale pumped hydro locations as it gives the best results (i.e. minimum system wide operating costs) when used in a two bus example.

Case 3.1: Pumped hydro energy storage added to Lake Mead S. bus

One possible location for a large scale pumped hydro energy storage is near Hoover (Boulder) Dam located in the Black Canyon of the Colorado River, on the border between the US states of Arizona and Nevada. Hoover Dam has a nameplate capacity of 2080 MW, so this is assumed the maximum value of the pumped hydro placed at this location. There are two buses located near Hoover Dam, one on both the north and south end of the river. This case will test the scenario where pumped hydro is added to the south bus. Again, pumped hydro is also placed at Horse Mesa Dam with a capacity of 130 MW.

Using the program created in MATLAB shown in Appendix A, storage is added to the Lake Mead S. Bus (Bus 149) and studied. The pumped storage is set to have three different values of energy / power (E/P) ratios: 2, 5, and 10. The ratio describes the size of the upper reservoir, or how much water can be stored. For a higher ratio, the reservoir can store more water thus it has a higher energy (MWh) rating. The E/P ratio determines how long the pumped hydro energy storage can provide rated power (assuming the water is already stored in the upper reservoir). Table 3.4 provides some existing PHES in the United States and their E/P ratios [65.]. A range of 4-12 hours at rated power is shown in Table 3.4 with an average of around 8 hours. Table 3.5 shows the three different cases that are studied at the Lake Mead S. bus.

Each E/P scenario shown in Table 3.5 is studied at different levels of storage ranging from a power level of 600-2080 MW. This test shows how increasing the storage power limit effects the system wide operating cost as well as how various system limits are effected such as generation or line limits. The results are plotted together along with the base case yearly value of $1.294 billion. The results can be seen in Figure 3.4.

Table 3.4 Power and energy ratings of selected PHES in the U.S.

Pumped hydro storage name	Power (MW)	Energy (MWh)	E/P ratio	Location
Bath County	3003	30030	10	Virginia
Ludington	1872	14976	8	Michigan
Olivenhain-Hodges	40	320	8	California
Castaic	1427	14270	10	California
Mount Elbert	200	2400	12	Colorado
Bear Swamp	600	3600	6	Massachusetts
Yards Creek	400	2400	6	New Jersey
Taum Sauk	440	3520	8	Missouri
Cabin Creek	324	1296	4	Colorado

Table 3.5 Lake Mead S. bus pumped storage scenarios

Scenario	E/P ratio	Lake Mead S. bus charging power limit (MW)	Lake Mead S. bus charging energy limit (MWh)
1	2	2080	4160
2	5	2080	10400
3	10	2080	20800

From Figure 3.4, it can be seen that with energy storage added to Lake Mead S. bus, the system wide operating cost is lower than the base case cost for an E/P ratio of 5 or 10. The plot of the E/P = 2 scenario however is actually higher than the base case cost up until about 800 MW. This is because the small amount of storage available causes the system to hit more generation and line limits. Once the 800 MW of storage is reached, there is enough storage in the system and the operating cost decreases below the base case value. It can be seen from Figure 3.4 that as the E/P ratio increases, the operating cost decreases.

Also, when the energy storage power limit increases in each case, the operating cost decreases as expected. This occurs because the pumped hydro storage can "shave" more of the peak demand. An example of peak shaving from the simulations is shown in Figure 3.5 using an E/P ratio of 10 and storage charging power of 2080 MW, where the minimum operating cost occurs of $1.216 billion per year.

Another important calculation that can be made to determine the value of the energy storage is the payback period. The payback period compares the investment cost of the energy storage with the annual savings. The time period calculated illustrates how long it would take to recover the investment. Using the yearly operating cost savings and an estimate of the capital costs of pumped hydro storage, a payback period can be calculated using,

$$C = OC_{saved} Y \tag{3.1}$$

where C is the overall capital cost in dollars, OC_{saved} is the yearly operating cost savings in dollars, and Y is the payback period in years. To estimate the payback period for the storage used in at Lake Mead S. bus, two costs are used based on the nameplate power and energy ratings. The power related costs, in $/kW, include the various pumps and turbines while the energy related costs, in $/kWh, contain the reservoir costs. Table 3.6 shows a range of typical power and energy related costs for pumped hydro storage.

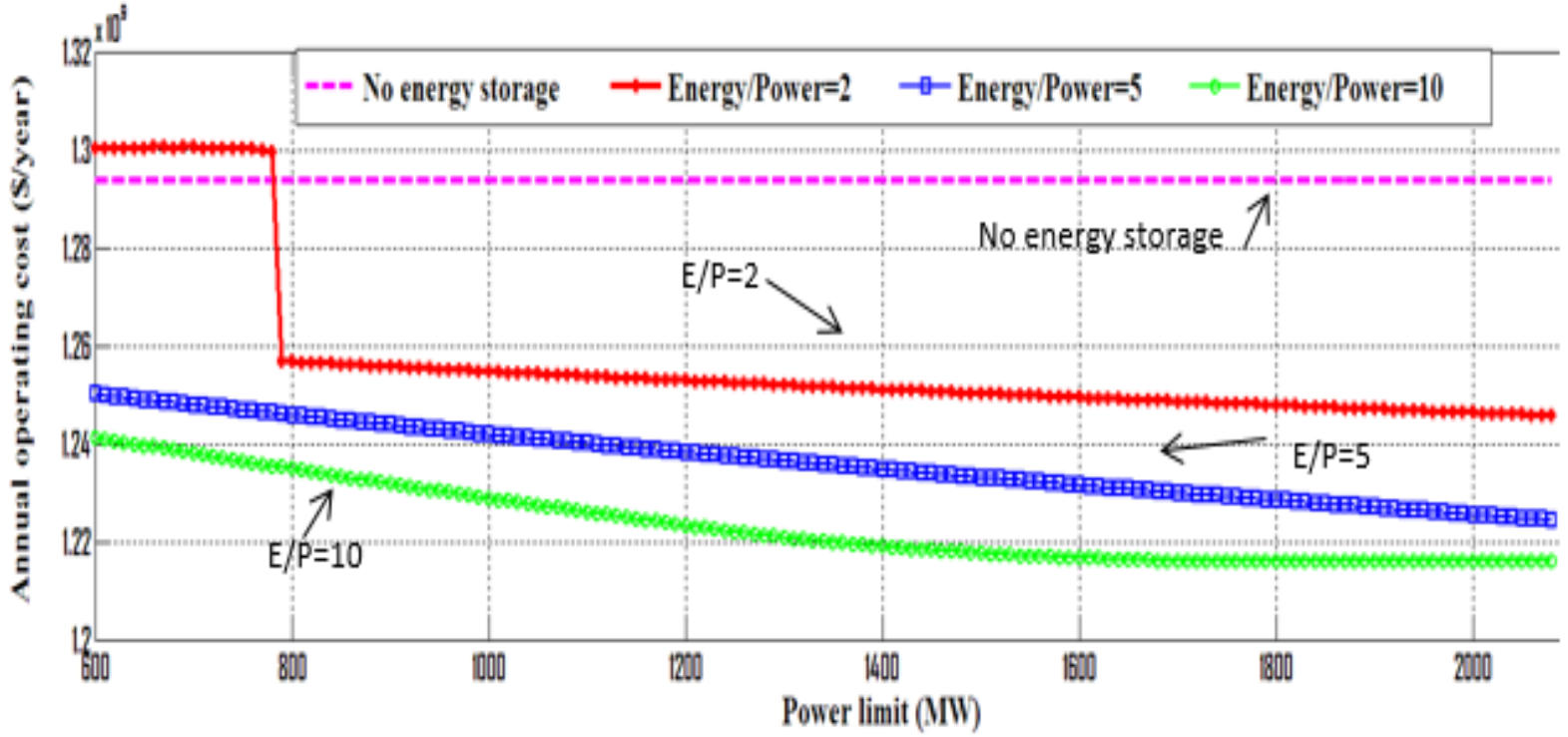

Figure 3.4 Case 3.1 system wide annual operating cost with storage at Lake Mead S. bus

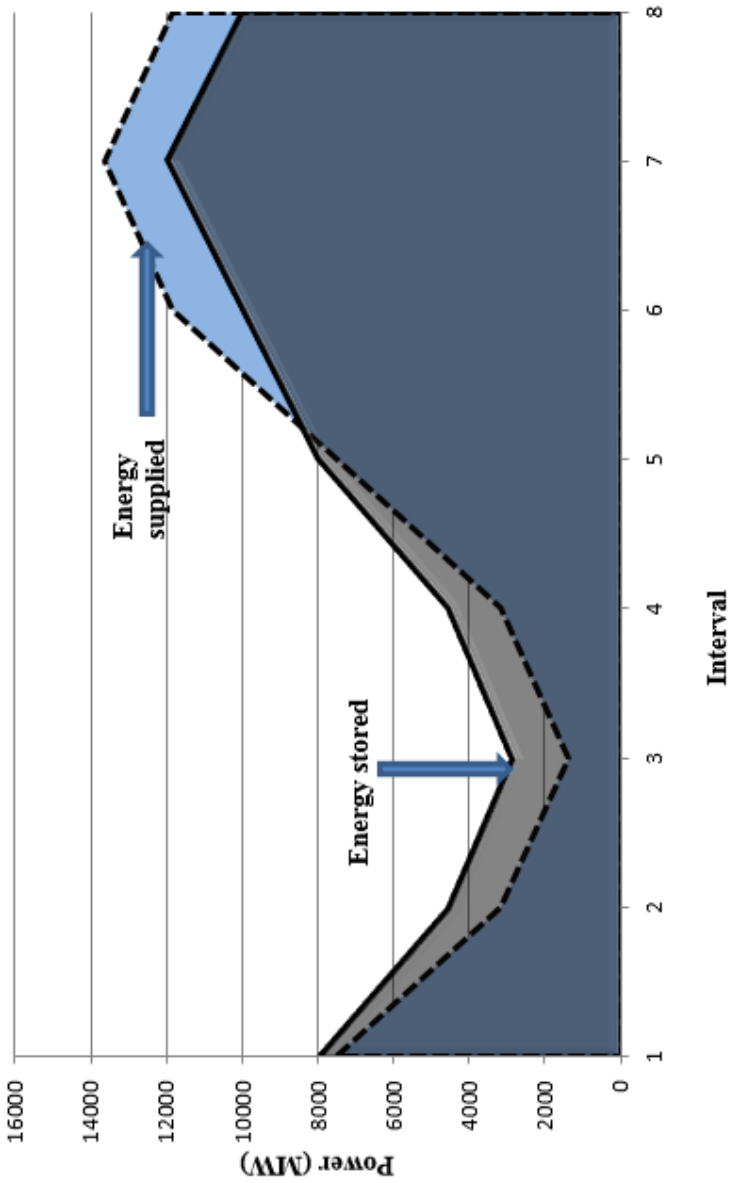

Figure 3.5 Example of peak shaving at Lake Mead S. bus

Table 3.6 Assumed pumped hydro storage power and energy related costs [18, 20]

	Minimum	*Maximum*
Power related costs ($/ kW)	500	2000
Energy related costs ($/kWh)	7	20

Using the values from Tables 3.5 and 3.6 and the operating costs shown in Figure 3.3, (3.1) is used to determine the payback period. The payback period for the three scenarios at each power level is shown in Figure 3.6.

Figure 3.6 shows that with added storage the payback period increases. This is due to the fact that a decrease in operating cost is less than the cost to add that amount of storage. However, with a higher E/P ratio, the capital costs increase but the annual operating cost decrease is greater allowing a lower payback period. The plot of E/P = 2 starts at about 800 MW because the operating cost is higher than the base case before that point, thus $OC_{saved} = 0$. In the range shown in Figure 3.5, a reasonable payback period is shown for the Lake Mead S. bus with a minimum value of 7.95 years when an E/P ratio of 10 is used and a maximum value of 23.69 years when an E/P ratio of 2 is used. With a typical lifetime of pumped hydro storage being 40 years, the range would give a practical length of time where the investment is already covered and the system is saving a significant amount of money.

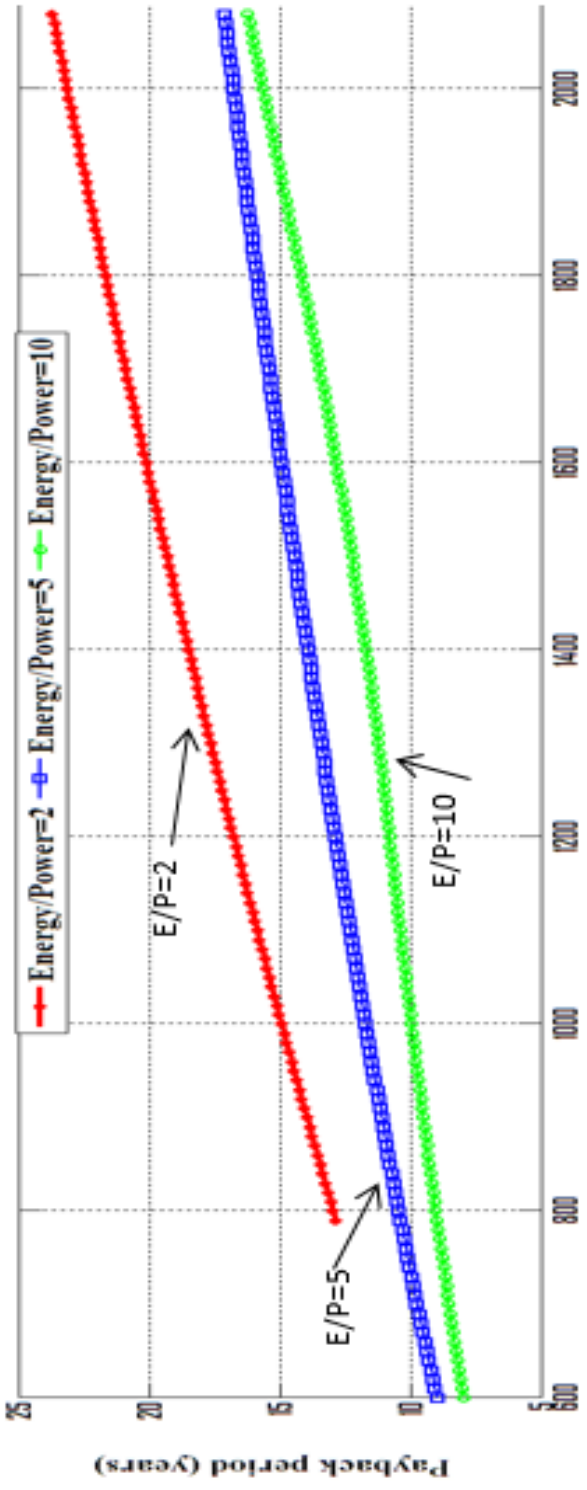

Figure 3.6 Case 3.1 payback periods for Lake Mead S. bus

Case 3.2: Pumped hydro energy storage added to Lake Mead N. bus

Similar to Case 3.1, pumped hydro energy storage is added near Hoover Dam but on the Lake Mead N. bus (bus 150). Comparable results are expected because of its close vicinity to the south bus. Once again, the pumped storage is set to have three different values of an E/P ratio: 2, 5, and 10. The three scenarios being tested are the same as what is shown in Table 3.5.

The three scenarios are again studied at different levels of storage ranging from a power level of 600-2080 MW. The variation in power allows the possibility to analyze the effect of more storage on operating cost, various system limits, and the payback discussed earlier. The results are again plotted together along with the base case yearly value of $1.294 billion. The plots for storage at Lake Mead N. bus can be seen in Figure 3.7.

The operating costs shown in Figure 3.7 display that energy storage added to Lake Mead N. bus also help decrease the system wide operating cost between power levels of 600 and 2080 MW for an E/P ratio of 5 and 10. Similar to Case 3.1 however, when the E/P ratio is 2, the operating cost is higher than the base case value up until around 800 MW. This is once again due to the small amount of storage available that causes more generation and line limits to be reached. Again, once around 800 MW of storage is added, there is enough storage in the system and the operating cost decreases below the base value. Figure 3.6 shows that both as the E/P ratio and the storage power limit increases at the Lake Mead N. bus, the operating cost decreases. This is again demonstrating how added storage is "shaving" more of the peak demand, as shown in Figure 3.5. The minimum operating cost for all three scenarios occurs between 1150 and 2080 MW where the system wide operating cost levels off at $1.2317 billion.

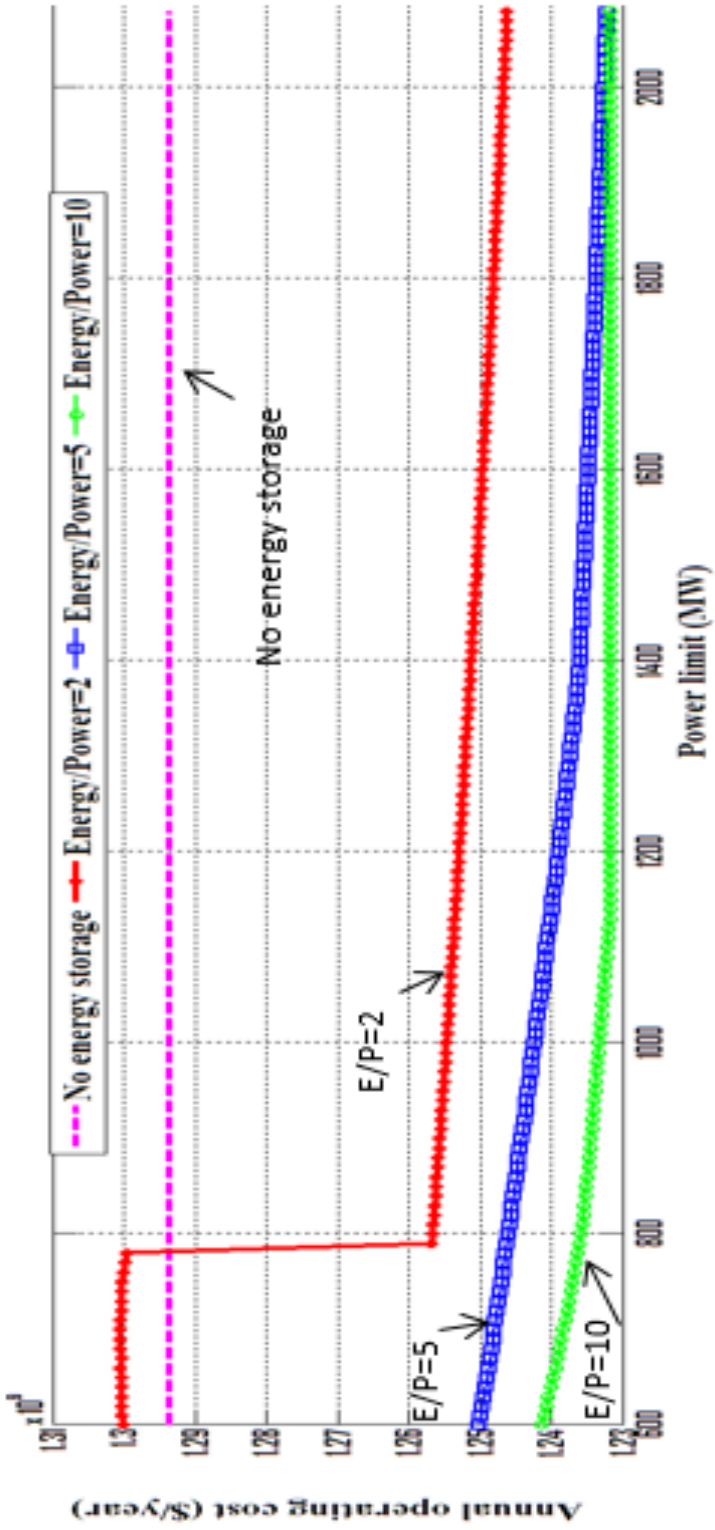

Figure 3.7 Case 3.2 system wide annual operating cost with storage at Lake Mead N. bus

The payback period is calculated for the Lake Mead N. bus using the operating costs from Figure 3.7 and the capital costs found from the numbers in Tables 3.5 and 3.6. These values along with (3.1) are used to determine the payback period for the three scenarios at each power level. The results are shown in Figure 3.8.

In Figure 3.8, the various payback periods show similar results as in Case 3.1. All three scenarios show a positive slope as the energy storage power limit is increased at the bus. This is again due to the decrease in operating cost being less than the cost to increase the power limit. However, in this case increasing the E/P ratio only decreases the payback period up until a certain power level once the ratio gets higher. As seen in Figure 3.8, the plots for E/P = 5, 10 intersect around 1600 MW and the plot of E/P=10 continues above the plot of E/P = 5. The plot of E/P=2 again starts around 800 MW because the operating cost is higher than the base case before that point, thus $OC_{saved} = 0$. The minimum payback period occurs at 600 MW when the E/P ratio is 10 at a value of 7.97 years, slightly above the minimum from Case 3.1. The longest payback period occurs at an E/P ratio of 2 when the power limit is raised to 2080 MW at a length of 23.92 years. This is once again a reasonable range compared to the typical 40 year lifetime of a pumped hydro energy storage plant.

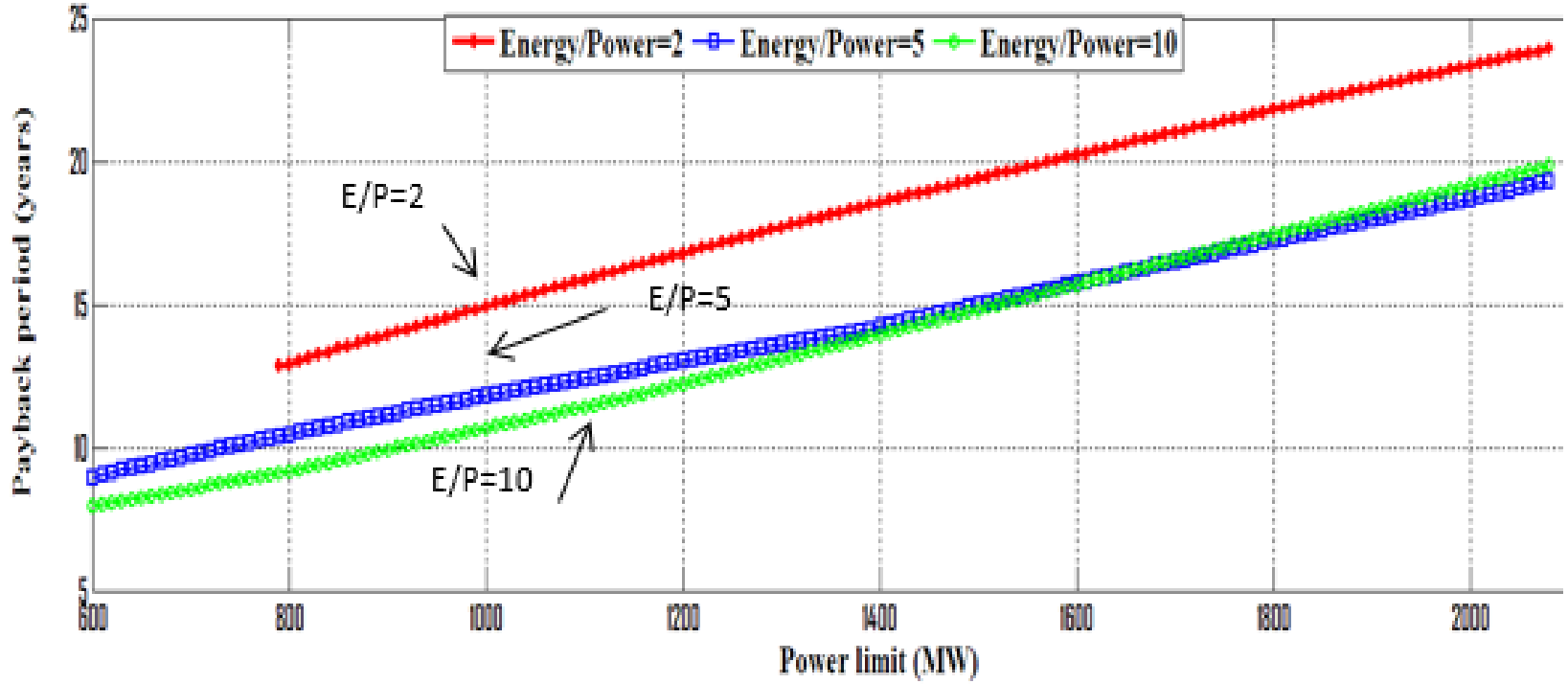

Figure 3.8 Case 3.2 payback periods for Lake Mead N. bus

Case 3.3: Pumped hydro energy storage added to Glen Canyon S. bus

Another possible location for a large scale pumped hydro energy storage plant is near Glen Canyon Dam, which is on the Colorado River near the town of Page, AZ, on the border of Arizona and Utah. Glen Canyon Dam has a nameplate capacity of 1296 MW, thus this is assumed the maximum value of the pumped hydro plant place at this location. There are two buses located near Glen Canyon Dam, one on both the north and south end of the river. Both buses will be tested but this case will test the scenario where pumped hydro is added to the south bus. Once again, pumped hydro is placed at Horse Mesa Dam with a capacity of 130 MW in both cases.

The program shown in Appendix A is used again but storage is this time added to the Glen Canyon S. bus (bus 187) and studied. The pumped storage is set to have three different values of E/P ratios: 2, 5 and 8. It was found this time that at an E/P ratio of 8 or greater, the operating cost remains constant over all power levels, or an increase in the ratio has no effect on the solution. Thus, a value of E/P = 8 is chose as the maximum E/P ratio. Table 3.7 shows the three different cases that are studied at the Glen Canyon S. bus.

Table 3.7 Glen Canyon S. bus pumped storage scenarios

Scenario	E/P ratio	Glen Canyon S. bus charging power limit (MW)	Glen Canyon S. bus charging energy limit (MWh)
1	2	1296	2592
2	5	1296	6480
3	8	1296	10368

Each E/P ratio scenario shown in Table 3.7 is studied over the energy storage power rating range of 500-1296 MW. The results are plotted together along with the base case yearly value of $1.294 billion. The results plotted together can be seen in Figure 3.9.

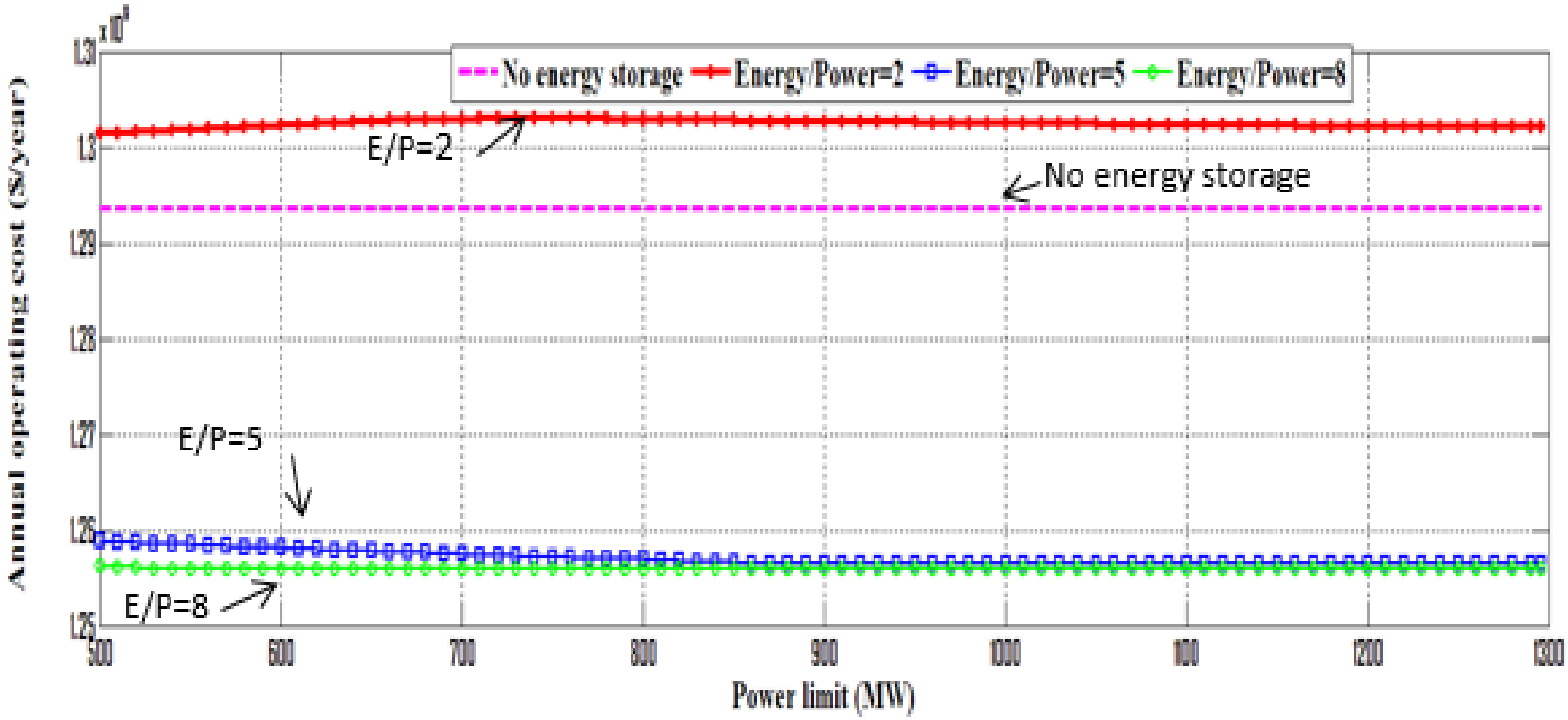

Figure 3.9 Case 3.3 system wide annual operating cost with storage at Glen Canyon S. bus

In Figure 3.9, for an E/P ratio of 5 and 8, the operating cost is lower than the base case. However, it seems that increasing the E/P ratio from 5 to 8 has little effect on the cost as the two plots begin to converge around 900 MW. It is evident that there is a limit on how much the E/P ratio can be increased before there is little to no effect on the system wide operating cost. In the case of the plot of E/P = 2, the limit on how much energy can be stored being so small causes the operating cost to always be higher than the base case. It seems there is never a sufficient amount of energy storage available and more generation and line limits are hit. It is apparent that at the Glen Canyon S. bus, the increase of the energy storage power limit or the E/P ratio has little effect on the operating cost after a certain point. The minimum operating cost for this case is $1.2559 billion which occurs for a ratio of E/P = 8 over the range of 550-1296 MW.

The payback periods are calculated for the Glen Canyon S. bus using the operating costs from Figure 3.8 and the capital costs using Tables 3.6 and 3.7. The values are inserted into (3.1) and the payback periods are calculated. The results can be seen in Figure 3.10. The payback periods for E/P = 5 and 8 are shown above in Figure 3.10. There is no plot for E/P = 2 because the operating cost is always greater than the base case, thus OC_{saved} = 0. The plots for E/P = 5 and 8 both display a positive slope, meaning the annual system wide operating cost savings is less than the added cost to increase the energy storage power limit. Also, the plot of E/P = 8 crosses and eventually increases above the plot of E/P = 5 around 700 MW. Around this point, the added cost of energy for E/P = 8 exceeds the operating cost savings and causes the payback period to increase above the E/P = 5 plot. This can be observed in Figure 3.10 where the plots converge.

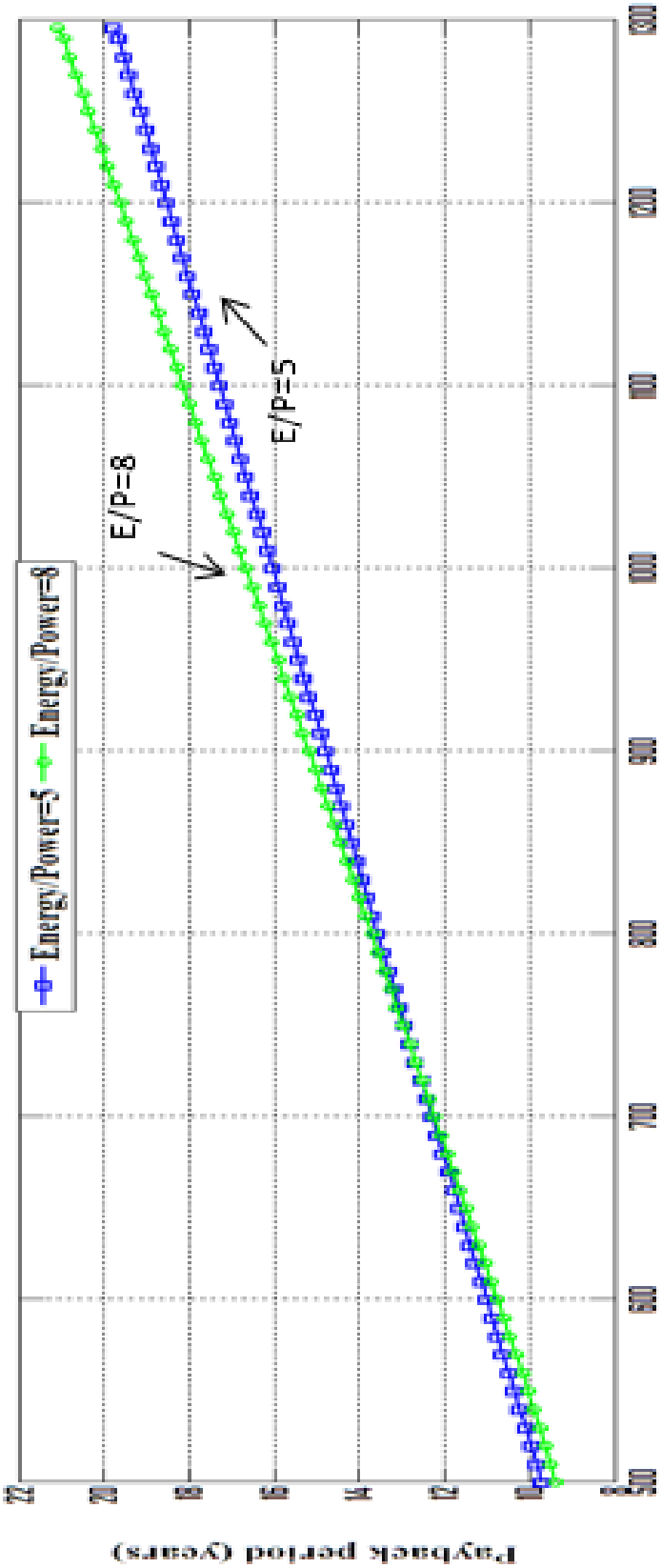

Figure 3.10 Case 3.3 payback periods for Glen Canyon S. bus

The operating costs for the two plots in Fig. 3.10 are roughly equal; however, the energy storage plant with E/P = 8 would cost more due to the higher energy rating. The minimum payback occurs at 500 MW at an E/P ratio of 8 for a length of 9.39 years, higher than the minimum values for both Cases 3.1 and 3.2. The longest payback period occurs for the same E/P ratio when the power limit reaches 1296 MW at a length of 21.09 years. This range is also reasonable when compared to the average lifetime of a pumped hydro energy storage plant.

Case 3.4: Pumped hydro energy storage added to Glen Canyon N. bus

Pumped hydro energy storage is also added to the north bus located near the Glen Canyon Dam to compare the results with Case 3.3. In this case, the energy storage is set to have three different E/P ratios: 2, 5, and 10. The Glen Canyon N. (bus 186) bus does not have a limit at an E/P of 8 or 10, thus 10 is used as the maximum value. The three scenarios being tested are shown in Table 3.8.

Table 3.8 Glen Canyon N. bus pumped storage scenarios

Scenario	E/P ratio	Glen Canyon N. bus charging power limit (MW)	Glen Canyon N. bus charging energy limit (MWh)
1	2	1296	2592
2	5	1296	6480
3	10	1296	12960

The three scenarios shown in Table 3.8 are again studied at different levels of energy storage power ratings ranging from 500-1296 MW. The results are then plotted together with the annual base case value of $1.2945 billion calculated earlier. The results for storage at the Glen Canyon N. bus can be seen in Figure 3.11.

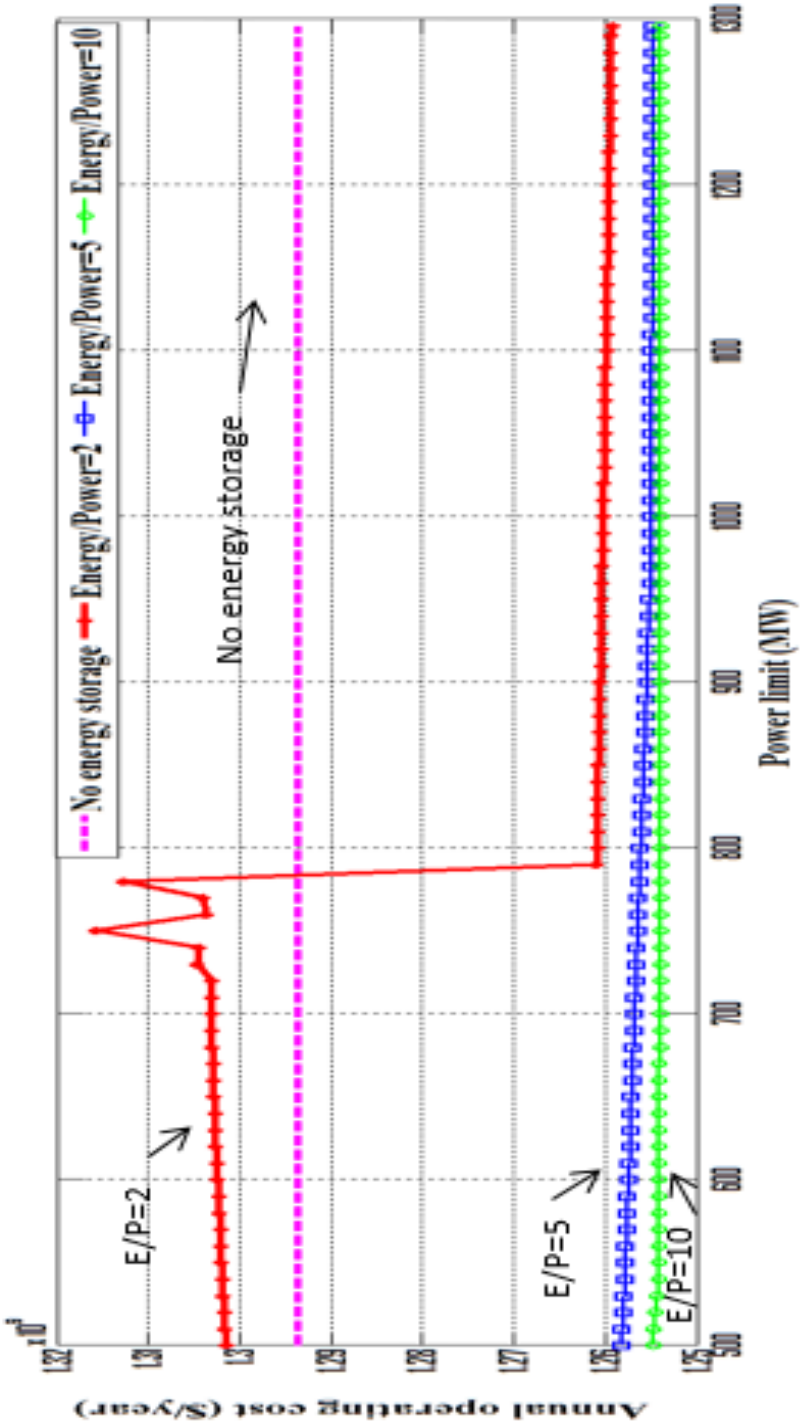

Figure 3.11 Case 3.4 system wide annual operating cost with storage at Glen Canyon N. bus

The operating costs shown in Figure 3.11 demonstrate a similar trend as previous cases. Other than the plot of E/P = 2, adding energy storage cause a decrease in system wide operating cost at all power levels. For the plot of E/P = 2, the results show a similar trend as in Cases 3.1 and 3.2 where the operating cost is higher than the base case value up until 790 MW. After this point, there is enough storage at the bus and the operating cost drops below the base case value. For this case, the operating cost seems to level out around one number for all three E/P ratios and the plots for E/P = 5 and 10 start to converge at higher power limits. It is also apparent that an increase in the E/P ratio to higher values has little effect on the operating cost as there is very little difference between the E/P = 5 and 10 plots even at lower power levels.

The payback periods are calculated for the Glen Canyon N. bus from Figure 3.10 and the capital costs using Tables 3.6 and 3.8. The values are inserted into (3.1) and the payback periods are calculated. The results can be seen in Figure 3.12.

The payback periods shown in Figure 3.12 all have a positive slope, meaning the operating cost savings is less than the cost to add the same amount of storage. For each E/P ratio, the slope is roughly the same which is about 0.0178 $\frac{yrs}{MW}$. For this case, the higher E/P ratio of 10 eventually intersects and increases above the payback period of E/P = 5. This occurs once again because the operating costs for both ratios eventually converge towards each other. With the added cost for an E/P ratio, the payback period is eventually higher around 750 MW.

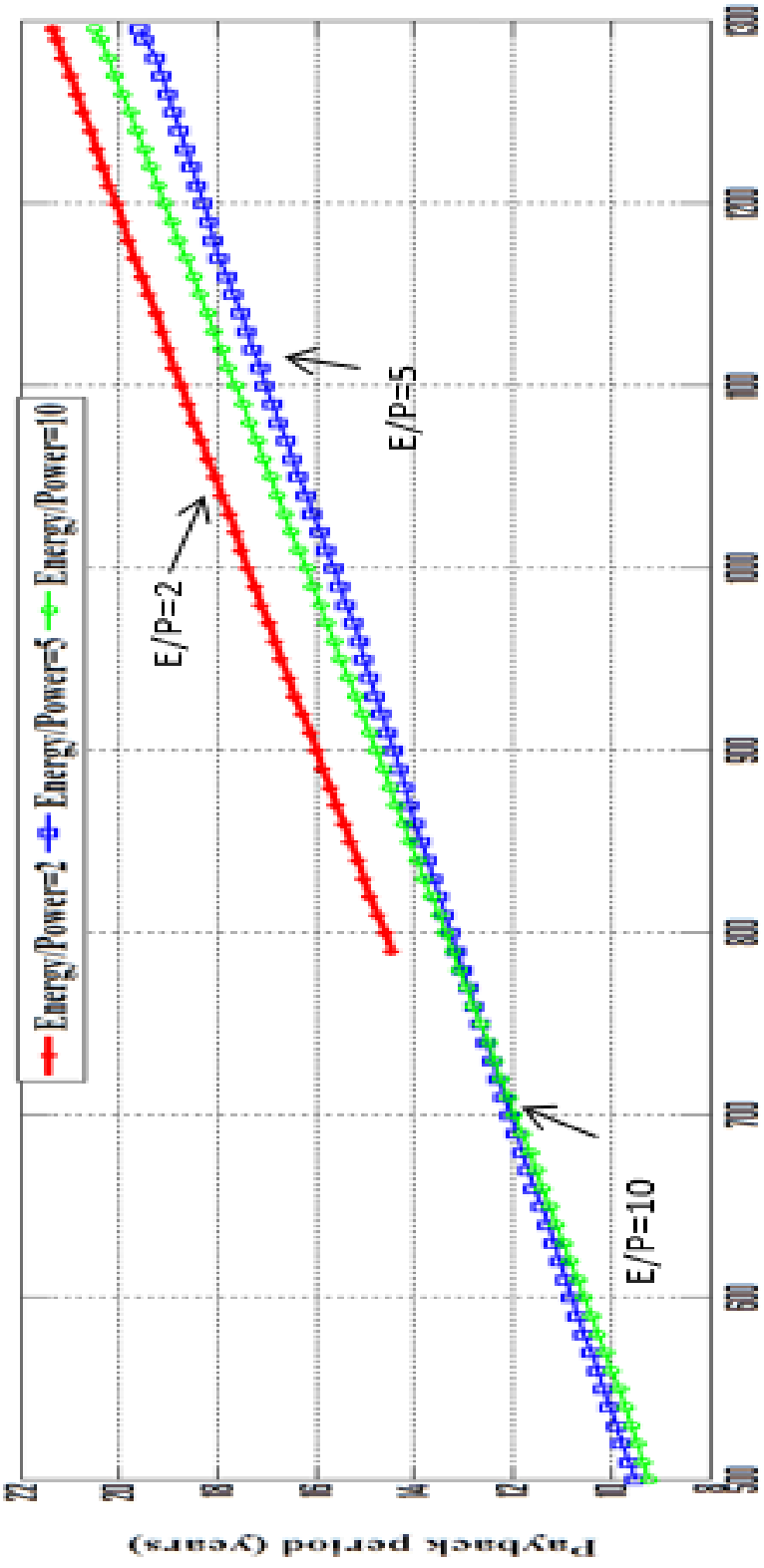

Figure 3.12 Case 3.4 payback periods for Glen Canyon N. bus

The lowest payback period for the Glen Canyon N. bus is 9.25 years, which is at an E/P ratio of 10 at 500 MW, slightly lower than Glen Canyon S. bus. The maximum payback period length occurs at the same E/P ratio at 1296 MW for a length of 20.5 years. This range is a reasonable length compared to the average 40 year lifetime of a pumped hydro energy storage plant.

3.5 Summary of results

The previous section showed through four cases that the use of bulk energy storage can lower the system wide generator operating cost. This is accomplished by the peak shaving application discussed in Chapter 1. A payback period calculation was also specified and used to calculate a range of payback periods for each case. Table 3.9 summarizes the results from the base case and cases 3.1-3.4 including the operating cost and payback period ranges. The table will show the ranges for the E/P ratio in each case with the best results.

Table 3.9 Summary of Arizona test bed case results with bulk energy storage

Case	Best E/P ratio	Minimum annual operating cost (billion-$/yr)	% decrease	Maximum annual operating cost (billion-$/yr)	% decrease	Minimum payback period (years)	Maximum payback period (years)
Base	0	1.294	N/A	1.294	N/A	N/A	N/A
3.1	10	1.216	6.03	1.2413	4.07	7.95	16.22
3.2	10	1.2317	4.81	1.2444	3.83	7.97	19.85
3.3	8	1.2559	2.94	1.2563	2.91	9.39	21.09
3.4	10	1.2538	3.11	1.2548	3.03	9.25	20.5

Table 3.9 shows that the best E/P ratio in all four cases is the maximum ratio tested, or between 8-10 hours at rated power. This length matches well when compared with the E/P ratios displayed in Table 3.4 of existing PHES in the United States. Also, a range of 3-6% annual operating cost savings was found when using high levels of energy storage in the Arizona test bed. This percentage of annual savings equates to between $37.8-78 million each year, depending on the location and size of the PHES. Note that the operating cost savings only includes the difference in the generator operating cost of the specified case and the base case. The operating cost savings does not include any capital costs including the power and energy costs specified earlier. Using the range of operating cost savings and (3.1), the payback period was found to be between 8-21 years. When compared to average lifetime of PHES, the payback period range seems feasible.

A common occurrence in all four cases is as both the E/P ratio and the power limit of the PHES increases, the operating cost decreases. However, there were a few scenarios where increasing either one had no effect on the operating cost. This could be caused by different limits in the system and is looked into with more detail in Chapter 5. Another observation related to the payback period is that in every case, the slope of the payback period versus the power limit is positive. A positive slope in this case means that the additional operating cost savings from increasing the PHES power limit is less than the added capital cost. However, in most cases the payback period did decrease as the E/P ratio increased.

CHAPTER 4

BULK ENERGY STORAGE AT VERY HIGH LEVELS OF PUMPED HYDRO IMPLEMENTATION

4.1 Description of high level test cases

The focus of this chapter is to analyze the effect of adding very high levels of bulk energy storage to the Arizona test bed described in Section 3.1. With a load ranging between 1.36-13.6 GW, the best case scenario for "shaving" the peak would be to completely flatten the load profile, which is known as load leveling. For 100 % load factor, it would be necessary to add bulk storage with a total simultaneous power limit of at least 6 GW.

Three cases are studied using bulk energy storage between power ratings of 5-6 GW. The locations chose to add PHES include the different combinations of the three simulated locations used in Chapter 3 as well as three additional PHES waiting approval from FERC. These locations include:

- Longview Pumped Storage located in Big Chino Valley, southeast of Seligman, AZ which would tie into the El-Dorado – Moenkopi 500 kV line [66].
- Table Mountain Pumped Storage located near the towns of Peach Springs and Kingman, AZ that would tie into the Mead – Phoenix 500 kV line [67].
- Eagle Mountain Pumped Storage located northeast of Palm Springs, CA which would tie into the Devers – Palo Verde 500 kV line [68].

Figure 4.1 shows the locations of the proposed pumped hydro energy storage added that will be analyzed using the Arizona test bed. Appendix C has a very brief discussion of environmental issues related to large scale pumped hydro at the sites listed.

Figure 4.1 Locations of pumped hydro energy storage proposed to FERC

Tables 4.1 and 4.2 provide information on the three proposed locations [66-68]. Some of this information includes reservoir volume and area as well as power limits and operating entities.

Table 4.1 Proposed PHES location information and operating entity

	Location	County	Nearby bus	Year of development	Water source	Operating entity	Power limit (MW)
▲	Longview	Yavapai AZ	Moenkopi	2012	Local ground water	Energy Storage Systems	2000
■	Table Mountain	Mohave AZ	Mead	2011	Colorado River	Table Mountain Hydro, Arizona	400
●	Eagle Mountain	Riverside CA	Palo Verde	2009	Chuckwalla ground water	Eagle Crest Energy	1300

Table 4.2 Proposed PHES location reservoir numbers

	Lower reservoir volume (acre-ft.)	Lower reservoir surface area (acres)	Lower reservoir average depth (ft.)	Upper reservoir volume (acre-ft.)	Upper reservoir surface area (acres)	Upper reservoir average depth (ft.)
▲	17,400	175	99.4	17,400	209	83.3
■	5,683	68	83.6	5,280	66	80
●	17,700	163	108.6	17,700	191	92.7

4.2 Case 4.1: Longview and Table Mountain pumped storage

The first case tested for very high levels of energy storage includes five locations in Arizona. The locations tested using the Arizona test bed described in Section 3.1 includes: Longview Pumped Storage, Horse Mesa Pumped Storage, Boulder Pumped Storage, Table Mountain Pumped Storage, and Glen Canyon Pumped Storage. Table 4.3 shows the locations, system bus numbers, and the power limit of each PHES.

Table 4.3 Case 4.1 PHES locations and power limit

Location of PHES	Bus number	Power capacity (MW)
Longview	3	2000
Horse Mesa	83	130
Boulder	149	2080
Table Mountain	153	400
Glen Canyon	186	1296
	Total	5906

Case 4.1 has a total power limit of 5.91 GW, which is very close to the maximum power limit of 6 GW to perform load leveling. This case is tested over a range of energy / power ratios to see the effect on operating cost, payback period, peak shaving, and the load factor. The program created in MATLAB shown in Appendix A is again used with the PHES in Table 4.2 added to their specified bus.

Case 4.1 operating cost and payback period evaluation

The first test run on Case 4.1 is to see how varying the E/P ratio between 1-10 hours for each PHES location and seeing its effect on the output. This test gives a good understanding as to how large the upper reservoir should be in order to get the lowest operating cost and payback period. The payback period is calculated using the operating cost savings found using the $1.294 billion value from the base case in Section 3.3, the

capital cost calculated for each location using the values in Table 3.6, and (3.1). The results are shown in Table 4.4 and plotted in Figures 4.2 and 4.3.

Table 4.4 Case 4.1 annual operating cost and payback period as E/P ratio increases

E/P ratio	Annual operating cost (billion $/ year)	Payback period (year)
1	1.2423	58.4
2	1.2247	44.1
3	1.2103	36.9
4	1.1994	33.1
5	1.1924	31.2
6	1.1886	30.5
7	1.1869	30.4
8	1.1861	30.6
9	1.1858	30.9
10	1.1858	31.2

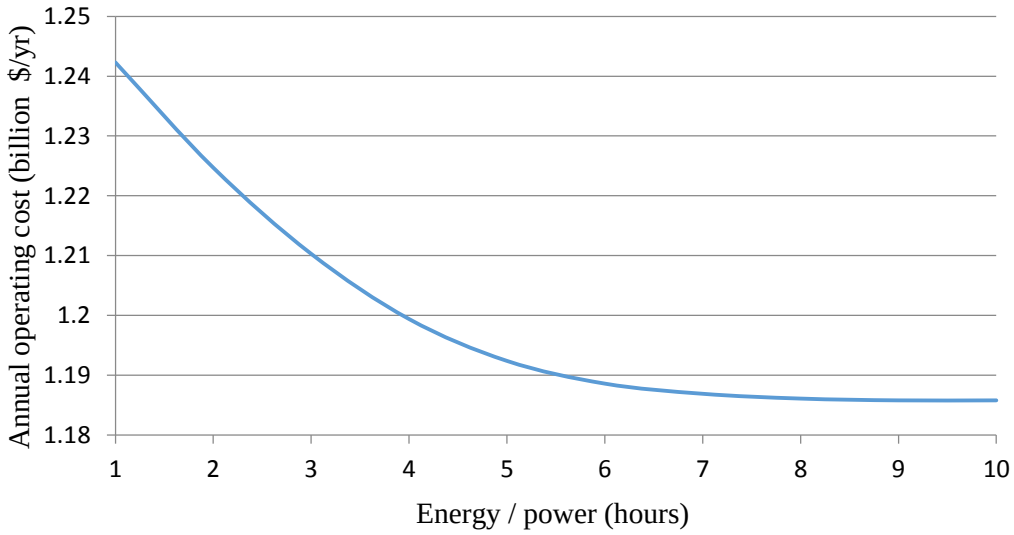

Figure 4.2 Case 4.1 annual operating cost as E/P ratio varies

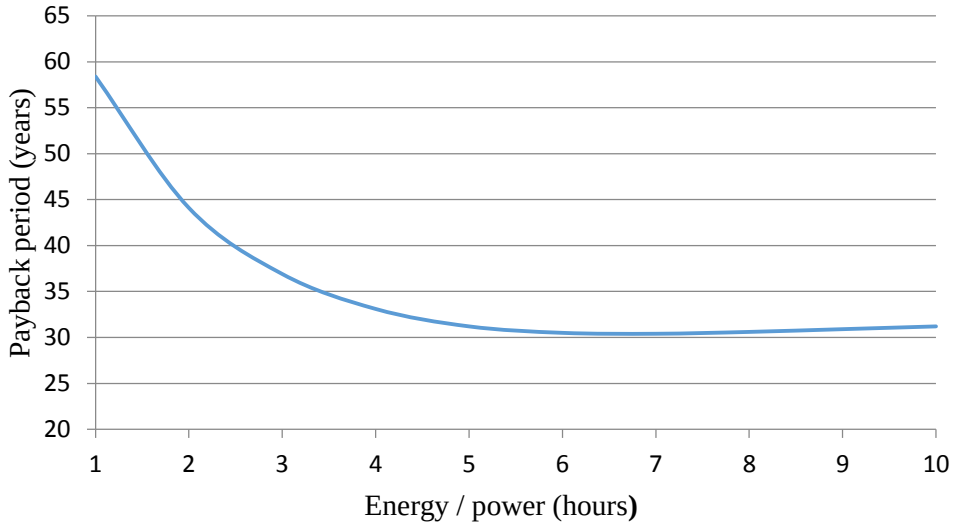

Figure 4.3 Case 4.1 payback period as the E/P ratio varies

Figures 4.2 and 4.3 show that as the E/P ratio increases, the operating cost and payback period both decrease and eventually level off to a constant value. However, if the E/P ratio was to continue to past 10 hours, the payback period would continue to slowly increase because the operating cost savings would remain constant but the power related capital costs would increase. For Case 4.1, the minimum operating cost was found to be $1.1858 billion at E/P ratios of 9 and 10 hours, or an annual operating cost savings of 8.4%. This percentage savings equates to roughly $108 million of annual generator operating cost savings. The minimum payback period occurs at an E/P ratio of 7 hours at a length of 30.4 years. The payback period begins to increase above 30.4 years because the operating cost savings to capital cost ratio begins to decrease.

Case 4.1 peak shaving evaluation

The next test used on Case 4.1 is how much energy is stored and recovered to "shave" the peak as the E/P ratio increases for each location. Based on the results from Section 4.2, the amount of the peak "shaved" should increase as the E/P ratio increases because the operating cost is decreasing. Figures 4.4-4.6 show plots of the generation level

plotted with the load profile to show how the amount of energy stored / recovered change as the E/P ratio increases. This is done using E/P ratios of 2, 5 and 10.

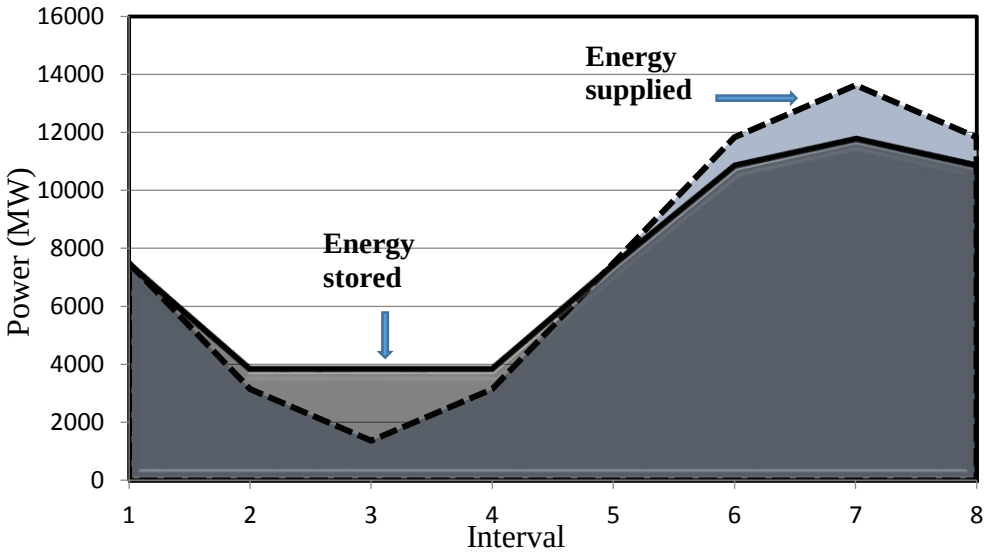

Figure 4.4 Case 4.1 daily generation output and load profile: E/P = 2

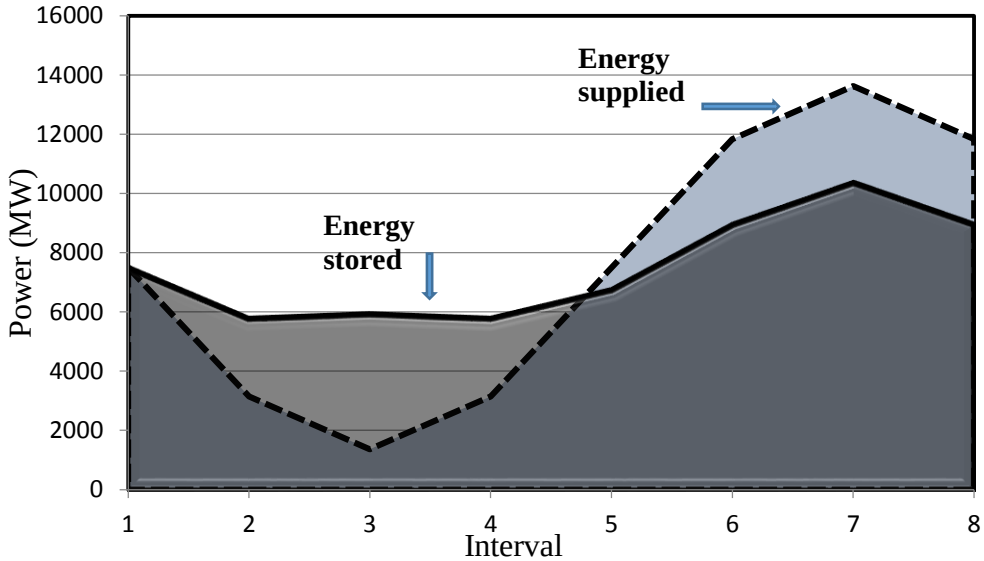

Figure 4.5 Case 4.1 daily generation output and load profile: E/P = 5

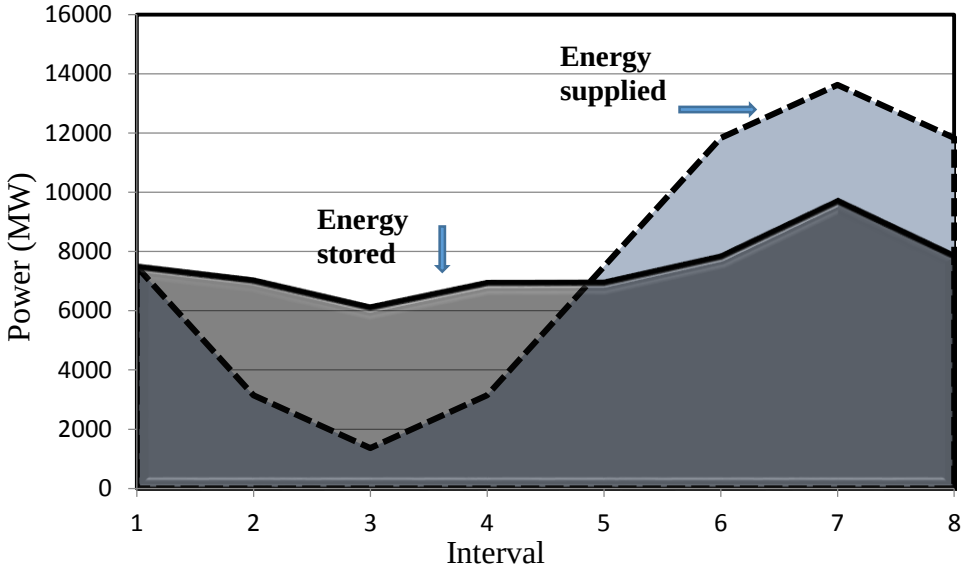

Figure 4.6 Case 4.1 daily generation output and load profile: E/P = 10

Figures 4.4 – 4.6 demonstrate that as the E/P ratio increases, more energy can be stored during off peak hours and recovered when the demand increases towards a peak. The figures display that with very high amounts of energy storage available close to the average of the load, the generation output begins to flatten out to a constant value. However, the output never completely flattens out meaning there is some limit preventing this from occurring. Chapter 5 will look into how the system limits affect the amount of energy storage and its energy rating. Table 4.5 quantifies the amount of energy shaved from the peak demand period for each E/P ratio and Figure 4.7 plots the results.

Figure 4.7 shows that as the E/P ratio increases, more energy is stored/ recovered during periods of peak demand. This result is expected because as the ratio increases, the PHES has a larger upper reservoir and can store more water / energy (MWh). However, as the E/P ratio increases to around 9 hours, it begins to flatten out to a constant value of

around 36.6 GWh. Chapter 5 will investigate why there is a limit on the amount of energy stored and used to "shave" the peak demand.

Table 4.5 Case 4.1 daily energy recovered as E/P ratio varies

Energy / power (hours)	Daily energy recovered* (MWh)
1	5905.9757
2	11730.757
3	17249.767
4	22988.487
5	28403.799
6	31792.531
7	33880.329
8	35528.326
9	36550.404
10	36577.106

*"Energy recovered" refers to the energy stored during off peak, and this is identical to the energy recovered and used during on-peak

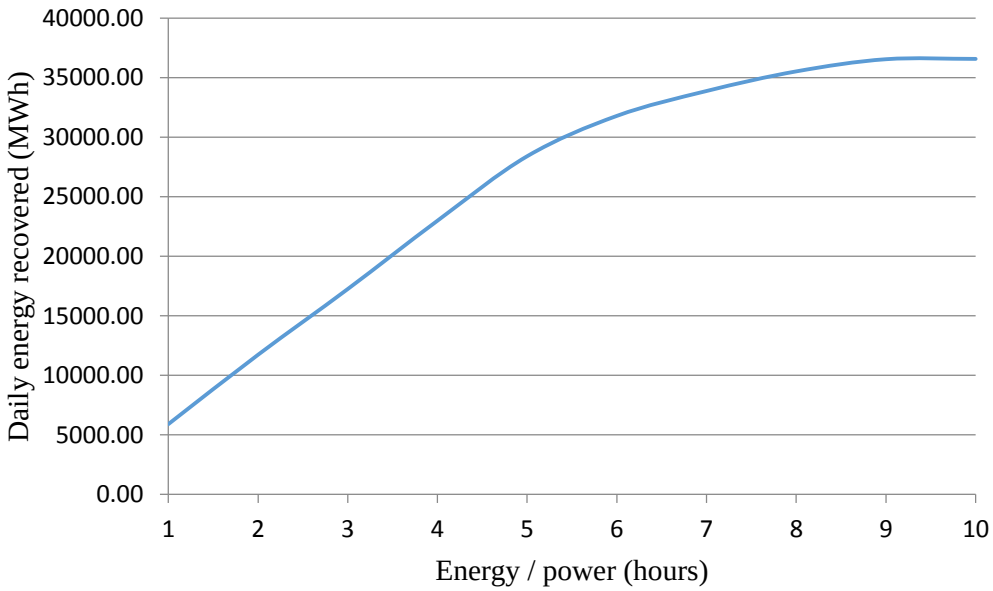

Figure 4.7 Case 4.1 daily energy recovered during peak demand as E/P ratio varies

Case 4.1 load factor evaluation

The final test used on Case 4.1 is to analyze the effect of the E/P ratio on the load factor. The load factor is defined as the "ratio of the average load over a designated period to the peak load occurring in that period [69]." The load factor is a measure of the utilization rate, or efficiency of electrical energy usage. The higher the load factor, the better the system is utilizing its generation resources. The load factor is formulated as,

$$LF = \frac{E_T}{P_{peak}T} \tag{4.1}$$

where

E_T Total energy supplied in MWh

P_{peak} Peak power demand in MW

T Time period in hours (e.g., T=8760 h for annual LF)

Using (4.1), the load factor is calculated for each E/P ratio including the base case to see how energy storage and the size of the upper reservoir can improve the load factor of the Arizona test bed. The results can be seen in Table 4.6 and Figure 4.8 plots the results.

Table 4.6 Case 4.1 annual load factor as E/P ratio varies

E/P Ratio	Annual load factor (%)
0	54.98
1	61.60
2	63.78
3	66.10
4	69.03
5	72.51
6	74.45
7	75.73
8	76.64
9	77.00
10	77.31

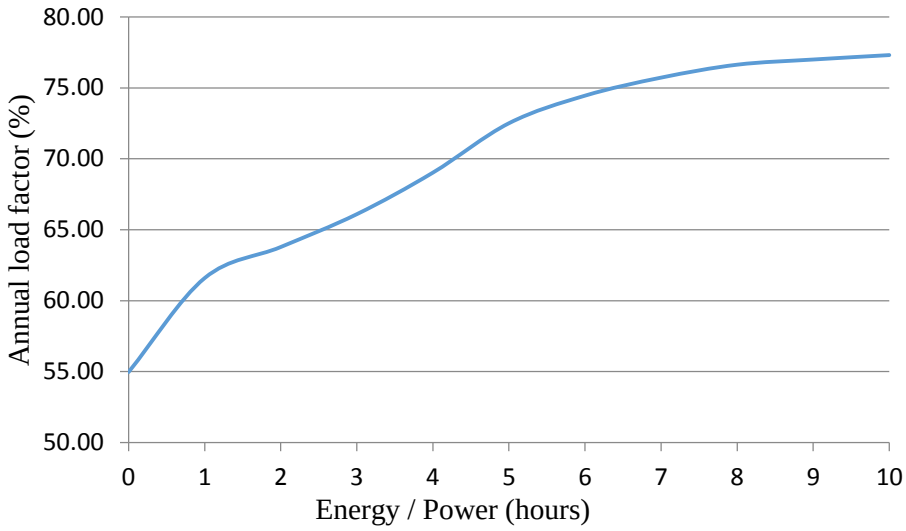

Figure 4.8 Case 4.1 annual load factor percentage as the E/P ratio increases

Figure 4.8 shows that as the E/P ratio increases to around 9 hours, the load factor also increases. After 9 hours, the load factor remains constant at around 77% which is expected because the energy recovered during periods of peak demand shown in Table 4.5 also remains constant. By adding very high amounts of energy storage to the test bed and increasing the E/P ratio close to the typical values seen in existing PHES locations, the load factor was able to improve by about 22%. This load factor increase shows that for Case 4.1, energy storage can help improve the utilization of the generators significantly.

4.3 Case 4.2: Eagle Mountain and Table Mountain pumped storage

The second case tested for very high levels of energy storage includes five locations again, with four in Arizona and one location in California close to the California Arizona border. The locations include: Eagle Mountain Pumped Storage, Horse Mesa Pumped Storage, Boulder Pumped Storage, Table Mountain Pumped Storage, and Glen Canyon Pumped Storage. Eagle Mountain Pumped Storage is a location pending approval from

FERC and is located in California close to the border with Arizona. Table 4.7 provides the locations, system bus numbers, and the power limit of each PHES location added to the system in Case 4.2.

Table 4.7 Case 4.2 PHES locations and power limit

Pumped storage location	Bus number	Power capacity (MW)
Eagle Mountain (CA)	66	1300
Horse Mesa	83	130
Boulder	149	2080
Table Mountain	153	400
Glen Canyon	186	1296
	Total	5206

Case 4.2 has a total power limit of 5.21 GW, which is closer to the 5 GW minimum needed to perform load leveling to the system. With a lower amount of energy storage available, it is expected that the amount of energy "shaved" from the peak will be less than what occurred in Case 4.1. Again, the MATLAB program in Appendix A is used to test the effect of the E/P ratio on the operating cost, payback period, peak shaving, and the load factor.

Case 4.2 operating cost and payback period evaluation

Similar to Case 4.1, the E/P ratio is varied between 1-10 hours of rated power output for each location and the operating cost and payback period are analyzed. The base case operating cost of $1.294 billion is compared with the operating cost savings and the capital costs of the five PHES locations to determine a payback period for each E/P ratio using (3.1). The results are shown in Table 4.8 and plotted in Figures 4.9 and 4.10.

Table 4.8 Case 4.2 annual operating cost and payback period as E/P ratio increases

E/P ratio	Annual operating Cost (billion $ / year)	Payback period (year)
1	1.2452	54.5
2	1.2297	41.9
3	1.2167	35.3
4	1.2068	31.7
5	1.2016	30.3
6	1.1992	29.9
7	1.1984	30.0
8	1.1983	30.4
9	1.1983	30.8
10	1.1983	31.1

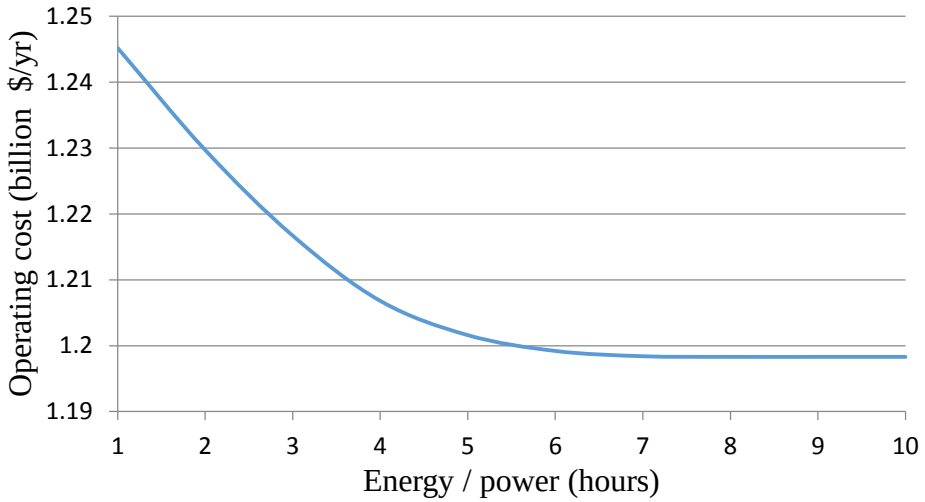

Figure 4.9 Case 4.2 annual operating cost as E/P ratio varies

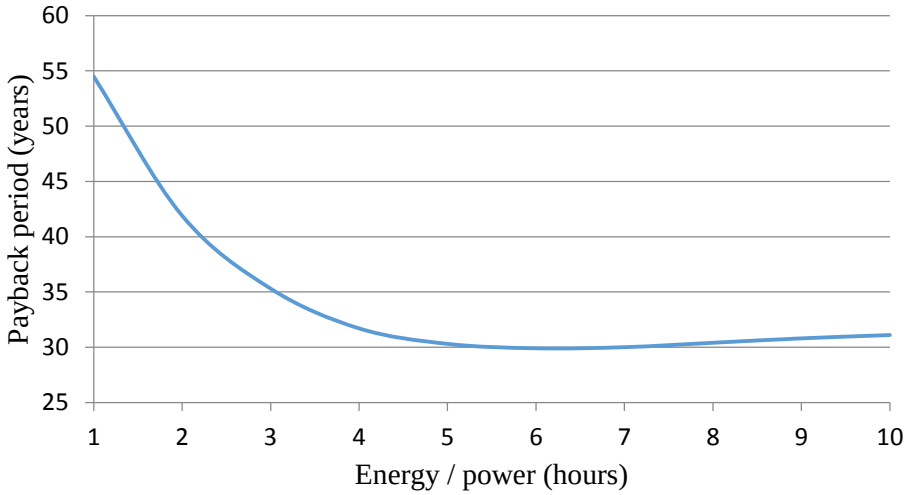

Figure 4.10 Case 4.2 payback period as the E/P ratio varies

Figures 4.9 and 4.10 show similar results to Figures 4.2 and 4.3 in Case 4.1. As the E/P ratio increases, the operating cost decreases and levels out to an operating cost of $1.983 billion between $8 \leq E/P \leq 10$. Compared to Case 4.1, the minimum system wide operating cost is slightly higher because there is 700 MW less of storage available. However, the minimum payback period is slightly less in this case resulting from a lower total capital cost than Case 4.1 but only a $12.5 million difference is operating cost savings. The minimum operating cost savings is around $95.7 million or around 7.4%. The payback period decreases to a minimum length of 29.9 years at $E/P = 6$ and starts to increase as the E/P ratio increases past 6. Again, the payback period approaches a minimum and increases because the operating savings to capital cost ratio begins to decrease.

Case 4.2 peak shaving evaluation

Case 4.2 is tested for how much energy is stored and recovered to "shave" the peak as the E/P ratio increases. Again, the results are expected to be very similar to Case 4.1 in that the amount of energy recovered during the peak demand should increase because the operating cost decreases up until $E/P = 8$. After that point, the amount of energy recovered should remain constant because the system wide operating cost does not change. Figures 4.11-4.13 show plots of the generation output and load profile for E/P ratios of 2, 5, and 10 to show how much energy is stored / recovered as the ratio is varied.

Again, Figures 4.11-4.13 are very similar to Figures 4.4-4.6 in Case 4.1. As the E/P ratio increases, more energy is recovered during peak demand hours. However, as the ratio increases from 5 to 10 hours, there is very little change in the energy recovered. This small change in the peak "shaved" is quantified by the small change in the system wide operating

cost. Similar to Case 4.1, the generation output never completely flattens out due to a limit preventing the maximum amount of energy being stored. Table 4.9 shows the amount of energy recovered during the period of peak demand for each E/P ratio and Figure 4.14 plots the results.

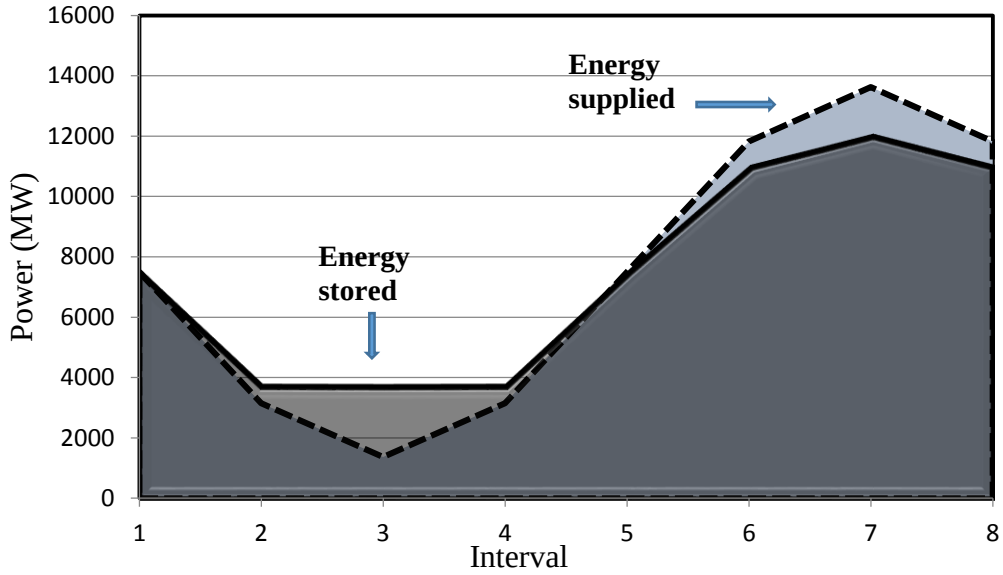

Figure 4.11 Case 4.2 daily generation output and load profile: E/P = 2

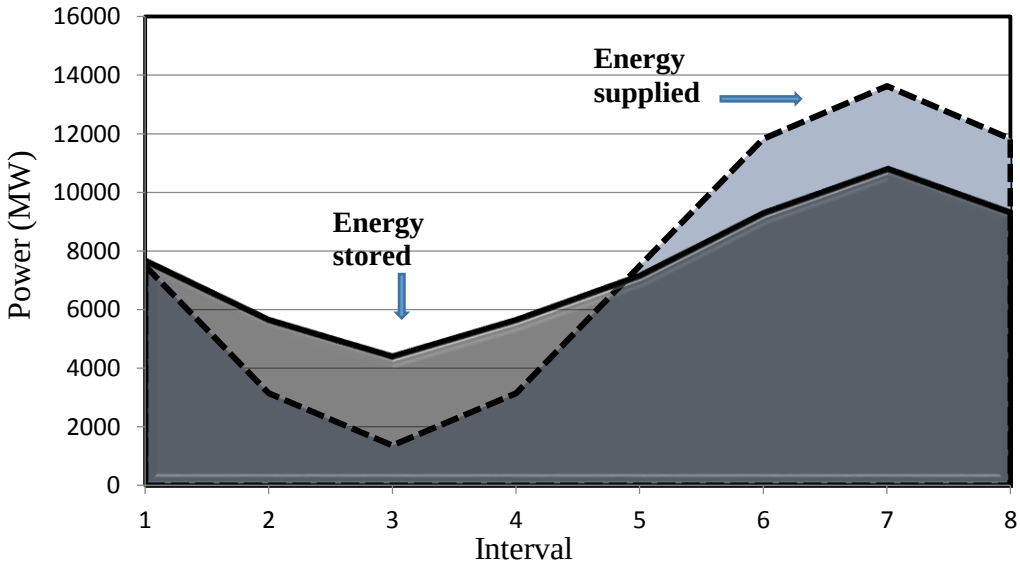

Figure 4.12 Case 4.2 daily generation output and load profile: E/P = 5

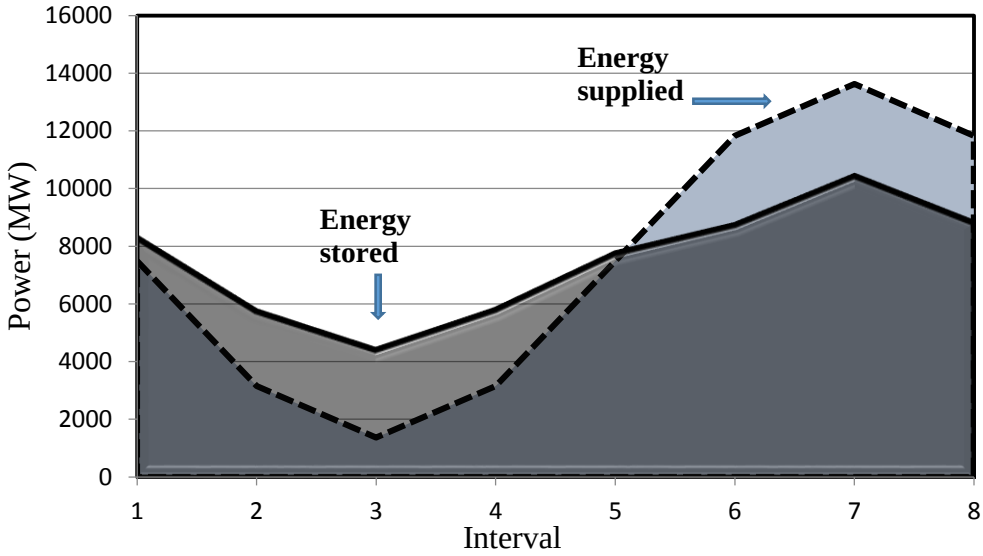

Figure 4.13 Case 4.2 daily generation output and load profile: E/P = 10

Table 4.9 Case 4.2 energy recovered as E/P ratio varies

E/P Ratio	Daily energy recovered (MWh)
1	5205.96
2	10348.19
3	15145.21
4	20181.07
5	23971.18
6	25654.34
7	26301.00
8	26425.89
9	26520.13
10	26514.12

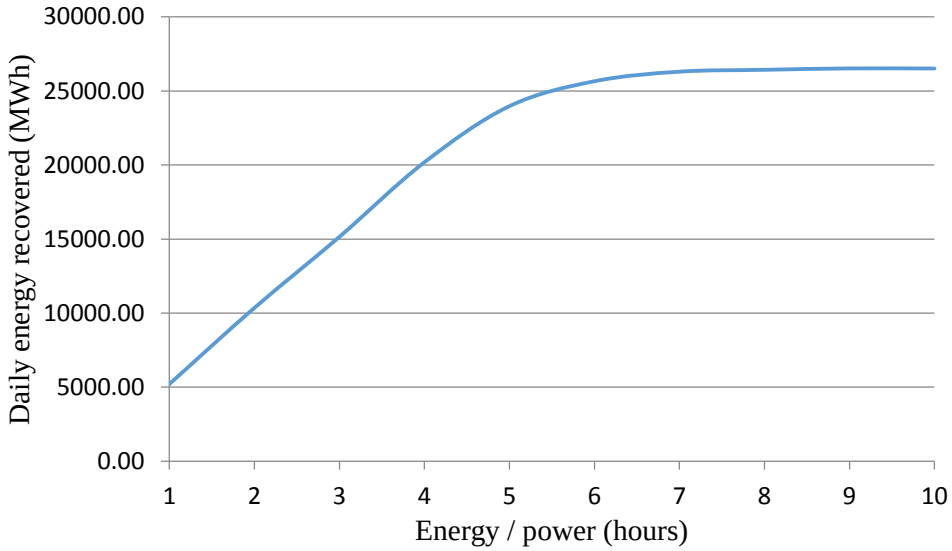

Figure 4.14 Case 4.2 daily energy recovered as E/P ratio increases

Similar to Case 4.1, as the E/P ratio increases, more energy is stored/ recovered when the load profile as a higher demand. However, in this case the amount of energy "shaved" from the peak actually starts to flatten out earlier around 7 hours rather than 9 hours. Also, the maximum amount of energy recovered is around 26.5 GWh which is about 10 GWh less than the first case. This decrease is partially the result of having 700 MW less energy storage available.

Case 4.2 load factor evaluation

Case 4.2 is analyzed using the load profile test discussed in Case 4.1. Using (4.1), the load factor is calculated at each E/P ratio and compared with the base case load factor to understand how the PHES locations in Case 4.2 can improve the load factor for the Arizona test bed. The results are also compared with Case 4.1. Table 4.10 shows the resulting load factor percentages and Figure 4.15 graphs the results versus the E/P ratio.

Table 4.10 Case 4.2 annual load factor as E/P ratio varies

E/P Ratio	Annual load factor (%)
0	54.98
1	60.93
2	62.62
3	64.46
4	66.68
5	69.45
6	71.01
7	71.69
8	72.00
9	72.00
10	71.99

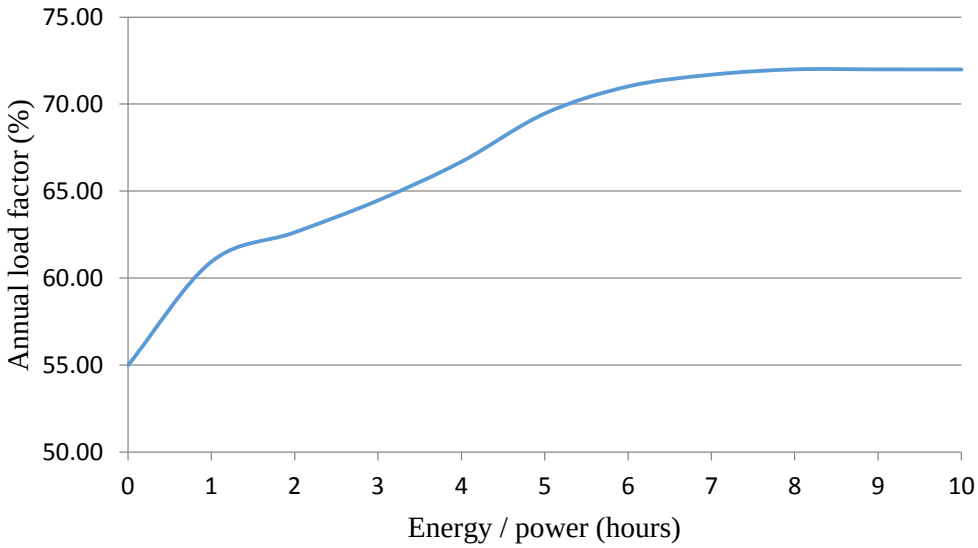

Figure 4.15 Case 4.2 annual load factor as the E/P ratio increases

Figure 4.15 shows that the load factor increases to a minimum of 60.9% from 55% using the locations in Case 4.2 with the minimum E/P ratio of 1. As the ratio increases to 7 hours, the load factor increases up to 72% and remains constant. The results when testing the load factor change show that by adding the PHES shown in Table 4.7, the load factor

can improve by as much as 17%. However, this load factor increase is 5% less than in Case 4.1.

4.4 Case 4.3: Longview, Eagle Mountain, and Table Mountain pumped storage

Case 4.3 uses five of the six locations shown in Section 4.1 to try to accomplish load leveling in the Arizona test bed. The locations include: Longview Pumped Storage, Eagle Mountain Pumped Storage, Horse Mesa Pumped Storage, Boulder Pumped Storage, and Table Mountain Pumped Storage. Again, one PHES location in California, Eagle Mountain Pumped Storage, is chose because of its high energy capacity. Table 4.11 gives the PHES locations, test bed bus numbers, and the power limit of each location in Case 4.3.

Table 4.11 Case 4.3 PHES locations and power limits

Pumped storage location	Bus number	Power capacity (MW)
Longview	3	2000
Eagle Mountain (CA)	66	1300
Horse Mesa	83	130
Boulder	149	2080
Table Mountain	153	400
	Total	5910

Case 4.3 has a total power limit of 5.91 GW, the maximum level of storage of all three cases and closest to the 6 GW needed to completely level the load. With a slightly higher level of storage available, the minimum operating cost should be the lowest of all three cases, and thus the energy recovered should be the maximum of the three. Again, the E/P ratio is varied to study its effect on operating cost, payback period, peak shaving, and the change in load factor.

Case 4.3 operating cost and payback period evaluation

Using the PHES locations shown in Table 4.11, the E/P ratio is varied again between 1 and 10 hours of rated power output to determine how this affects the operating

cost and payback period. The total capital costs of all five PHES locations are first determined to be used in (3.1). The operating cost savings found from the difference of the base case cost of $1.294 billion are then with the total capital cost to find the payback period at each E/P ratio. The results are shown in Table 4.12 and plotted in Figures 4.16 and 4.17.

Table 4.12 Case 4.3 annual operating cost and payback period as E/P ratio increases

E/P ratio	Annual operating cost (billion $ / year)	Payback period (year)
1	1.2398	55.7
2	1.2203	41.4
3	1.2048	34.8
4	1.1934	31.1
5	1.1884	30.1
6	1.1871	30.1
7	1.1866	30.3
8	1.1864	30.7
9	1.1863	31.0
10	1.1863	31.4

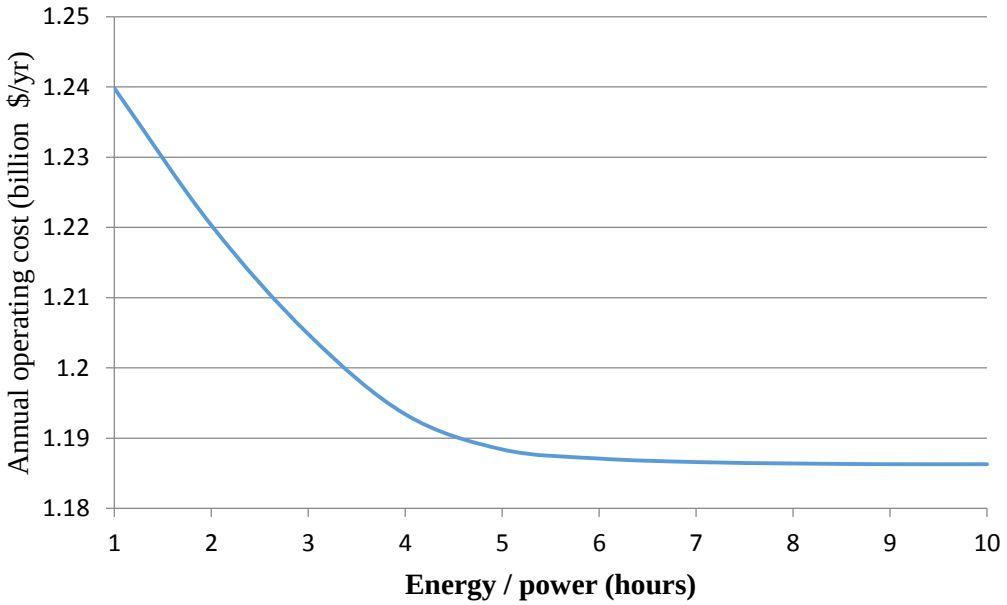

Figure 4.16 Case 4.3 annual operating cost as E/P ratio varies

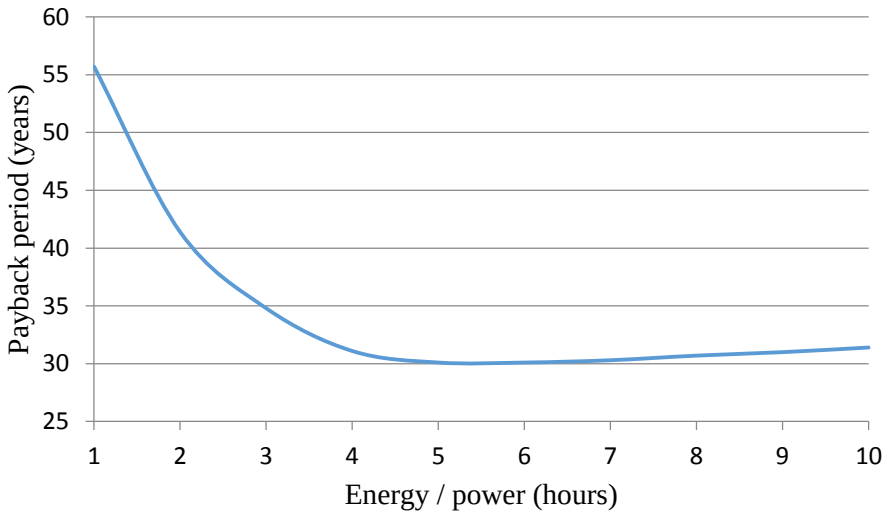

Figure 4.17 Case 4.3 payback period as the E/P ratio varies

Similar results to the previous two cases are found when observing Figures 4.16 and 4.17. Figure 4.16 shows that increasing the E/P ratio decreases the operating cost before it levels off to $1.1863 billion at E/P = 9 and 10. Even with a slightly higher total power rating, the minimum operating cost is barely higher than the minimum found in Case 4.1. The annual operating cost savings for Case 4.3 is calculated at $107.7 million for an annual savings percentage of 8.32%. Figure 4.13 shows that the minimum payback period occurs for E/P = 5 and 6 at a length of 30.1 years. The payback period increase above the minimum after E/P = 6 because of the operating cost to capital cost ratio decreasing.

Case #3 peak shaving evaluation

The E/P ratio of the locations in Case 4.3 are varied to analyze how this affects the energy recovered during the period of peak demand. The amount of the peak "shaved" as the E/P ratio increases is expected to increase because, similar to Cases 4.1 and 4.2, the operating cost decreases up until E/P = 9 and 10. The energy recovered for these two ratios should remain constant and there should be no change in the plots. Figures 4.18-4.20

display the generation output plotted with the load profile for E/P ratios 2, 5, and 10 to analyze the effect on peak shaving.

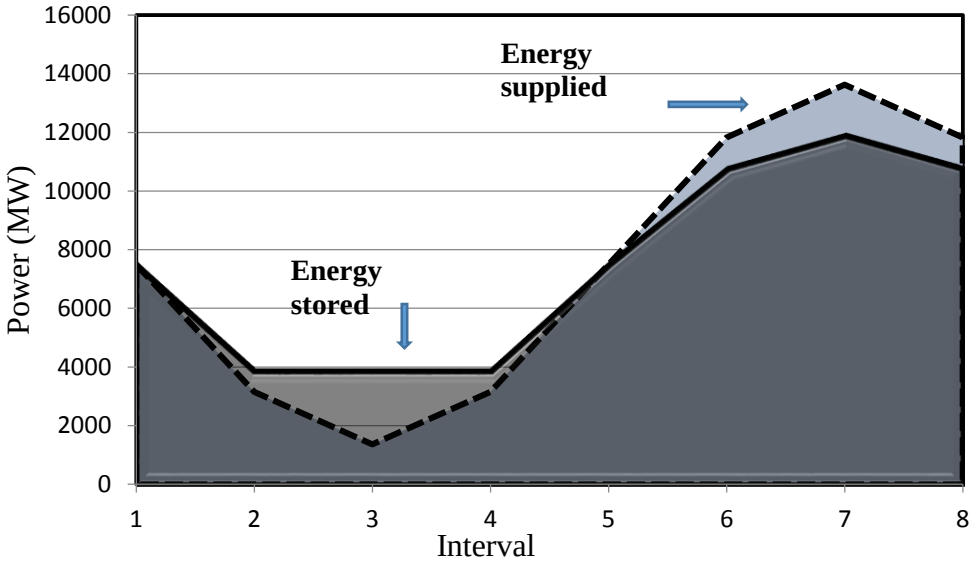

Figure 4.18 Case 4.3 daily generation output and load profile: E/P = 2

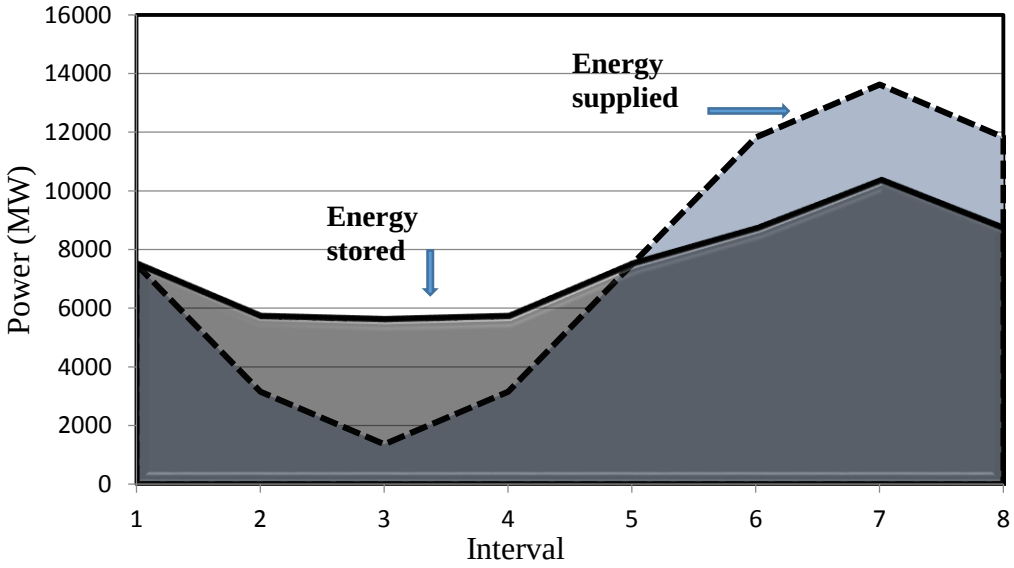

Figure 4.19 Case 4.3 daily generation output and load profile: E/P = 5

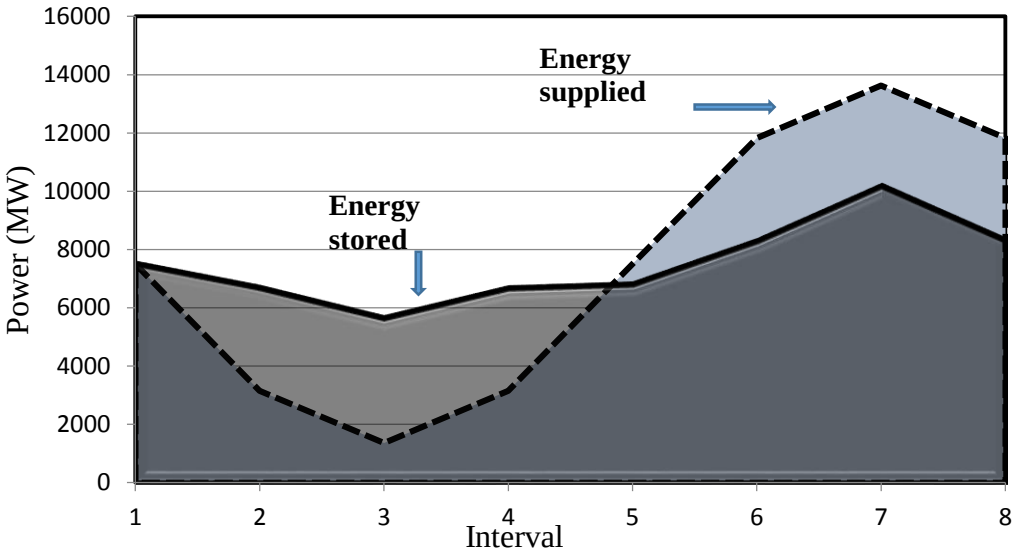

Figure 4.20 Case 4.3 daily generation output and load profile: E/P = 10

Figures 4.18-4.20 demonstrate that as the E/P ratio increases, the energy recovered during the intervals of peak demand also increase. As the E/P ratio approaches 10 hours, the generation output begins to level out with a small peak occurring around interval 7. Similar to Cases 4.1 and 4.2 however, some limit(s) in the system are preventing the maximum amount of energy from being stored. This problem is again analyzed in Chapter 5 to determine the limiting constraint. Table 4.13 shows the amount of energy recovered at each E/P ratio and Figure 4.21 plots the results.

As shown in Cases 4.1 and 4.2, the energy stored / recovered increase as the E/P ratio increases. Again, this result is expected because as the ratio increases, the size of the upper reservoir also increases and can store more water as potential energy. In Case 4.3, the energy recovered remains constant around 8 hours at rated power, which is between the lengths of Cases 4.1 and 4.2. The maximum amount of energy recovered during periods of

peak demand is around 32.8 GWh, which is also in between the amount of Cases 4.1 and 4.2.

Table 4.13 Case 4.3 daily energy recovered as E/P ratio varies

E/P Ratio	Daily energy recovered (MWh)
1	5909.97
2	11819.10
3	17729.61
4	23639.25
5	28386.53
6	30418.58
7	31817.35
8	32472.11
9	32819.92
10	32834.19

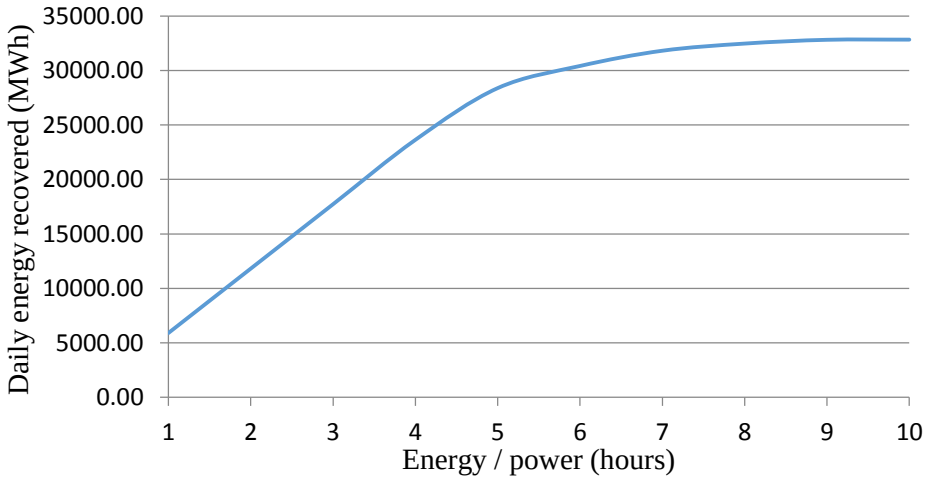

Figure 4.21 Case 4.3 daily energy recovered as the E/P ratio increases

Case 4.3 load factor evaluation

The final test used to analyze the PHES locations added to the Arizona test bed in Case 4.3 is the load factor test discussed in Case 4.1. The E/P ratio is varied and using the generation output, the load factor is calculated using (4.1). The load factor is then compared

with the base case and Cases 4.1 and 4.2. Table 4.14 shows the load factor percentages at each E/P ratio and Figure 4.22 graphs the results from the table.

Table 4.14 Case 4.3 annual load factor percentage as the E/P ratio varies

E/P Ratio	Annual load factor (%)
0	54.98
1	60.40
2	63.15
3	65.77
4	68.80
5	72.36
6	73.35
7	73.57
8	73.60
9	73.84
10	73.86

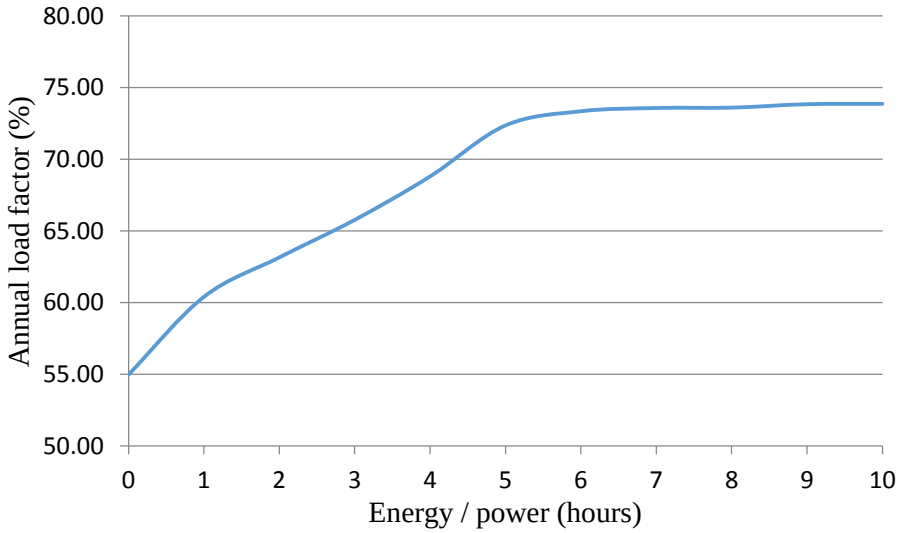

Figure 4.22 Case 4.3 annual load factor as the E/P ratio increases

Figure 4.22 displays the results of the load factor test for Case 4.3. By adding the PHES locations shown in Table 4.11 to the Arizona test bed, the load factor was able to improve from 55% to between 66.9% and 73.9%. The load factor begins to level out around an E/P ratio of 5 hours at rated power. When compared to Cases 4.1 and 4.2, Case 4.3 has

a load factor around 3% less than Case 4.1 and 2% greater than Case 4.2. The load factor increase for Case 4.3 when compared to the base case is about $\Delta LF = 19\%$.

4.5 Summary of results for very high levels of storage

In all three cases using very high levels of pumped hydro energy storage, the operating cost was reduced from the base case value of $1.294 billion. This operating cost savings was achieved using the method of peak shaving and in some cases, the load was almost completely leveled. The payback period, energy recovered, and the load factor were also calculated in all three cases to compare with the base case. Table 4.15 summarizes the results of the three cases. The table displays the minimum operating cost and payback period as well as the maximum energy recovered and load factor in each case.

Table 4.15 Summary of best case results for Cases 4.1-4.3

Case	Minimum annual operating cost (billion $ / yr.)	Annual operating cost savings (million $ / yr.)	Operating cost savings (%)	Minimum payback period (years)	Maximum daily Energy recovered (MWh)	Maximum annual load factor (%)
4.1	1.1858	108.2	8.36	30.40	36.58	77.31
4.2	1.1983	95.7	7.40	29.90	26.51	72.00
4.3	1.1863	107.7	8.32	30.10	32.83	73.86

Table 4.15 shows a maximum operating cost savings in the range of $95.7 – 108.2 million per year when using the three cases of very high levels of PHES. This savings equates to between 7.4-8.4% of savings each year, which is higher than the results from Chapter 3. The minimum payback period was calculated to be between 29.9 – 30.4 years. For high levels of energy storage, the payback period is significantly higher because of the large increase in energy storage capital costs that exceed the additional operating cost savings. When looking at the magnitude of the peak “shaved” from adding large amounts

of energy storage, the energy stored/ recovered is between 26.5 – 26.6 GWh, which helped increase the 55% load factor of the base case to between 72-77.3%. This equates to a 17-22% increase which is a significant improvement in utilizing the system generation.

This chapter showed that adding very high levels of energy storage to the Arizona test bed had a notable impact on various aspects. It is evident that the PHES locations in Case 4.1 produced the best results for all four test analyzed on the system. Case 4.1 was able to decrease the operating cost by almost $110 million annually and improved the load factor 22%. However, it was observed in all three cases that even with high amounts of storage as well as high E/P ratios that some system constraint(s) were preventing load leveling from occurring. This result was apparent from the operating cost, energy recovered, and load factor all eventually approaching a limit after the E/P ratio increased to a certain point. Chapter 5 will examine the relaxation of selected constraints and how the previously stated advantages and observations change.

CHAPTER 5

RELAXATION OF SELECTED CONSTRAINTS

5.1 Description of relaxed constraint cases

The results from Chapters 3 and 4 make it apparent that some system constraint(s) are *active constraints* that impact load leveling, attaining maximum operating cost savings, and attaining the maximum amount of energy storage. These observations come from the various system tests approaching limits as the E/P ratio is increased. The most evident indicator of the foregoing is that the load factor does not increase above 80% even with enough energy storage available to completely levelize the load. In order to analyze the system constraint(s) effect on the various tests, several relaxation scenarios are tested: e.g., the system line limits, the storage energy limits; and the storage power limits. Figure 5.1 displays the eight selected relaxation scenarios studied.

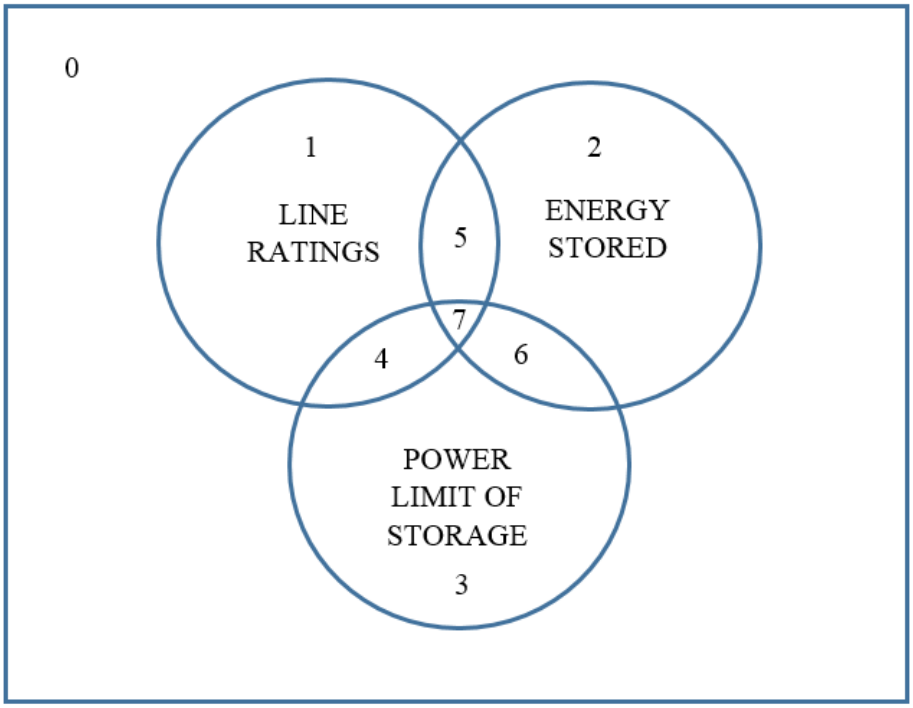

Figure 5.1 System constraint relaxation tests

Figure 5.1 displays the eight tests that are used with the Case 4.1 PHES test bed from Chapter 4. Inspection of Figure 5.1 shows a base case denominated by the numeral '0'; a test in which line rating limits are relaxed denominated by the numeral '1'; and so forth to a test in which the line ratings and storage power limits are relaxed (denominated by '4' in the figure); and so forth to the case in which all limits are relaxed. The latter is denominated by the numeral '7' in Figure 5.1.

The first test, Case 5.0, involves relaxing none of the constraints and uses the results from Chapter 4 to compare with Cases 5.1 – 5.7 which are described in this chapter. The following numbering system is used to distinguish the eight cases studied. Cases 5.*k*, *k* = 0, 1, 2, 7, refer to case *k* shown in Figure 5.1. In order to relax any of the constraints, the corresponding limit is increased to 10^9 to remove the constraint from the system.

5.2 Case 5.0, no constraint relaxations

Case 5.0 is defined as the base case and thus has no constraints that are relaxed. The PHES locations from Case 4.1 in Chapter 4 are chosen as the test case for all seven constraint relaxation tests. The results from this case are thus the exact same seen in Case 4.1. The operating cost, operating cost savings, load factor, and the total energy stored from Case 4.1 will be used for comparisons with Cases 5.1- 5.7 to see how the various constraints affect the listed tests.

5.3 Case 5.1, relaxation of system line limits

The first test is the relaxation of the system transmission line limits. The relaxation of the line limits analyzes the outcome when the system transmission lines have no maximum operating limit. By removing the line limits, the system wide operating cost should be minimized as there would nothing preventing the maximum amount of energy

from being stored as well as the cheaper generators being utilized at their maximum power output levels. The E/P ratio is varied between 1 and 10 and the results are compared with Case 4.1. Tables 5.1 and 5.2 displays the results from Cases 4.1 and 5.1 with the line limits relaxed. Figures 5.1-5.4 plot the results from Table 5.1 together to show how the relaxation of the line limits improve the various tests from Chapter 4.

Table 5.1 Case 4.1 test results as the E/P ratio varies

E/P ratio	Annual operating cost (billion $/year)	Payback period (years)	Daily energy recovered (GWh)	Annual load factor (%)
1	1.2423	58.4	5.91	61.6
2	1.2247	44.1	11.73	63.8
3	1.2103	36.9	17.25	66.1
4	1.1994	33.1	22.99	69.0
5	1.1924	31.2	28.40	72.5
6	1.1886	30.5	31.79	74.5
7	1.1869	30.4	33.88	75.7
8	1.1861	30.6	35.53	76.6
9	1.1858	30.9	36.55	77.0
10	1.1858	31.2	36.58	77.3

Table 5.2 Case 5.1 test results as the E/P ratio varies

E/P ratio	Annual operating cost (billion $/year)	Payback period (years)	Daily energy recovered (GWh)	Annual load factor (%)
1	1.2329	26.15	5.90	63.5
2	1.2149	22.91	11.81	67.4
3	1.2001	20.89	17.72	71.6
4	1.1885	19.63	23.62	76.4
5	1.1802	18.90	29.53	81.9
6	1.1754	18.61	35.42	88.2
7	1.1733	18.62	41.33	95.6
8	1.1731	18.84	43.74	97.0
9	1.1731	19.08	43.75	97.0
10	1.1730	19.30	43.76	97.0

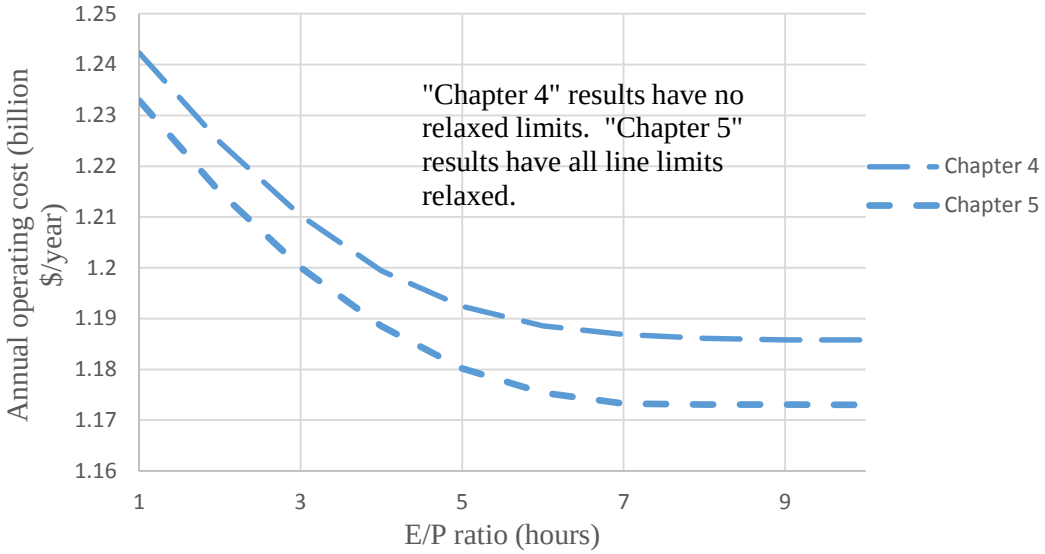

Figure 5.2 Cases 4.1 and 5.1 annual operating cost as the E/P ratio varies

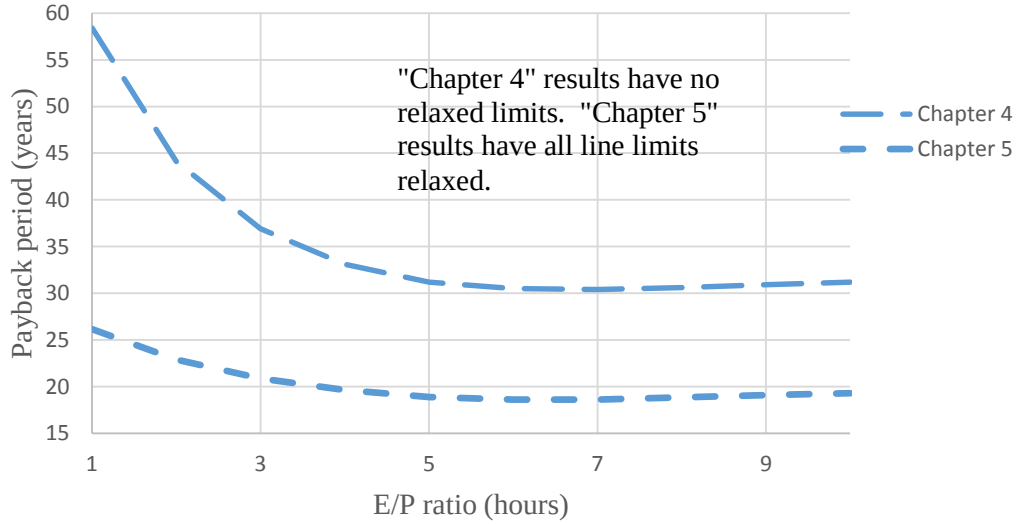

Figure 5.3 Cases 4.1 and 5.1 payback period as the E/P ratio varies

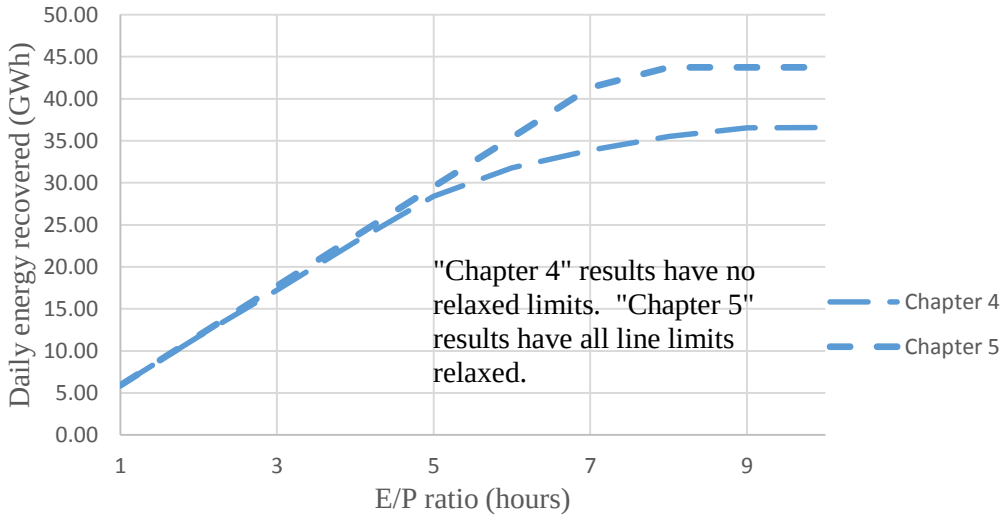

Figure 5.4 Cases 4.1 and 5.1 daily energy stored / recovered as the E/P ratio varies

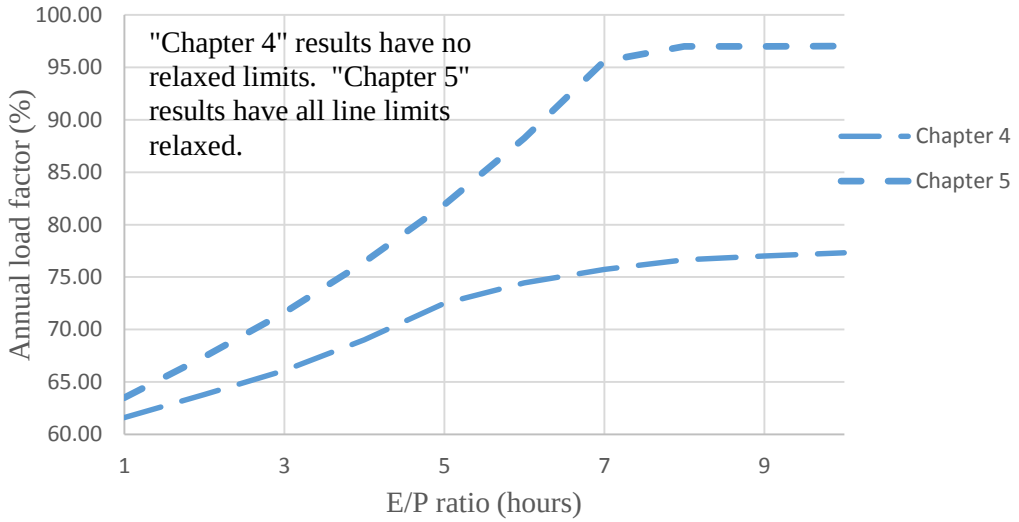

Figure 5.5 Cases 4.1 and 5.1 annual load factor percentage as the E/P ratio varies

As expected, all four test results improved with the line limits relaxed. Figure 5.2 shows that at all E/P ratios, the operating cost decreases for Case 5.1. The minimum operating decreases by as much as 1.09%, or $12.8 million for a minimum of $1.173 billion. The payback periods in Figure 5.3 show a significant decrease for Case 5.1 compared to Case 4.1 with as much as a 38.8% decrease. This equates to an 11.8 year

decrease for a minimum of 18.61 years at E/P = 6. Note that the payback period does not include the added cost to increase the transmission line limits and only calculates the PHES payback period. Figure 5.4 displays that for higher E/P ratios, the energy stored / recovered increases up to 16.4%, or 7.18 GWh with a maximum value of 43.8 GWh. Finally, Figure 5.5 shows a very large increase at higher E/P ratios by as much as 19.7% and a load factor as high as 97%. These results show that the existing line limits have a significant impact on the various tests run on Case 4.1. The line limits are preventing the load factor from increasing to nearly 100% and are increasing the payback period by a considerable amount.

5.4 Case 5.2, relaxation of storage energy limits

Case 4.2 studies the effect of relaxing the pumped hydro energy limits. By relaxing the energy limits of the storage, the PHES upper reservoir is modeled to have an infinite volume. An infinite reservoir is unrealistic; however, the relaxation analyzes the limitations the storage energy limit is having on the four test results from Case 4.1. Using the PHES locations form Case 4.1, the results of Case 5.2 can be seen in Table 5.3. Table 5.3 includes the system wide operating cost when there is no energy storage present in the system. The generation output plotted and the load profile can be seen in Figure 5.6 to model peak shaving.

Table 5.3 Case 5.2 test results

Annual operating cost (billion $/year)	Annual operating cost savings (%)	Annual operating cost savings (million $/year)	Daily energy recovered (GWh)	Annual load factor (%)	No energy storage annual operating cost (billion $/year)
1.1858	8.33	107.8	36.60	77.4	1.2936

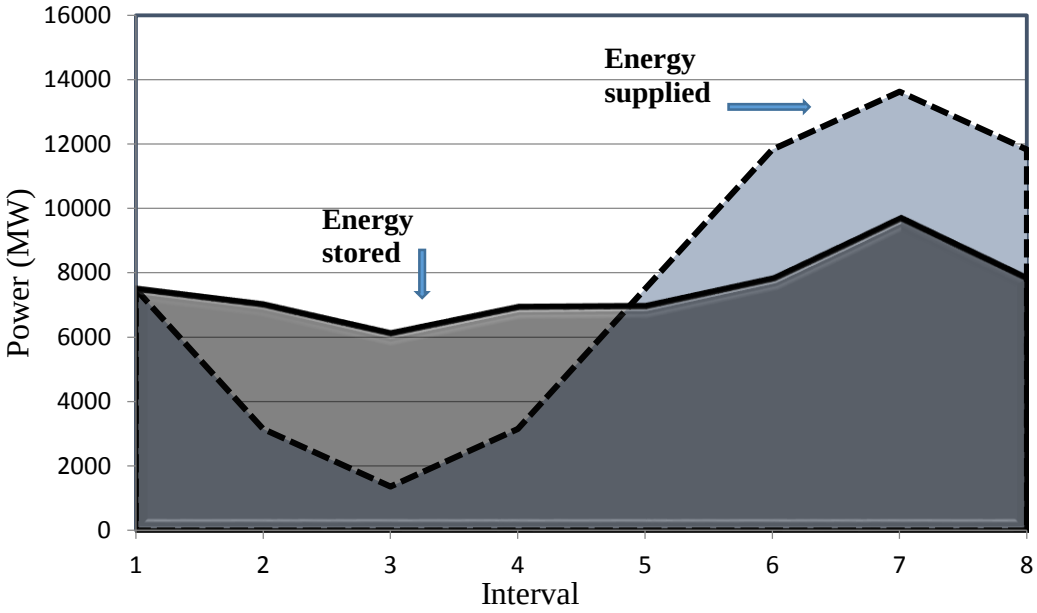

Figure 5.6 Case 5.2 daily generation output and load profile

When comparing the results from Table 5.3 and Figure 5.6 with the results from Case 4.1 at its maximum E/P ratio of 10, there is little to no change. The operating cost remains at $1.1858 billion with an annual savings of $107.8 million, which is an 8.33% reduction when compared to the no storage case. The load factor also remains constant at 77.4% which is why the generation output in Figure 5.6 looks the same as in Figure 4.6 seen in Case 4.1. From these results compared with Case 4.1, it is evident that relaxing the pumped hydro energy limits has no effect on the output. All items tested seem to remain constant as the energy ratio increases to unrealistic numbers.

5.5 Case 5.3, relaxation of storage power limits

The results when the PHES power limits are relaxed are analyzed in Case 5.3. A relaxation of all of the storage power limits indicates replacing the turbine and generator of all existing PHES locations with ones that have impractically high power ratings. The storage power rating relaxations is only to evaluate the constraints effect on the tests run in

Case 4.1 and do not represent a realistic upgrade that could be made to the PHES. For this case, the energy ratings of each PHES remain at the same values as they were with an E/P ratio of 10 before the power limits are relaxed. The results of Case 5.3 can be seen in Table 5.4 and the generator output and load profile are plotted in Figure 5.7.

Table 5.4 Case 5.3 test results

Annual operating cost (billion $/year)	Annual operating cost savings (%)	Annual operating cost savings (million $/year)	Daily energy recovered (GWh)	Annual load factor (%)	No energy storage annual operating cost (billion $/year)
1.1852	8.38	108.40	38.06	78.3	1.2936

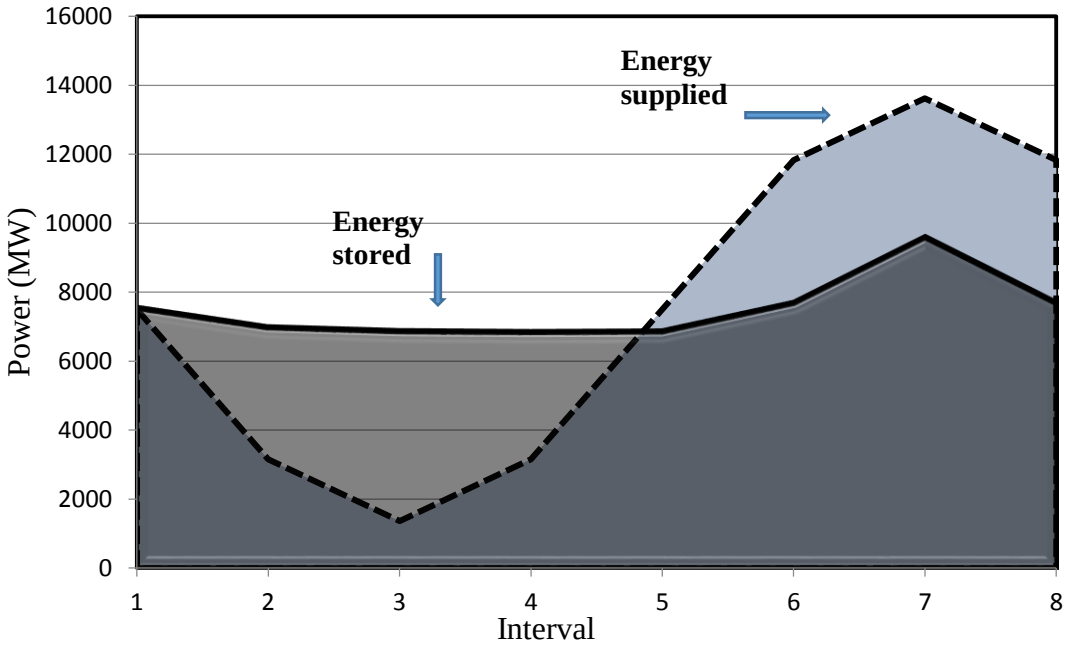

Figure 5.7 Case 5.3 daily generation output and load profile

Table 5.4 shows that by relaxing only the storage power limits, the system wide operating cost decreases by only a small amount when compared with Case 4.1 at an E/P = 10. The operating cost decreases by .05%, or $0.6 million to a value of $1.1852 when compared with Case 4.1 When compared with the base case, or no energy storage, the

operating cost improves by $108.4 million, or 8.38%. The load factor increases to 78.3%, or a 1% improvement from the highest load factor in Case 4.1. By relaxing the storage power limits, only a small improvement can be made to the items tested including operating cost and load factor. The small additional operating cost savings may not enough to make up for the high added capital costs that would occur for a significant turbine / generator power limit increase.

5.6 Case 5.4, relaxation of line / storage power limits

The fourth case is the relaxation of both the line and storage power limits in the Arizona test bed. These two relaxations are equivalent to having an infinite bus with all generators, loads, and storage elements connected to it and the PHES turbines having an infinite power rating. Both cases are unrealistic, similar to previous cases, and are purely to analyze the two constraints effect on the test results. Table 5.5 shows the outcome of the various tests when both the line and storage power limits are relaxed. Figure 5.8 displays the generator output and load profile for a 24 hour day.

Table 5.5 Case 5.4 test results

Annual operating cost (billion $/year)	Annual operating cost savings (%)	Annual operating cost savings (million $/year)	Daily energy recovered (GWh)	Annual load factor (%)	No energy storage annual operating cost (billion $/year)
1.1730	12.94	174.41	44.44	100.0	1.3474

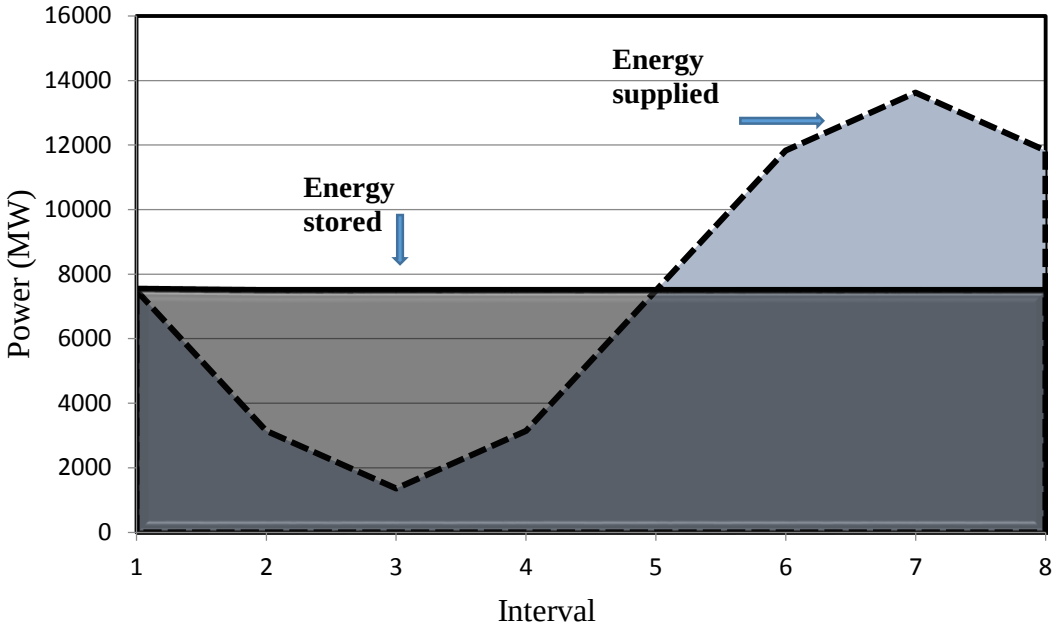

Figure 5.8 Case 5.4 daily generation output and load profile

The results in Table 5.5 and Figure 5.8 show that when relaxing both the line and storage power limits, a 100% load factor can be achieved. A complete load shave results in the minimum operating cost of $1.173 billion. This equates to an operating cost savings of 12.94% or $174.41 million when compared to the case with no storage. Compared to Case 5.1 with only a relaxation of the line limits, the operating cost is about the same but the load factor increased by 3% to 100%. A combination of relaxing the line and storage power limits allows enough energy to be stored to completely shave the peak and minimize operating costs. However, the additional energy shaved during peak hours from the power limit increasing decreases the operating cost by only a small amount.

5.7 Case 5.5, relaxation of line / storage energy limits

Case 5.5 involves relaxing both the line limits and the storage energy limits. This test analyzes the effect of removing all transmission lines and replacing them with an infinite bus. Also, the reservoirs of all PHES locations would be unrealistically large in

volume and can store very large amounts of water. Again, these two relaxations are purely to see how the two constraints affect the various tests on the test bed. Table 5.6 shows the results of case 5.5 and Figure 5.9 plots the generation output with the load profile.

Table 5.6 Case 5.5 test results

Annual operating cost (billion $/year)	Annual operating cost savings (%)	Annual operating cost savings (million $/year)	Daily energy recovered (GWh)	Annual load factor (%)	No energy storage annual operating cost (billion $/year)
1.1730	12.94	174.40	43.74	97.0	1.3474

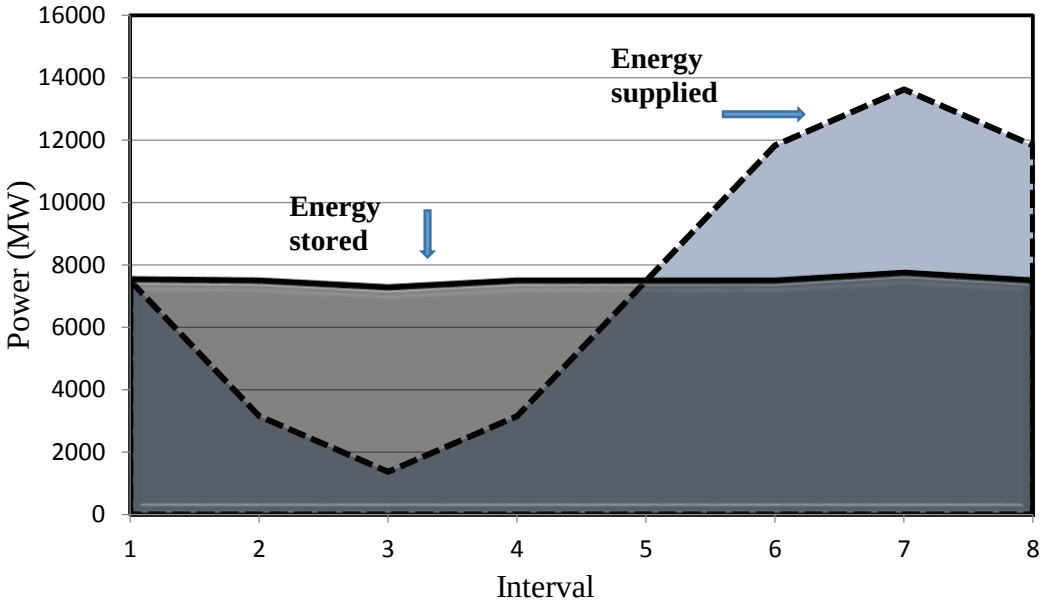

Figure 5.9 Case 5.5 daily generator output and load profile

The results in Table 5.6 are very similar to the higher E/P ratio results in Case 5.1 with only the line limits relaxed. The annual operating cost is the same at $1.173 billion and an operating cost savings of $174.4 million. This equates to a 12.94% annual operating

cost savings. The generation output in Figure 5.9 is very similar to the output in Case 5.1 with the load factor the same at 97%. From these results, it can be concluded that relaxing the storage energy limits has no effect on the generation output when the line limits are already relaxed. The results from Case 5.1 where only the line limits are relaxed remain exactly the same when the storage energy limits are relaxed.

5.8 Case 5.6, relaxation of storage energy and power limits

The sixth case involves relaxing a combination of both the PHES energy and power ratings. By relaxing both limits of the pumped hydro locations in Case 4.1, the reservoirs are assumed unrealistically large and the turbines and generators are replaced with ones that have unconventionally high power limits. Again, these two relaxations do not represent real world applications and are merely to analyze the effect of the storage energy and power limits on the previous tests. The results of Case 5.6 can be seen in Table 5.7 and Figure 5.10 displays the generation output and load profile for the purpose of demonstrating peak shaving.

Table 5.7 Case 5.6 test results

Annual operating cost (billion $/year)	Annual operating cost savings (%)	Annual operating cost savings (million $/year)	Daily energy recovered (GWh)	Annual load factor (%)	No energy storage annual operating cost (billion $/year)
1.1852	8.38	108.40	38.12	78.2	1.2936

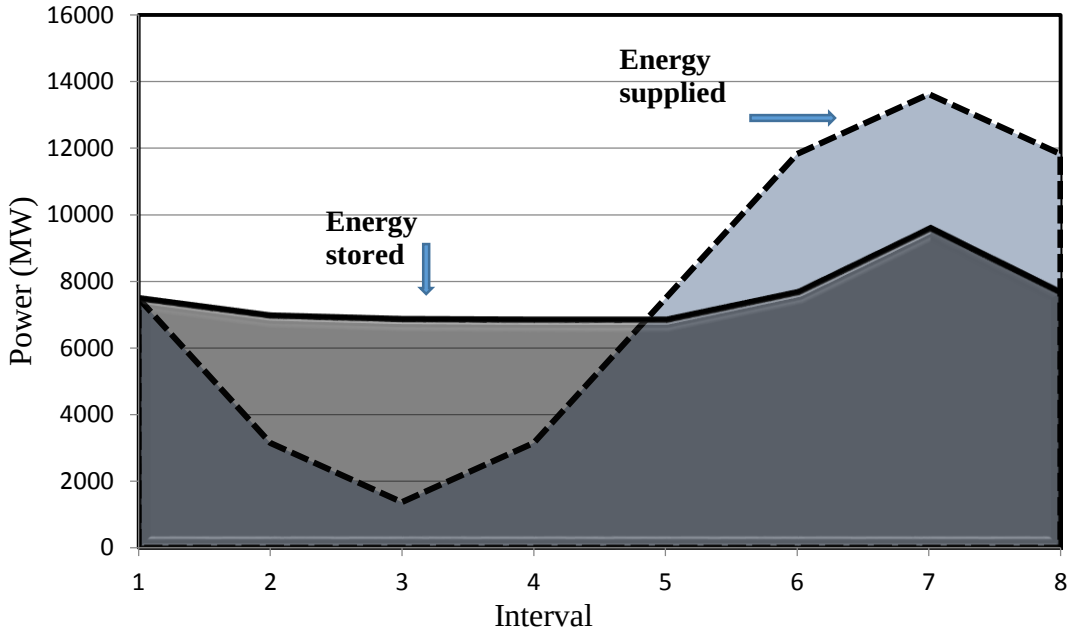

Figure 5.10 Case 5.6 daily generation outputs and load profile

It is found that by relaxing both the storage energy and power limits, the results do not change when compared with relaxing only the storage power limits. The results in Table 5.7 and the generation output in Figure 5.10 remain exactly the same as Table 5.1 and Figure 5.7 in Case 5.3. From these results, it is further evident that the storage energy rating has no effect on the system operating costs after an E/P ratio of around 10. Increasing the reservoir volume would only increase capital costs and would have no effect on the system operating costs.

5.9 Case 5.7, relaxation of line / storage energy and power limits

The last case is the relaxation of all three constraints tested in this chapter. Case 5.7 involves replacing all transmission lines with an infinite bus, increasing the volume of all PHES locations to an extremely high value, and replacing all PHES turbines with ones with unrealistically high power ratings. Similar to all previous relaxation cases, all three relaxations are just to see how relaxing all three constraints effects the system results. The

results of Case 5.7 can be seen in Table 5.8 and Figure 5.11 plots the generation outputs with the load profile.

Table 5.8 Case 5.7 test results

Annual operating cost (billion $/year)	Annual operating cost savings (%)	Annual operating cost savings (million $/year)	Daily energy recovered (GWh)	Annual load factor (%)	No energy storage annual operating cost (billion $/year)
1.1730	12.95	174.5	44.44	100.0	1.3474

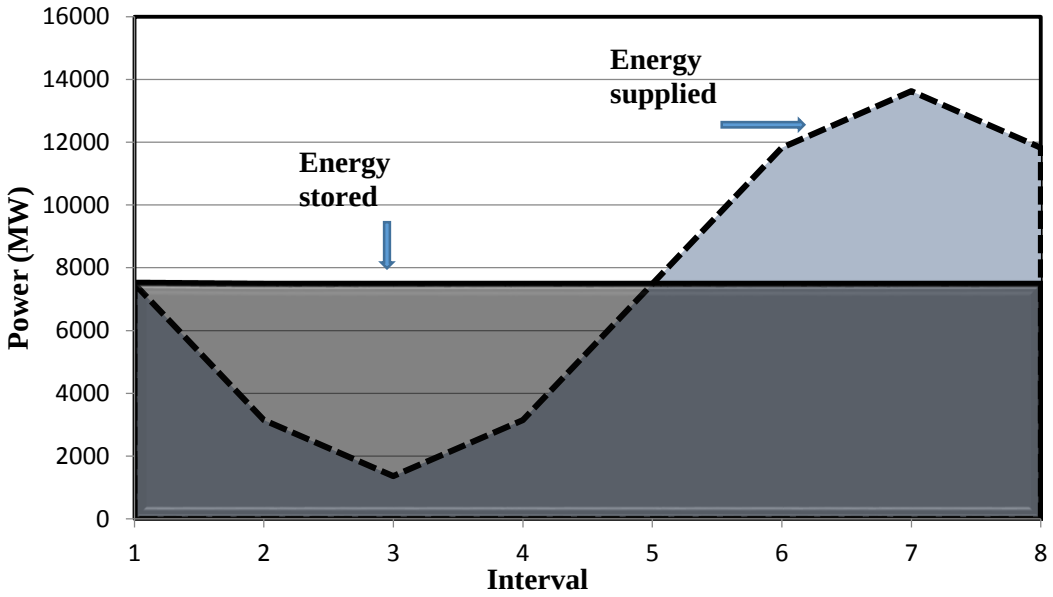

Figure 5.11 Case 5.7 daily generator output and load profile

The results for Case 5.7 shown in Table 5.8 are almost exactly the same as in Case 5.4 with the line and storage power limit relaxed. The annual operating cost is $1.173 billion for a $174.5 million per year savings. This savings is 12.95% less when compared to the same case with no energy storage. Also, the load factor is calculated to be 100% meaning the peak is completely shaved. Again, the results of Case 5.7 are very close to Case 5.4 meaning that relaxing the storage energy limits has little to no effect on the output when the line and storage power limits are also relaxed. Similar to Case 5.4, the relaxation

of the storage power limits improves the load factor by 3% and decreases the operating cost by a very small amount.

5.10 Summary of results

This chapter focused on relaxing various constraints to see the effect on the results obtained in Chapter 4. The results from the previous chapter showed that some constraint(s) were limiting load leveling, and attainment of the minimal operating cost. Seven relaxed cases using combinations of the line limits, storage energy limits, and the storage power limits were analyzed and the results were compared with Case 4.1 from Chapter 4. Table 5.9 displays the results of Case 4.1 and the seven relaxation cases studies.

Table 5.9 Chapter 5 relaxed constraint case results

Case	Annual operating cost (billion $/year)	Annual operating cost savings (%)	Annual operating cost savings (million $/year)	Daily energy recovered (GWh)	Annual load factor (%)	No energy storage annual operating cost (billion $/year)
5.0*	1.1858	8.33	107.8	33.66	77.3	1.2936
5.1*	1.1730	12.94	174.4	43.76	97.0	1.3474
5.2	1.1858	8.33	107.8	36.60	77.4	1.2936
5.3	1.1852	8.38	108.4	38.06	78.3	1.2936
5.4	1.1730	12.94	174.4	44.44	100.0	1.3474
5.5	1.1730	12.94	174.4	43.74	97.0	1.3474
5.6	1.1852	8.38	108.4	38.12	78.2	1.2936
5.7	1.1730	12.94	174.4	44.44	100.0	1.3474

* Includes the minimum value for each test

When comparing the cases in Table 5.9 with the base case (Case 5.0), it is evident that the cases that relax the line limits have the best improvements for all tests. The cases that relax line power ratings are Cases 5.1, 5.4, 5.5, and 5.7. This is clear when Case 5.1, which relaxes only the line limits, is compared with the other three cases (5.4, 5.5, 5.7) that

also relax the line limits. In Cases 5.4, 5.5, and 5.7, the system wide operating cost does not change from what was found in Case 5.1. However, in Cases 5.4 and 5.7 where the storage power limits are also relaxed, the load factor does improve to 100% as more energy is stored / recovered. Also, when the storage power limit is relaxed in Cases 5.2 and 5.6 but not the line limits, the operating cost does improve slightly.

The cases that relax the storage energy limit (Cases 5.2, 5.5, and 5.7) have no change in performance indicators (i.e., load factor or annual operating cost measures) compared to those that do not. This result apparently means that the energy stored / recovered during every time interval is not approaching or hitting the energy limit of each PHES. Thus relaxation of the energy storage limits has no effect. By increasing the line limits in the system, high levels of PHES would realize improvement of load factor and annual operating cost. In a realistic analysis, upgrading line ratings should be done so that the desired system operating metrics are improved in an optimal way. The foregoing study employed wholesale upgrading of transmission circuits system-wide; a realistic study would need to identify those circuits which have the greatest impact on the system performance metrics as well as cost / benefit effectiveness. The latter is relegated to 'future work'. For example, this approach is applied by Tokombayev in [70] to identify transmission circuits for upgrade by high temperature, low sag construction.

CHAPTER 6

CONCLUSIONS AND FUTURE WORK

6.1 Conclusions

In this thesis, a test bed utilizing the Arizona transmission system with a 2010 summer peak load, was used to demonstrate several topics related to bulk energy storage. The following conclusions can be made based on the research and results discovered:

- *Literature review:* the literature review offered in Chapter 2 explained important applications that bulk energy storage can provide including:
    - peak shaving
    - frequency and area control regulation
    - transmission line expansion deferral
    - integration of renewables
    - lowering transmission line congestion
    - Improving regional reserve margins.
- *The economic dispatch problem:* the second chapter gave a review of the economic dispatch problem and provided various methodologies to solve that problem. Quadratic programming was chosen as the method to solve the economic dispatch problem and simulate energy storage and its effect on the Arizona test bed.
- *Addition of modest levels of energy storage:* the third chapter illustrates the calculation of the minimum annual operating cost of the system with no energy storage. This is denominated as the base case. The annual operating cost for a stated load scenario was found to be $1.294 billion with a 55% load factor. By adding energy storage to different locations in the system, a maximum annual

savings of 6% or $78 million was determined. The maximum saving was then utilized to show that the corresponding minimum payback period for the locations tested was about 8 years.

- *Addition of high levels of energy storage:* Chapter 4 illustrates the result of adding very high amounts (e.g., ~6 GW) of pumped hydro storage to the Arizona test bed. This is done to model load leveling in the system. The goal was to add enough storage such that the energy stored during off peak intervals would be enough to completely "shave" the peak during the peak demand intervals. From the results in the three cases, an annual operating cost savings of up to $108.8 million or 8.4% was found. The load factor for the corresponding case was found to be 77.3%. Note that this is an improvement from the case without storage in which the load factor was 55%.
- *Relaxation of line, storage-energy, and storage-power limits:* the final chapter looked into relaxing various system constraints and analyzing the change in the operating cost and load factor. The results showed that relaxing the line limits had the greatest change with a minimum operating cost of $1.173 billion. This stated operating cost represents a decrease of about $174 million annually. The operating cost savings represents about 12.94% annually compared to the base case. In order to have a 100% load factor, the line and storage power limits had to be relaxed. Also, the relaxation of the storage energy limits showed that there was no effect on the results.
- *Load factor:* it was shown that large scale energy storage can decrease generation operating costs in the system by storing off peak energy and recovering this energy

during peak demand periods. By doing so, the load factor of the system increases. However, a 100% load factor is not necessarily the desired operational goal.

6.2 Future work

In the research and tests performed for this thesis, the economic dispatch was studied using the Arizona test bed with various simplifying assumptions, mainly omission of: modeling reactive power flows, transmission losses, energy storage losses, and system voltages and their limits. The research discussed could be extended in the following ways:

- modeling the losses related to the transmission and energy storage devices
- performing an ACOPF on the Arizona test bed to examine system stability related to both the system bus voltages and a *N*-1 analysis
- including reactive power in the system analysis and quantifying its effects
- modeling correct bus voltages in the system
- identifying the transmission circuits that have the greatest impact on the system performance metrics as well as a cost / benefit effectiveness
- extending the analysis out to the entire WECC and determining PHES locations in this larger milieu
- modeling large scale non-hydro energy storage and showing the resulting operating cost and load factor changes
- demonstrating examples of lowering the transmission line congestion in the system with correct placement of energy storage
- creating a program to make pumped storage (or other energy storage) "off the shelf" technology.

REFERENCES

[1] S. Olea, “Renewable energy standard and tariff,” available at: http://www.azcc.gov/divisions /utilities/electric/environmental.asp.

[2] S. Vazquez, S.M. Lukic, E. Galvan, L.G. Franquelo, J.M. Carrasco, "Energy storage systems for transport and grid applications," *IEEE Transactions on Industrial Electronics*, Dec. 2010, vol. 57, no. 12, pp. 3881-3895.

[3] R.J. Kerestes, G.F. Reed, A.R Sparacino, "Economic analysis of grid level energy storage for the application of load leveling," *IEEE Power and Energy Society General Meeting*, 22-26 July 2012, pp. 1-9.

[4] J. Mankansi, J. Abboud, “Energy storage- the missing link in the electricity value chain,” available at: http://www.energystoragecouncil.org/ESC%20White%20Paper%20.pdf.

[5] B. Wollenberg, A. Wood, *Power generation operation and control*, J Wiley and Sons, New York, Second edition, 1996.

[6] EPRI-DOE Handbook, “Energy storage for transmission and distribution applications,” Dec. 2003.

[7] M.T. Holmberg, M. Lahtinen, J. McDowall, T. Larsson, "SVC light with energy storage for frequency regulation," *IEEE Conference on Innovative Technologies for an Efficient and Reliable Electricity Supply (CITRES)*, 27-29 Sept. 2010, pp. 317-324.

[8] L. Liang, J. Zhong, Z. Jiao, "Frequency regulation for a power system with wind power and battery energy storage," *IEEE International Conference on Power System Technology*, Oct. 30 -Nov. 2 2012, pp. 1-6.

[9] D. Rastler, “Electric energy storage technology options,” available at: http://www.electricitystorage.org/images/uploads/static_content/technology/resources/ESA_TR_5_11_EPRIStorageReport_Rastler.pdf.

[10] J. A. Jardini, D. Missali, M. G. Jardini, R. L. Vasquez-Arnez, M. Masuda, "On the analysis and evaluation of a transmission line upgrading assisted by line arresters," *IEEE Power & Energy Society General Meeting*, 26-30 July 2009, pp. 1-7.

[11] I. Zamora, A. J. Mazon, P. Eguia, R. Criado, C. Alonso, J. Iglesias, J. R. Saenz, "High-temperature conductors: a solution in the uprating of overhead transmission lines," *IEEE Porto Power Tech Proceedings*, 10-13 September 2001, vol. 4, pp. 1-6.

[12] D. P. Manjure, M. D. McMullen, D. O. Subakti, D. Tewari, "Managing wind energy: from interconnection planning to real time operations, an integrated approach to ensure energy and transmission capacity," *IEEE Power & Energy Society General Meeting*, 26-30 July 2009, pp. 1-8.

[13] D. M. Larruskain, I. Zamora, O. Abarrategui, A. Iraolagoitia *et al.*, "Power transmission capacity upgrade of overhead lines," University of the Basque Country, San Sebastián, Spain, 2006.

[14] A. Oudalov, T. Buehler, D. Chartouni, "Utility scale applications of energy storage," *IEEE Energy 2030 Conference*, 17-18 Nov. 2008, pp. 1-7.

[15] R. Ayyanar, V. Vittal, *Grid integration and dynamic impact of wind energy (power electronics and power systems)*, Springer, New York, 2012.

[16] M. Patel, *Wind and solar power systems: design, analysis, and operation*, CRC Press, Florida, Second edition, 1996.

[17] P. Gevorkian, *Large-scale solar power system design*, McGraw-Hill Professional, New York, 2011.

[18] G. Boyle, *Renewable energy: power for a sustainable future*, Oxford University Press, England, Third edition, 2012.

[19] S.C. Smith, P.K. Sen, B. Kroposki, "Advancement of energy storage devices and applications in electrical power systems," *IEEE Power and Energy Society General Meeting – Conversion and Delivery of Electrical Energy in the 21st Century*, 20-24 July 2008, pp. 1-8.

[20] S. Yeleti, F. Yong, "Impacts of energy storage on the future power system," *North American Power Symposium*, 26-28 Sept. 2010, pp. 1-7.

[21] J. Kleissl, M. Lave, M. Jamaly, J. Bosch, "Aggregate solar variability," *IEEE Power and Energy Society General Meeting*, 22-26 July 2012, pp. 1-3.

[22] N. Ming, Z. Zheng, D. Osborn, "Economic and operation benefits of energy storage — a case study at MISO," *IEEE Power and Energy Society General Meeting*, 22-26 July 2012, pp. 1-7.

[23] S.O. Geurin, A.K. Barnes, J.C. Balda, "Smart grid applications of selected energy storage technologies," *IEEE PES Innovative Smart Grid Technologies*, 16-20 Jan. 2012, pp. 1-8.

[24] W. Jewell, H. Zhouxing, "The role of energy storage in transmission and distribution efficiency," *IEEE PES Transmission and Distribution Conference and Exposition*, 7-10 May 2012, pp. 1-4.

[25] K. Furusawa, H. Sugihara, K. Tsuji, Y. Mitani, "A new operation framework of demand-side energy storage system cooperated with power system," *International Conference on Power System Technology*, 21-24 Nov. 2004, vol. 1, pp. 385-390.

[26] H. Zhouxing, W. T. Jewell, "Optimal power flow analysis of energy storage for congestion relief, emissions reduction, and cost savings," *IEEE/PES Power Systems Conference and Exposition*, 20-23 March 2011, pp. 1-8.

[27] M.S. Habibi, "Model for impact of storage on spinning reserve requirements and distributed generation," *Proceedings of the 33rd Southeastern Symposium on System Theory*, Mar. 2001, pp. 161-165.

[28] A.L. de Sebastian, "Investment requirements in generation capacity and reserve margin," *IEEE Power Engineering Society General Meeting*, June 2004, pp. 1023-1025.

[29] US Energy Information Administration, "Reserve electric generating capacity helps keep the lights on," available at: http://www.eia.gov/todayinenergy/detail.cfm?id=6510.

[30] D. Connolly," A review of energy storage technologies," available at: http://www.dconnolly.net/files/David%20Connolly,%20UL,%20Energy%20Storage%20Techniques,%20V3.pdf.

[31] Q. Hao, Z. Jianhui, L. Jih-Sheng, "A grid-tie battery energy storage system," *IEEE 12th Workshop on Control and Modeling for Power Electronics*, 28-30 June 2010, pp. 1-5.

[32] S. Kalyani, S. Nagalakshmi, R. Marisha, "Load frequency control using battery energy storage system in interconnected power system," *Third International Conference on Computing Communication & Networking Technologies*, 26-28 July 2012, pp. 1-6.

[33] M. C. Such, C. Hill, "Battery energy storage and wind energy integrated into the Smart Grid," *IEEE PES Innovative Smart Grid Technologies*, 16-20 Jan. 2012, pp. 1-4.

[34] K.Y. Cheung, S.T. Cheung, R.G. Navin De Silva, M.P. Juvonen, R. Singh, "Large-scale energy storage systems," Imperial College, London, England, 2003.

[35] A. Gonzalez, B. Ó'Gallachóir, E. McKeogh, K. Lynch, "Study of electricity storage technologies and their potential to address wind energy intermittency in Ireland," Sustainable Energy Ireland, 2004.

[36] R.E. Horn," Supercapacitor energy storage," available at: http://www.macrovu.com /image/PVT/NASA/RPC/uc%3DSupercapacitors.v3.pdf.

[37] E. Harkins, M. Prado, D. Sodel," Electrical energy storage using fuel cell technology," available at: http://www.esru.strath.ac.uk/EandE/Web_sites/0001/fuel_cells/Fuel%20cell%20advantages.htm.

[38] The University of Strathclyde in Glasgow, "Fuel cell advantages," available at: http://www.esru.strath.ac.uk/EandE/Web_sites/0001/fuel_cells/Fuel%20cell%20advantages.htm.

[39] FERC, "Economic dispatch: concepts, practices and issues," available at: http://www.ferc.gov/eventcalendar/Files/20051110172953-FERC%20Staff%20Presentation.pdf.

[40] W. Caisheng, M. H. Nehrir, "Distributed generation applications of fuel cells," *Power Systems Conference: Advanced Metering, Protection, Control, Communication, and Distributed Resources*, 14-17 March 2006, pp. 244-248.

[41] X. Yu, M. R. Starke, L. M. Tolbert, B. Ozpineci, "Fuel cell power conditioning for electric power applications: a summary," *IET Electric Power Applications*, Sept. 2007, vol. 1, no. 5, pp. 643-656.

[42] S. Srinivasan, *Fuel cells: from fundamentals to applications*, Springer, New York, 2006.

[43] J. Zhu, *Optimization of power system operation*, J Wiley and Sons, New Jersey, First edition, 2009.

[44] W. Ongsakul, V. N. Dieu, *Artificial intelligence in power system optimization*, CRC Press, Florida, 2013.

[45] N. M. Pindoriya, S.N. Singh, K.Y. Lee, "A comprehensive survey on multi-objective evolutionary optimization in power system applications," *IEEE Power and Energy Society General Meeting*, 25-29 July 2010, pp. 1-8.

[46] H. H. Happ, "Optimal power dispatch-a comprehensive survey," *IEEE Transactions on Power Apparatus and Systems*, May-June 1977, vol. 96, pp. 841-854.

[47] F. Gao, G. Sheble, "Economic dispatch algorithms for thermal unit system involving combined cycle units," *15th Power Systems Computation Conference*, 22-26 August 2005.

[48] R. Bellman, "The theory of dynamic programming," RAND Corporation, Proc. National Academy of Sciences, 1952, pp. 503-715.

[49] A. Richards, J. How, "Mixed-integer programming for control," *American Control Conference*, 8-10 June 2005, vol. 4, pp. 2676-2683.

[50] D. Bertsimas, J. N. Tsitsiklis, *Introduction to Linear Optimization*, Athena Scientific, Belmont, MA, 1997.

[51] C. A. Floudas, *Nonlinear and Mixed-Integer Programming – Fundamentals and Applications*, Oxford University Press, 1995.

[52] J. Linderoth, M. Savelsbergh, "A computational study of branch and bound search strategies for mixed integer programming," *INFORMS Journal on Computing*, Nov. 1999, pp. 173–187.

[53] G. Pengfui, W. Xuezhi, H. Yingshi, "The enhanced genetic algorithm for the optimization design," *3rd International Conference on Biomedical Engineering and Informatics*, 16-18 Oct. 2010, vol. 7, pp. 2990-2994.

[54] M. R. Nayak, K. R. Krishnanand, P. K. Rout, "Modified differential evolution optimization algorithm for multi-constant optimization power flow," *International Conference on Energy, Automation, and Signal*, 28-30 Dec. 2011, pp. 1-7.

[55] Y. Xiaohi, Z. Yunlong, Z Wenping, "A hybrid artificial bee colony algorithm for numerical function optimization," *11th International Conference on Hybrid Intelligent Systems*, 5-8 Dec. 2011, pp. 127-132.

[56] D. Simon, "Biogeography based optimization," *IEEE Transactions on Evolutionary Computation*, Dec. 2008, vol. 12, no. 6, pp. 702-713.

[57] M. Dorigo, M. Biratteri, T. Stutzle, "Ant colony optimization," *IEEE Computational Intelligence Magazine*, Nov. 2006, vol. 1, no. 4, pp. 28-39.

[58] M. Hai, W. Yanjiang, "An artificial fish swarm algorithm based on chaos search," *Fifth International Conference on Natural Computation*, 14-16 Aug. 2009, vol. 4, pp. 118-121.

[59] S. Yichuan, C. Hanning, "Cooperative bacterial foraging optimization," *International Conference on Future Biomedical Information Engineering*, 13-14 Dec. 2009, pp. 486-488.

[60] J. Blondin, "Particle swarm optimization: a tutorial," available at: http://cs.armstrong.edu/saad/csci8100/pso_tutorial.pdf.

[61] J. Kennedy, R. Eberhart, "Particle swarm optimization," *Proceedings of the IEEE International Conference on Neural Networks*, 1995, volume IV, pp. 1942–1948.

[62] J. Kennedy, R. Eberhart, Y. Shi, *Swarm Intelligence,* Morgan Kaufmann Publishers, San Francisco, 2001.

[63] Frans van den Bergh, "An analysis of particle swarm optimizers," PhD thesis, University of Pretoria, South Africa, 2001.

[64] S. Eftekharnejad, "The Impact of increased penetration of photovoltaic generation on smart grids," PhD. dissertation, Arizona State University, Tempe AZ, December 2012, p. 48.

[65] "DOE international energy storage database: open loop pumped hydro storage," available at: http://www.energystorageexchange.org/projects?utf8=%E2%9C%93&technology_type_sort_eq=Open+Loop++Pumped+Hydro+Storage&country_sort_eq=&state_sort_eq=&kW=&kWh=&benefit_stream_inf=&ownership_model_eq=&status_eq=&siting_eq=&show_unapproved=%7B%7D&order_by=&sort_order=&search_page=1&size_kw_ll=&size_kw_ul=&size_kwh_ll=&size_kwh_ul=.

[66] K. F. Kumli, "Application for preliminary permit for the Longview Pumped Storage project," available at: http://longviewee.com/admins/wp-content/uploads/2012/02/Application%20for%20Preliminary%20Permit.pdf.

[67] Table Mountain LLC, "Table Mountain Pumped Storage project: notice of preliminary permit," available at: http://www.gpo.gov/fdsys/pkg/FR-2011-11-14/pdf/2011-29248.pdf.

[68] G. Gillen *et. al*., "Eagle Mountain Pumped Storage project draft environmental impact report volume I," GEI Consultants, Inc., Rancho Cordova, CA, Report No. 2009011010, July 2010, vol. 1.

[69] V. M. Montsinger, "Effect of load factor on operation of power transformers by temperature," *Transactions of the American Institute of Electrical Engineers*, Nov. 1940, vol. 59, no. 11, pp. 632-636.

[70] A. Tokombayev, G. T. Heydt, "HTLS upgrades for the economic operation improvement of power systems," paper submitted October 2013 to the IEEE Power and Energy Society, *Transactions on Power Delivery*.

[71] MATLAB, ”Interior-point-convex quadprog algorithm,” available at: http://www.mathworks.com/help/optim/ug/quadratic-programming-algorithms.html#bsqspm.

[72] J. Ruggiero, G. Heydt, “Making the economic case for bulk energy storage in electric power systems,” *North American Power Symposium*, 22-24 Sept. 2013, pp. 1 – 8.

[73] United States Congress, “The Endangered Species Act of 1973,” 7 U.S.C. § 136, 16 U.S.C. § 1531 and subsequent acts, Washington DC, 1973.

APPENDIX A

MATLAB CODE

A.1 MATLAB code used in this project

```
clear;
clc;

%Changes specific options in the quadprog algorithm including a change
to
%the interior-point-convex.
options= optimset('MaxIter',50,'LargeScale','off', 'Display', 'off',...
'Diagnostics','off', 'MaxFunEvals',100,'TolFun',.0001,...
'TolX',.0001,'Algorithm','interior-point-convex');

%Reads xlsx file with network data
 A=xlsread('Large System Casev2.xlsx','System data');
%Determines number of each category
 b=A(1,1);                                          % b=# of buses
 l=A(1,2);                                          % l=# of lines
 g=A(1,3);                                          % g=# of generators
 s=A(1,4);                                          % s=# of storage units
int=A(1,5);                                        % int=# of load
intervals
dT=A(1,6);                                         % dT= delta t or hours
per interval
 d=A(1,7);                                          % d=number of days
  B=xlsread('Large System Casev2.xlsx','Bus data');       %Extracts bus
data
 L=xlsread('Large System Casev2.xlsx','Line data');      %Extracts line
data
 G=xlsread('Large System Casev2.xlsx','Generator data'); %Extracts
generator data
 S=xlsread('Large System Casev2.xlsx','Storage data');   %Extracts
storage data

 X=(3*b+l-1)*int;                                %Creates size of 'x'
matrix

%GENERATION OF THE Q MATRIX (QUADRATIC COSTS)
%Extracts generator quadratic cost terms and inputs into a matrix
 c=1;
 j=1;
 a=zeros(b,b);
for k=1:1:g

a(G(c,1),G(c,1))=G(c,5)*2;
    c=c+1;
    j=j+1;
end
%Matrix of generator quadratic costs at each hour
c=1;
j=1;
for k=1:1:int

    Q1(c:c+b-1,j:j+b-1)=a;
    c=c+b;
```

```
    j=j+b;
end
%Overall Q matrix with Q1 in the correct location
Q=zeros(X,X);
Q((b+l-1)*int+1:(2*b+l-1)*int,(b+l-1)*int+1:(2*b+l-1)*int)=Q1;
Q=sparse(Q);

%GENERATION OF THE C MATRIX (LINEAR COSTS)
%Extracts generator linear cost terms and inputs them into a matrix
c=1;
j=1;
C1=zeros(1,b);
for k=1:1:g

C1(1,G(c,1))=G(c,4);
    c=c+1;
    j=j+1;
end
%Repeats the linear costs over the amount of hours
j=1;
for k=1:1:int

CT(1,j:j+b-1)=C1;
    j=j+b;
end
%Inputs the total linear costs into the overall C matrix
C=zeros(1,X);
C(1,(b+l-1)*int+1:(2*b+l-1)*int)=CT;
C=sparse(C);

%GENERATION OF THE B MATRIX (INEQUALITY LIMITS)
%Generates vector of line limits
c=1;
j=1;
b1=zeros(2*l*int,1);
for k=1:1:l

        b1(c:2*j*int,1)=L(j,6);
        c=c+2*int;
        j=j+1;
end
%Generates vector of generator limits
i=1;
j=1;
b2=zeros(2*b*int,1);
b2i=zeros(2*int,1);
for k=1:1:g
for u=1:1:int
b2i(i,1)=G(j,3);
b2i(i+1,1)=-G(j,2);
        i=i+2;
end
b2(2*G(j,1)*int-(2*int-1):2*G(j,1)*int,1)=b2i;
    j=j+1;
```

```
    i=1;
    b2i=zeros(2*int,1);
end
%Generates vector of storage charging power limits
i=1;
j=1;
b3=zeros(2*b*int,1);
b3i=zeros(2*int,1);
for k=1:1:s
for u=1:1:int
b3i(i:i+1,1)=S(j,2);
        i=i+2;
end
b3(2*S(j,1)*int-(2*int-1):2*S(j,1)*int,1)=b3i;
    j=j+1;
    i=1;
    b3i=zeros(2*int,1);
end
%Generates vector of generator ramp rate limits
i=1;
j=1;
b4=ones(2*b*(int-1),1)*10000;
b4i=zeros(2*(int-1),1);
for k=1:1:g
for u=1:1:(int-1)
b4i(i:i+1,1)=G(j,6);
        i=i+2;
end
b4(2*G(j,1)*(int-1)-(2*(int-1)-1):2*G(j,1)*(int-1),1)=b4i;
    j=j+1;
    i=1;
    b4i=zeros(2*(int-1),1);
end
%Generates vector of storage charging energy limits
i=1;
j=1;
b5=zeros(2*b*int,1);
b5i=zeros(2*int,1);
for k=1:1:s
for u=1:1:int
b5i(i,1)=S(j,3);
b5i(i+1,1)=0;
        i=i+2;
end
b5(2*S(j,1)*int-(2*int-1):2*S(j,1)*int,1)=b5i;
    j=j+1;
    i=1;
    b5i=zeros(2*int,1);
end
%Inputs 5 vectors (b1,b2,b3,b4 and b5) into overall b vector
bT=zeros(2*int*(l+2*b)+2*b*(int-1)+2*b*int,1);
bT(1:2*l*int,1)=b1;
bT(2*l*int+1:2*int*(l+b),1)=b2;
bT(2*int*(l+b)+1:2*int*(l+2*b),1)=b3;
bT(2*int*(l+2*b)+1:2*int*(l+2*b)+2*b*(int-1),1)=b4;
```

```
bT(2*int*(l+2*b)+2*b*(int-1)+1:2*int*(l+2*b)+2*b*(int-1)+2*b*int,1)=b5;
bT=sparse(bT);

%GENERATION OF THE beq MATRIX (EQUALITY LIMITS)

%Generates beq1 vector which contains the load value at each bus and
each
%interval
c=1;
j=1;
m=1;
beqa=zeros(int,1);
beq1=zeros(b*int,1);
for k=1:1:b
        p=5;
for u=1:1:int
beqa(c,1)=B(j,p);
        c=c+1;
        p=p+1;
end
        c=1;
beq1(m:int*j,1)=beqa;
    m=m+int;
    j=j+1;
end
%Inputs load values into the overall beq vector with zeros at every
other
%point
beq=zeros((b+l)*int+b,1);
beq(l*int+1:(l+b)*int,1)=beq1;
beq=sparse(beq);

%GENERATION OF THE A MATRIX (INEQUALITIES)
%Generates the A1 matrix(line inequalities)
t=1;
i=1;
j=1;
m=1;
A1=zeros(2*l*int,l*int);                    %Sets up size of A1 matrix
A1i=zeros(2*int,l*int);                     %Sets up size of inner A1i
matrix
for k=1:1:l
for u=1:1:int
A1i(i,j)=1;
A1i(i+1,j)=-1;
        i=i+2;
        j=j+l;
end
A1(m:2*t*int,1:l*int)=A1i;                  %Inputs inner matrix of each
    m=m+2*int;                                %line into the larger A1
matrix
    t=t+1;
    i=1;
    j=t;
    A1i=zeros(2*int,l*int);
```

```
end;
%Generates the A2 matrix(generator inequalities)
t=1;
i=1;
j=1;
m=1;
A2=zeros(2*b*int,b*int);                    %Sets up size of A2 matrix
A2i=zeros(2*int,b*int);                     %Sets up size of inner A2i
matrix
for k=1:1:b
for u=1:1:int
A2i(i,j)=1;
A2i(i+1,j)=-1;
            i=i+2;
            j=j+b;
end
A2(m:2*t*int,1:b*int)=A2i;
   m=m+2*int;
   t=t+1;
   i=1;
   j=t;
   A2i=zeros(2*int,b*int);
end
%Generates A3 matrix (storage inequalities)
t=1;
i=1;
j=1;
m=1;
A3=zeros(2*b*int,b*int);                    %Sets up size of A3 matrix
A3i=zeros(2*int,b*int);                     %Sets up size of inner A3i
matrix
for k=1:1:b
for u=1:1:int
A3i(i,j)=1;
A3i(i+1,j)=-1;
        i=i+2;
        j=j+b;
end
A3(m:2*t*int,1:b*int)=A3i;                  %Inputs inner matrix of each
    m=m+2*int;                                %storage into the larger
A3 matrix
    t=t+1;
    i=1;
    j=t;
    A3i=zeros(2*int,b*int);
end;
%Generates the A4 matrix(generator ramp rate inequalities)
i=1;
j=1;
m=1;
t=1;
A4=zeros(2*b*(int-1),b*int);
A4i=zeros(2*(int-1),b*int);
for k=1:1:b
for u=1:1:(int-1)
```

```
A4i(i,j)=1/dT;
A4i(i,j+b)=-1/dT;
A4i(i+1,j)=-1/dT;
A4i(i+1,j+b)=1/dT;
        i=i+2;
        j=j+b;
end
A4(m:2*t*(int-1),1:b*int)=A4i;
    m=m+2*(int-1);
    t=t+1;
    i=1;
    j=t;
    A4i=zeros(2*(int-1),b*int);
end
%Generates the A5 matrix (bulk energy storage limit on energy storage)
i=1;
j=1;
t=0;
z=1;
f=1;
y=int;
A5=zeros(2*b*int,b*int);
A5i=zeros(2*int,b*int);
for k=1:1:b
for m=1:1:int
for u=1:1:y
A5i(i+2*t,j)=dT;
A5i(i+2*t+1,j)=-dT;
           i=i+2;
end
        i=1;
        y=y-1;
        t=t+1;
        j=j+b;
end
A5(f:2*z*int,1:b*int)=A5i;
    y=int;
    f=f+2*int;
    z=z+1;
    j=z;
    t=0;
    A5i=zeros(2*int,b*int);
end
%Stores each of the smaller matrices (A1,A2,A3,A4, and A5) into the A
matrix
A=zeros(2*int*(l+2*b)+2*b*(int-1)+2*b*int,X);
A(1:2*l*int,(b-1)*int+1:(b+l-1)*int)=A1;
A(2*l*int+1:2*int*(l+b),(b+l-1)*int+1:(2*b+l-1)*int)=A2;
A(2*int*(l+b)+1:2*int*(l+2*b),(2*b+l-1)*int+1:X)=A3;
A(2*int*(l+2*b)+1:2*int*(l+2*b)+2*b*(int-1),(b+l-1)*int+1:(2*b+l-
1)*int)=A4;
A(2*int*(l+2*b)+2*b*(int-1)+1:2*int*(l+2*b)+2*b*(int-1)+2*b*int,(2*b+l-
1)*int+1:X)=A5;
%A=sparse(A);
```

```
%GENERATION OF THE AEQ MATRIX (EQUALITIES)
Aeq=zeros((b+l)*int+s,X);                %Sets up the size of the Aeq
matrix
%GENERATION OF AEQ1A MATRIX(LINE DELTA VALUES)
p=1;
t=1;
i=1;
j=0;
m=1;
Aeq1a=zeros(l*int,b*int);                %Sets up the size for the
Aeq1a matrix
Aeq1ai=zeros(int,b*int);                 %Sets up the size for the
Aeq1ai matrix
for k=1:1:l
    kV2=B(L(p,2),4)*B(L(p,3),4);
for u=1:1:int
if (L(p,2)< L(p,3))
Aeq1ai(i,L(p,2)+j)=-kV2/L(p,5);
Aeq1ai(i,L(p,3)+j)=kV2/L(p,5);
            i=i+1;
            j=j+b;
elseif (L(p,2) > L(p,3))
Aeq1ai(i,L(p,2)+j)=kV2/L(p,5);
Aeq1ai(i,L(p,3)+j)=-kV2/L(p,5);
            i=i+1;
            j=j+b;
end
end
Aeq1a(m:t*int,1:b*int)=Aeq1ai;
    m=m+int;
    t=t+1;
    Aeq1ai=zeros(int, b*int);
    i=1;
    p=p+1;
    j=0;
end
%Deletes the swing bus because it has an angle of zero
i=1;
j=0;
for k=1:1:b
if B(i,2)==3
for u=1:1:int
Aeq1a(:,B(i,1)+j)=[];
            j=j+b-1;
end
end
     i=i+1;
end
Aeq(1:l*int,1:(b-1)*int)=Aeq1a; %Stores the line delta values in the
Aeq matrix
%GENERATION OF AEQ1B MATRIX (LINE POWER FLOW VALUES)
m=1;
i=1;
j=1;
t=1;
```

```
Aeq1b=zeros(l*int,l*int);                %Sets up the size for the
Aeq1b matrix
Aeq1bi=zeros(int,l*int);                 %Sets up the size for the
Aeq1bi matrix
for k=1:1:l
for u=1:1:int
Aeq1bi(i,j)=1;
        i=i+1;
        j=j+l;
end
Aeq1b(m:t*int,1:l*int)=Aeq1bi;
    m=m+int;
    t=t+1;
    j=t;
    i=1;
    Aeq1bi=zeros(int,l*int);
end
Aeq(1:l*int,(b-1)*int+1:(b+l-1)*int)=Aeq1b; %Stores the Aeq1b matrix
into Aeq
%GENERATION OF THE AEQ2A MATRIX(BUS POWER FLOW VALUES)
i=1;
j=0;
t=1;
e=1;
m=1;
Aeq2a=zeros(b*int,l*int);                   %Sets up the Aeq2a matrix
size
Aeq2ai=zeros(int,l*int);
for k=1:1:b
for u=1:1:l
if ((L(i,2)== t) || (L(i,3) == t))  %Tests to see if a line contains a
bus number
%Determines which way power is flowing based on order of buses
for v=1:1:int
if L(i,2)==t
Aeq2ai(e,L(i,1)+j)=-1;
elseif L(i,3)==t
Aeq2ai(e,L(i,1)+j)=1;
end
                e=e+1;
                j=j+l;
end
            j=0;
            e=1;
end
        i=i+1;
end
Aeq2a(m:t*int,1:l*int)=Aeq2ai;
        m=m+int;
        t=t+1;
        i=1;
        j=0;
        e=1;
        Aeq2ai=zeros(int,l*int);
end
```

```
Aeq(l*int+1:(l+b)*int,(b-1)*int+1:(b+l-1)*int)=Aeq2a;   %Stores Aeq2a
into Aeq
%GENERATION OF THE AEQ2B MATRIX (BUS GENERATION VALUES)
i=1;
j=1;
t=1;
m=1;
Aeq2b=zeros(b*int,b*int);                    %Sets up the size of the
Aeq2b matrix
Aeq2bi=zeros(int,b*int);
for k=1:1:b
for u=1:1:int
Aeq2bi(i,j)=1;
            j=j+b;
            i=i+1;
end
Aeq2b(m:t*int,1:b*int)=Aeq2bi;
    m=m+int;
    t=t+1;
    i=1;
    j=t;

    Aeq2bi=zeros(int,b*int);
end
Aeq(l*int+1:(l+b)*int,(b+l-1)*int+1:(2*b+l-1)*int)=Aeq2b; %Stores it in
the Aeq matrix
%GENERATION OF THE AEQ2C MATRIX(BUS STORAGE VALUES)
i=1;
j=1;
t=1;
Aeq2c=zeros(b*int,b*int);                %Sets up the size of the Aeq2c
matrix
%Aeqxi=zeros(int,b*int);
for k=1:1:b
for u=1:1:int
Aeq2c(i,j)=-1;
        i=i+1;
        j=j+b;
end
    t=t+1;
    j=t;
end
Aeq(l*int+1:(l+b)*int,(2*b+l-1)*int+1:(3*b+l-1)*int)=Aeq2c;   %Stores
the Aeq2c matrix into Aeq
%GENERATION OF THE AEQ3 MATRIX(STORAGE VALUES AT EACH HOUR)
i=1;
j=1;
Aeq3=zeros(b,b*int);
for k=1:1:b
for u=1:1:int
Aeq3(i,j)=1;
        j=j+b;
end
    i=i+1;
    j=i;
```

```
end
Aeq((l+b)*int+1:(l+b)*int+b,(2*b+l-1)*int+1:(3*b+l-1)*int)=Aeq3;
%Stores the Aeq3 matrix into the Aeq matrix
Aeq=sparse(Aeq);
[x,fval,exitflag]=quadprog(Q,C,A,bT,Aeq,beq,[],[],[],options);
%Determines the x values and the final generation cost
formatlong
Cost=fval*dT*d
%Extracts line flows at each interval
x1=x(int*(b-1)+1:int*(b-1)+l);
x2=x(int*(b-1)+l+1:int*(b-1)+2*l);
x3=x(int*(b-1)+2*l+1:int*(b-1)+3*l);
x4=x(int*(b-1)+3*l+1:int*(b-1)+4*l);
x5=x(int*(b-1)+4*l+1:int*(b-1)+5*l);
x6=x(int*(b-1)+5*l+1:int*(b-1)+6*l);
x7=x(int*(b-1)+6*l+1:int*(b-1)+7*l);
x8=x(int*(b-1)+7*l+1:int*(b-1)+8*l);
%Extracts generator output at each interval
y1=x(int*(l+b-1)+1:int*(l+b-1)+b);
y2=x(int*(l+b-1)+b+1:int*(l+b-1)+2*b);
y3=x(int*(l+b-1)+2*b+1:int*(l+b-1)+3*b);
y4=x(int*(l+b-1)+3*b+1:int*(l+b-1)+4*b);
y5=x(int*(l+b-1)+4*b+1:int*(l+b-1)+5*b);
y6=x(int*(l+b-1)+5*b+1:int*(l+b-1)+6*b);
y7=x(int*(l+b-1)+6*b+1:int*(l+b-1)+7*b);
y8=x(int*(l+b-1)+7*b+1:int*(l+b-1)+8*b);
%Extracts storage output at each interval
z1=x(int*(l+2*b-1)+1:int*(l+2*b-1)+b);
z2=x(int*(l+2*b-1)+b+1:int*(l+2*b-1)+2*b);
z3=x(int*(l+2*b-1)+2*b+1:int*(l+2*b-1)+3*b);
z4=x(int*(l+2*b-1)+3*b+1:int*(l+2*b-1)+4*b);
z5=x(int*(l+2*b-1)+4*b+1:int*(l+2*b-1)+5*b);
z6=x(int*(l+2*b-1)+5*b+1:int*(l+2*b-1)+6*b);
z7=x(int*(l+2*b-1)+6*b+1:int*(l+2*b-1)+7*b);
z8=x(int*(l+2*b-1)+7*b+1:int*(l+2*b-1)+8*b);
%Writes line flows at each interval to excel file
xlswrite('Output.xlsx',x1,'Test output','C2:C278');
xlswrite('Output.xlsx',x2,'Test output','D2:D278');
xlswrite('Output.xlsx',x3,'Test output','E2:E278');
xlswrite('Output.xlsx',x4,'Test output','F2:F278');
xlswrite('Output.xlsx',x5,'Test output','G2:G278');
xlswrite('Output.xlsx',x6,'Test output','H2:H278');
xlswrite('Output.xlsx',x7,'Test output','I2:I278');
xlswrite('Output.xlsx',x8,'Test output','J2:J278');
%Writes generation output at each interval to excel file
xlswrite('Output.xlsx',y1,'Test output','N2:N207');
xlswrite('Output.xlsx',y2,'Test output','O2:O207');
xlswrite('Output.xlsx',y3,'Test output','P2:P207');
xlswrite('Output.xlsx',y4,'Test output','Q2:Q207');
xlswrite('Output.xlsx',y5,'Test output','R2:R207');
xlswrite('Output.xlsx',y6,'Test output','S2:S207');
xlswrite('Output.xlsx',y7,'Test output','T2:T207');
xlswrite('Output.xlsx',y8,'Test output','U2:U207');
%Writes storage output at each interval to excel file
xlswrite('Output.xlsx',z1,'Test output','Y2:Y207');
```

```
xlswrite('Output.xlsx',z2,'Test output','Z2:Z207');
xlswrite('Output.xlsx',z3,'Test output','AA2:AA207');
xlswrite('Output.xlsx',z4,'Test output','AB2:AB207');
xlswrite('Output.xlsx',z5,'Test output','AC2:AC207');
xlswrite('Output.xlsx',z6,'Test output','AD2:AD207');
xlswrite('Output.xlsx',z7,'Test output','AE2:AE207');
xlswrite('Output.xlsx',z8,'Test output','AF2:AF207');
%Equality limit testing
Eql=Aeq*x-beq;
%Inequality limit testing
Ineql=A*x-bT;
Llmt=Ineql(1:2*l*int,1);
Glmt=Ineql(2*l*int+1:2*int*(l+b));
CPlmt=Ineql(2*int*(l+b)+1:2*int*(l+2*b));
Rlmt=Ineql(2*int*(l+2*b)+1:2*int*(l+2*b)+2*b*(int-1));
CElmt=Ineql(2*int*(l+2*b)+2*b*(int-1)+1:2*int*(l+2*b)+2*b*(int-
1)+2*b*int);
i=1;
LlmtO=zeros(length(Llmt),1);
for k=1:1:length(Llmt)
ifLlmt(i,1) >= 0
LlmtO(i,1)=1;
else
LlmtO(i,1)=0;
end
    i=i+1;
end
LLreached=sum(LlmtO);
i=1;
LlmtA=zeros(length(Llmt),1);
for k=1:1:length(Llmt)
ifLlmt(i,1)/b1(i,1) >= -.05 &Llmt(i,1)/b1(i,1) < 0
LlmtA(i,1)=1;
else
LlmtA(i,1)=0;
end
    i=i+1;
end
LL95=sum(LlmtA);
i=1;
GlmtO=zeros(length(Glmt),1);
for k=1:1:length(Glmt)/2
ifGlmt(i,1)>=0 & b2(i,1) ~= 0
GlmtO(i,1)=1;
else
GlmtO(i,1)=0;
end
    i=i+2;
end
i=2;
for k=1:1:length(Glmt)/2
ifGlmt(i,1)>=0 & b2(i-1,1) ~= 0
GlmtO(i,1)=1;
else
GlmtO(i,1)=0;
```

```
end
    i=i+2;
end
GLreached=sum(GlmtO);
i=1;
GlmtA=zeros(length(Glmt),1);
for k=1:1:length(Glmt)
ifGlmt(i,1)/b2(i,1)>=-.05 & b2(i,1) ~= 0 &Glmt(i,1)/b2(i,1)<0
GlmtA(i,1)=1;
else
GlmtA(i,1)=0;
end
    i=i+1;
end
GL95=sum(GlmtA);
i=1;
CPlmtO=zeros(length(CPlmt),1);
for k=1:1:length(CPlmt)
ifCPlmt(i,1)>=0 & b3(i,1) ~= 0
CPlmtO(i,1)=1;
else
CPlmtO(i,1)=0;
end
    i=i+1;
end
CPLreached=sum(CPlmtO);
i=1;
CPlmtA=zeros(length(CPlmt),1);
for k=1:1:length(CPlmt)
ifCPlmt(i,1)/b3(i,1) >= -.05 &CPlmt(i,1)/b3(i,1) < 0
CPlmtA(i,1)=1;
else
CPlmtA(i,1)=0;
end
    i=i+1;
end
CPL95=sum(CPlmtA);
i=1;
RlmtO=zeros(length(Rlmt),1);
for k=1:1:length(Rlmt)
ifRlmt(i,1) < 0
RlmtO(i,1)=0;
else
RlmtO(i,1)=1;
end
    i=i+1;
end
RLreached=sum(RlmtO);
i=1;
RlmtA=zeros(length(Rlmt),1);
for k=1:1:length(Rlmt)
ifRlmt(i,1)/b4(i,1) >=-.05 &Rlmt(i,1)/b4(i,1) < 0
RlmtA(i,1)=1;
else
RlmtA(i,1)=0;
```

```
end
    i=i+1;
end
RL95=sum(RlmtA);
i=1;
CElmtO=zeros(length(CElmt),1);
for k=1:1:length(CElmt)/2
ifCElmt(i,1)>=0 & b5(i,1) ~= 0
CElmtO(i,1)=1;
else
CElmtO(i,1)=0;
end
    i=i+2;
end
i=2;
for k=1:1:length(CElmt)/2
ifCElmt(i,1)>=0 & b5(i-1,1) ~= 0
CElmtO(i,1)=1;
else
CElmtO(i,1)=0;
end
    i=i+2;
end
CELreached=sum(CElmtO);
i=1;
CElmtA=zeros(length(CElmt),1);
for k=1:1:length(CElmt)
ifCElmt(i,1)/b5(i,1) >= -.05 & b5(i,1) ~= 0 &CElmt(i,1)/b5(i,1) < 0
CElmtA(i,1)=1;
else
CElmtA(i,1)=0;
end
    i=i+1;
end
CEL95=sum(CElmtA);
Limits=[LLreached, LL95, GLreached, GL95, CPLreached, CPL95, RLreached,
RL95, CELreached, CEL95]
xlswrite('Output.xlsx',Eql,'Limit testing','B3:B4072');
xlswrite('Output.xlsx',Ineql,'Limit testing','H3:H17204');
xlswrite('Output.xlsx',x,'Limit testing','N3:N7154');
%Prints out line limits into the output spreadsheet for comparison
Linelim=L(:,6);
xlswrite('Output.xlsx',Linelim,'Test output','B2:B278');
%Prints out generator limits into the output spreadsheet for comparison
Genlim=zeros(206,1);
i=1;
for k=1:1:g
Genlim(G(i,1),1)=G(i,3);
    i=i+1;
end
xlswrite('Output.xlsx',Genlim,'Test output','M2:M207');
%Prints out storage power limits into the output spreadsheet for
comparison
Storlim=zeros(206,1);
i=1;
```

```
for k=1:1:s
Storlim(S(i,1),1)=S(i,2);
    i=i+1;
end
xlswrite('Output.xlsx',Storlim,'Test output','X2:X207');
%Prints out generator ramp rate limits into the output spreadsheet for
comparison
Ramplim=zeros(206,1);
i=1;
for k=1:1:g
Ramplim(G(i,1),1)=G(i,6);
    i=i+1;
end
xlswrite('Output.xlsx',Ramplim,'Ramp rates','B3:B208');
```

APPENDIX B

THE QUADRATIC PROGRAMMING METHOD

B.1 Quadratic programming

Quadratic programming is used in this thesis for optimization of a nonlinear (quadratic) performance index constrained by linear constraints. The method used was directly from the MATLAB toolbox. *The following description of quadratic programming largely comes directly from [71].*

Interior-point-convex quadprog algorithm

Quadratic programming is a technique to find a vector *x* that minimizes a quadratic objective function, subject to linear constraints,

$$\min_X f(x) = \min_X \frac{1}{2} x^T H x + c^T x$$

$$Ax \leq b$$

$$A_{eq} x = b_{eq}$$

$$l \leq x \leq u$$

where

c	Vector(*n x 1*) of linear terms of the quadratic objective function
H	Symmetric matrix ($n \times n$) describing the coefficients of the quadratic terms
A	Coefficient matrix (*m x n*) of inequality constraints
b	Vector (*m x 1*) of inequality right-hand side constraints
A_{eq}	Coefficient matrix (*k x n*) of equality constraints
b_{eq}	Vector (*k x 1*) of equality right-hand side constraints.
l	Vector of lower bound variables
u	Vector of upper bound variables

The quadratic programming in MATLAB uses the interior-point-convex algorithm which has the following steps:

1. Presolve / postsolve
2. Generate initial point
3. Predictor- corrector
4. Multiple corrections.

Each of these steps are described in [71] in more detail and are summarized below.

Presolve / postsolve

The interior-point-algorithm starts by trying to remove redundancies and constraints that simplify the problem. The presolve portion of the algorithm attempts to perform the following operations in order to simplify the problem can be seen in [71].

In the presolve step the algorithm searches for an infeasible or unbounded problem. If one is found, the program is terminated and displays the appropriate exit message. If an infeasible or unbounded problem is not detected, the algorithm continues on to the other steps. The algorithm then restructures the original problem removing any of the transformations performed during the presolve section. Finally, the postsolve is the last step performed.

Generate initial point

The initial point x_0 for the algorithm is:

1. Initialize x_0 to ones(n,1), where n is the number of rows in H.
2. For components that have both an upper bound u_b and a lower bound l_b, the component is set to $(u_b + l_b)/2$ if a component of x_0 in not inside these bounds.

3. For components that have only one bound, the component is modified to lie strictly inside the bound.

Predictor- corrector

The interior-point-convex algorithm tries to find a point where the Karush-Kuhn-Tucker (KKT) conditions hold. For the quadratic programming problem described, these conditions can be seen in [71].

Multiple corrections

The multiple corrections step is used after the Newton phase in the predictor/ corrector section and prepares the solution for better succeeding steps. The corrections are used to possibly improve the algorithm performance and robustness.

B.2 Observations in the use of MATLAB quadprog

The forgoing was a quick description of the in line function quadprog in MATLAB where the full description can be seen in [71]. The following observations are made by the author in the use of this software:

- Unlike linear programming, increasing the limit of various constraints in the system when the output variable is not at that limit can actually improve the results. This outcome does not happen in linear programming where a relaxation of a limit that the variable is not hitting has no effect on the optimization results. When a line in the Arizona test be was approaching the line limit, relaxing that limit showed that it is possible to improve the system wide operating cost.
- Utilization of different algorithms can improve simulation times in MATLAB. The interior-point-convex algorithm seemed to have the fastest simulation times compared to the other algorithms.

- Decreasing the program tolerance levels improved the optimization results and actually lowered the system operating cost in both the base case and the cases with energy storage.
- The portion of the simulation time that took the longest was reading and writing to / from the program Excel.

APPENDIX C

A BRIEF DISCUSSION OF ENVIRONMENTAL ISSUES RELATED TO THE SITES SELECTED FOR ENERGY STORAGE

C.1 Environmental issues

In this appendix, a few citations and comments are provided for the three bulk energy sites discussed in this thesis. This thesis focuses on the electric power engineering issues of bulk energy storage. The reader is directed to the citations listed below for a discussion of environmental issues.

C.2 Eagle Mountain Pumped Storage

The following comments apply to the Eagle Mountain Pumped Storage facility between Desert Center and Chiriaco Summit, California (a few miles north of Interstate 10):

- The project will have no impact on local surface waters as there are none in the area affected by the project [68]. There are no perennial streams in the area, therefore no in stream or out stream flows will be affected by the operation of the pumped hydro energy storage. A closed loop system will be used where the reservoir water is re-used and resupplied when needed due to evaporation. However, the water quality in the new reservoirs can be degraded through evaporation resulting in salts and pit material resulting in elevated metal concentrations.
- Section 7 of the Endangered Species Act (ESA) [73] requires that the building of this PHES does not affect the existence of endangered or threatened species or destroy local habits of these species. In this location, Coachella Valley, the species of concern are the milkvetch and the desert tortoise. In this location, there is a critical habitat for the desert tortoise that must be protected during construction and operation.

C.3 Table Mountain Pumped Storage

The following comments apply to the Table Mountain Pumped Storage facility between Peach Springs and Kingman Arizona:

- An environmental impact study has not been performed for this PHES location yet. Only a preliminary permit has been filed for the project [67]. The proposed location will be a closed loop orientation and the circulated reservoir will be reused. Its effect on the local steams has not been studied yet. Also, an analysis has yet to be performed on local endangered species and the local habitat that these species occupy.

C.4 Longview Pumped Storage

The following comments apply to the Longview Pumped Storage facility near Chino Valley (north of Prescott and south of Seligman), Arizona:

- The project reservoirs will be closed loop, meaning that water in the reservoirs will be reusable [66]. However, the source of water will be the locally available ground water that will come from the Big Chino aquifer. This aquifer is used downstream by residents in Prescott, Prescott Valley, and Chino Valley. There is some concern that the use of this water by the PHES will affect the water available for these residents as well as the water quality.
- Big Chino aquifer also supplies 80% of the backflow of the Upper Verde River, which is branded as one of the countries most endangered rivers because it is home to many endangered species. There is concern that these species could be affected if the PHES uses a significant amount of water from the aquifer.